Universidad del País Vasco Euskal Herriko Unibertsitatea

Universidad del País Vasco/Euskal Herriko Unibertsitatea
Facultad de Medicina y Enfermería
Departamento de Neurociencias

Lysophosphatidic Acid Receptor 1 Labels Seizure-induced Hippocampal Reactive Neural Stem Cells and Controls their Activation

Tesis doctoral para optar al grado de doctor
Por Roberto Valcárcel Martín

Director de tesis: Juan Manuel Encinas Pérez

2018

Index

Index

1. Abbreviations

1. Abbreviations

AHN	Adult hippocampal neurogenesis
ANP	Amplifying neural progenitor
AP	Anteroposterior
Ara-C	Cytosine β-D-arabinofuranoside
BDNF	Brain-derived neurotrophic factor
BLBP	Brain lipid-binding protein
BMP	Bone morphogenetic protein
BrdU	Bromodeoxyuridin
BSA	Bovine seroalbumin
BSAc	Acetylated bovine seroalbumin
CA	*Cornu Ammonis*
CSF	Cerebrospinal fluid
DAPI	4′,6-diamidino-2-phenylindole
DCX	Doublecortin
DG	Dentate gyrus
Dkk1	Dickkopf 1
DV	Dorsoventral
EA	Epileptiform activity

EC	Entorhinal cortex
ECS	Electroconvulsive shock
ECT	Electroconvulsive therapy
EGFR	Epidermal growth factor receptor
FGF-2 (bFGF)	Fibroblast growth factor 2
GABA	γ-aminobutyric acid
GC	Granule cell
GCL	Granule cell layer
GFAP	Glial fibrillary acidic protein
GFP	Green fluorescent protein
IEG	Immediate early gene
IGF	Insulin growth factor
IL	Interleukin
KA	Kainic acid
KO	Knockout
LL	Laterolateral
LPA	Lysophosphatidic acid
LPA_1	LPA receptor 1
LPS	Lipopolysaccharide
LTP	Long-term potentiation

maLPA$_1$	Málaga variant of LPA$_1$-null
ML	Molecular layer
MTLE	Mesial temporal lobe epilepsy
MTLE-a	Intraamygdalar MTLE model
MWM	Morris water maze
NB	Neuroblast
Nestin	*Ne*uroepithelial *s*tem prote*in*
NMDA	N-acetyl-D-aspartate
NSC	Neural stem cell
OB	Olfactory bulb
OPC	Oligodendrocyte progenitor cell
PBS	Phosphate-buffered saline
PFA	Paraformaldehyde
PLP	Periodate lysine PFA
PSA-NCAM	Polysialylated-neural cell adhesion molecule
PV	Parvalbumin
QNP	Quiescent neural progenitor
RA	Reactive astrocyte
React-NSC	Reactive NSC
RMS	Rostral migratory stream

Sal	Saline
Sal-a	Intraamygdalar Sal model
SE	*Status epilepticus*
sFRP3	Secreted Frizzled-related protein
SGZ	Subgranular zone
Shh	Sonic hedgehog
SVZ	Subventricular region
TEM	Transmission electron microscopy
WT	Wild type
YFP	Yellow fluorescent protein

2. Extracto/Abstract

2. Extracto/Abstract

2.1. Extracto

En la regulación de la neurogénesis del hipocampo adulto, un paso fundamental es la división de las células madre neurales (NSCs) ya que, tras activarse, se dividen varias veces consecutivas y se diferencian después en astrocitos. En esta tesis demostramos que aumentar su tasa de activación mediante hiperexcitación neuronal conduce a su agotamiento e incluso induce un cambio en su diferenciación. Tras provocar epilepsia directamente en el hipocampo de ratones, hemos observado que las NSCs aumentan su tasa de activación pero dejan de generar neuronas y sin embargo se transforman en NSCs reactivas (React-NSCs) que se diferencian en astrocitos reactivos (RAs). Hemos validado mediante el empleo de una cepa transgénica que la expresión del receptor 1 del ácido lisofosfatídico (LPA_1) sirve como marcador para rastrear las React-NSCs durante su conversión en RAs. Además, hemos probado que la deleción del gen LPA_1 disminuye la activación masiva de las NSCs producida por las convulsiones epilépticas. Al someter a ratones a un modelo alternativo de epilepsia, actuando en la amígdala, comprobamos que las NSCs también se dividen más y se transforman en React-NSCs, demostrando que independientemente del origen de las convulsiones las NSCs se ven afectadas. Estos resultados muestran cómo en condiciones de hiperexcitación neuronal severa las NSCs contribuyen a la gliosis reactiva, lo que puede empeorar el pronóstico de la epilepsia, y que el receptor LPA_1 participa en esta nueva función de las NSCs.

2.2. Abstract

In the regulation of adult hippocampal neurogenesis, a critical step is the division of neural stem cells (NSCs) since, following activation, they divide several times consecutively and differentiate themselves into astrocytes. In this thesis we prove that increasing their activation rate with neuronal hyperexcitation leads to their exhaustion and even induces a change in their differentiation. After causing epilepsy directly into the hippocampus of mice, we have observed that NSCs increase their activation rate but stop generating neurons and however transform into reactive NSCs (React-NSCs) that differentiate into reactive astrocytes (RAs). We have validated by employing a transgenic strain that the expression of lysophosphatidic acid receptor 1 (LPA_1) serves as a marker to trace React-NSCs during their conversion into RAs. Moreover, we have shown that deletion of the gene LPA_1 decreases NSC massive activation provoked by epileptic seizures. Subjecting mice to an alternative epilepsy model, acting into the amygdala, we proved that NSCs also divide more and transform into React-NSCs, demonstrating that regardless of the seizure origin NSCs are affected. These results show how in conditions of severe neuronal hyperexcitation NSCs contribute to reactive gliosis, which can impair the outcome of epilepsy, and that LPA_1 receptor is involved in this new function of NSCs.

3. Resumen/Summary

3. Resumen/Summary

3.1. Resumen

La neurogenesis adulta, el proceso de formación de nuevas neuronas en el cerebro adulto, persiste en dos regiones cerebrales de los mamíferos: la zona subventricular (*subventricular zone*, SVZ) de los ventrículos laterales, que genera interneuronas destinadas al bulbo olfativo; y la zona subgranular (*subgranular zone*, SGZ) del giro dentado (*dentate gyrus*, DG), que genera células granulares (*granule cells*, GCs) que se integran en los circuitos hipocampales. El proceso neurogénico en la última, llamado neurogénesis hipocampal adulta (*adult hippocampal neurogenesis*, AHN), está implicado en funciones tales como el aprendizaje, la adquisición de memorias espaciales, el condicionamiento al miedo, la ansiedad y las respuestas al estrés.

La AHN existe gracias a una población de células madre neurales (*neural stem cells*, NSCs) que permanece en la SGZ del DG adulto. Estas NSCs son en su mayoría quiescentes, pero cuando son activadas se dividen principalmente de manera asimétrica dando lugar a progenitores neurales amplificadores (*amplifying neural progenitors*, ANPs) que, a su vez, proliferan y originan los neuroblastos (NBs) que maduran y originan GCs, las cuales se integran en la circuitería hipocampal. Tras varias rondas de división, las NSCs se diferencian en astrocitos y salen de la reserva de células madre, a partir de lo cual son incapaces de generar más precursores neuronales. Este agotamiento acoplado a la activación es un mecanismo que contribuye al decremento de la neurogénesis con la edad, lo que hace más necesario el conocimiento acerca de la regulación de la activación de las NSCs.

En parte debido a este paulatino agotamiento de las NSCs acoplado a su activación, el estudio de la multipotencia y de las propiedades de la división de estas células madre se ha centrado en las condiciones en las que las NSCs son activadas y en la posibilidad de su regreso a la quiescencia. Se ha descrito que las vías de señalización de los Wnts y de las proteínas morfogenéticas de hueso (*bone morphogenetic proteins*, BMPs) y la proteína proactivadora Ascl1, entre otros, están implicadas en el mantenimiento de su quiescencia, pero los datos sugieren cada vez más que cuando las NSCs se activan su vuelta a la quiescencia a largo plazo es improbable. Por tanto, los estímulos que inducen su activación favorecerían en último término su agotamiento.

En la complicada regulación que gobierna la neurogénesis y la dinámica de división de las NSCs, se ha demostrado que la actividad neuronal excitadora promueve la activación de las NSCs, mientras que la inhibidora mantiene su quiescencia. Apoyando esta idea, se ha observado que modelos animales y alteraciones cerebrales que incrementan la actividad eléctrica en el hipocampo alteran la AHN y el reclutamiento de las NSCs. En la misma línea, en el tipo más frecuente de epilepsia, la epilepsia del lóbulo temporal mesial (*mesial temporal lobe epilepsy*, MTLE), se ha observado neurogénesis aberrante y una disminución a largo plazo de la AHN. Además, en

modelos experimentales de este trastorno neurológico se ha documentado la acumulación de astrocitos de nueva formación. En situaciones patológicas como esta, los astrocitos a menudo se transforman en astrocitos reactivos (*reactive astrocytes*, RAs), un tipo celular glial que se cree implicado en el desequilibrio eléctrico y las convulsiones recurrentes que constituyen un rasgo de la MTLE.

Teniendo en cuenta el agotamiento progresivo de las NSCs acoplado a su división, propusimos que **la activación de las NSCs es un evento único que conduce inevitablemente a su agotamiento y que el regreso a la quiescencia tras la activación inicial, así como la autorrenovación, son insignificantes a nivel poblacional**. Para poner a prueba esta hipótesis, nuestro **Objetivo 1** fue **evaluar la dinámica de división frente a la quiescencia en el nicho neurogénico del hipocampo**. Con este propósito, sometimos a ratones Nestin-GFP, en los que las NSCs y los ANPs del DG pueden ser fácilmente visualizados, a la administración continua del análogo de la timidina bromodesoxiuridina (BrdU) en el agua de bebida para marcar todas las células en división y realizamos análisis de imagen cuantitativo basado en la microscopía confocal tras la tinción inmunohistoquímica de marcadores celulares específicos. En un primer análisis de la proliferación, confirmamos la contribución predominante de los ANPs a las células en división del DG seguida de una baja proporción de NSCs. En dos análisis de diferenciación distintos, tanto administrando BrdU durante una semana como un mes, encontramos una mayoría de neuronas y la generación de algunos astrocitos entre las células procedentes de división. Debido a la escasa capacidad mitótica mostrada por los astrocitos en el análisis de proliferación, concluimos que los astrocitos de nueva formación observados a largo plazo eran aquellos derivados de la diferenciación de las NSCs.

De forma destacable, las NSCs y ANPs marcados con BrdU fueron casi inexistentes en los análisis de diferenciación a largo plazo. Además, la reentrada al ciclo celular de las NSCs fue muy alta a corto plazo pero no se encontró ningún caso a largo plazo, revelando que en efecto la activación de las NSCs lleva a su agotamiento como células madre y que la vuelta a la quiescencia es un evento extremadamente infrecuente.

En conjunto, estos resultados sugirieron que la cascada neurogénica en el DG sigue los mismos principios que se han propuesto a nivel poblacional sin importar la aproximación, habiendo obtenido resultados similares a los descritos en estudios que emplearon pulsos concretos de BrdU. En primer lugar, en un momento dado pocas NSCs se están dividiendo pero, cuando lo hacen, vuelven a entrar en el ciclo celular de forma consecutiva, encontrándose el 75% de ellas en división una semana después de la activación inicial. Nuestros resultados concuerdan con la esperada mayoría de divisiones asimétricas de las NSCs debido al decremento en la contribución de las NSCs a las células marcadas con BrdU que encontramos en ambos análisis de diferenciación. La mayor parte de las divisiones en el DG originan a progenitores neuronales que en último término dan lugar a neuronas, pero también se generan astrocitos. Dado que los astrocitos manifestaron una capacidad proliferativa muy limitada, los astrocitos de nueva formación fueron muy probablemente generados mediante diferenciación

terminal de las NSCs dado que los ANPs generan solo neuronas. Esta diferenciación es un proceso largo en el que se podría pensar que las pocas NSCs $BrdU^+$ que quedan se encuentran en un estado quiescente tras la activación inicial, pero no se ha documentado nunca una nueva activación durante este periodo de tiempo, mientras que la conversión astrocítica final sí ha sido demostrada.

A continuación, hipotetizamos que los **estímulos que favorecen la entrada en el ciclo celular de las NSCs como la hiperactividad neuronal acelerarían su agotamiento o incluso provocarían un cambio en sus propiedades y alterarían el progreso correcto de la cascada neurogénica**. Nuestro **Objetivo 2** derivado de esta hipótesis fue **estudiar la respuesta a niveles diferentes de hiperexcitación neuronal del nicho neurogénico y específicamente de las NSCs**. Con este objetivo, inyectamos dos dosis diferentes de ácido kaínico (*kainic acid*, KA, un agonista del glutamato) directamente en el DG de ratones Nestin-GFP para inducir actividad epileptiforme (*epileptiform activity*, EA, descargas que no llegan a generar convulsiones) y MTLE (donde sí se dan convulsiones epilépticas), respectivamente, y marcamos las células en división con BrdU antes de analizar el nicho neurogénico mediante la tinción inmunohistoquímica para marcadores celulares. Encontramos un incremento en la proliferación celular y en la activación de las NSCs en ambos modelos de hiperactividad neuronal pero además un cambio cualitativo en la cascada neurogénica solo en ratones MTLE: mientras que la EA se asemejaba a una versión acelerada de la producción neurogénica normal derivada de la división asimétrica, en la MTLE la división de los ANPs disminuyó y las NSCs adquirieron una morfología reactiva (React-NSCs).

Por consiguiente, caracterizamos el tipo de división celular de las NSCs en la MTLE, para lo cual aprovechamos la línea transgénica Nestin-$CreER^{T2}$/R26R:YFP para rastrear inequívocamente y de manera inducible a las NSCs y su progenie. En ratones inyectados con salino (Sal) la división asimétrica (NSC+ANP) suponía la mayoría de las divisiones de las NSCs; sin embargo, en la MTLE las React-NSCs se dividían simétricamente dando lugar a más React-NSCs. Interesados en esta característica, estudiamos entonces la diferenciación de las células YFP^+ en estos animales y descubrimos una nueva propiedad de las células madre: las React-NSCs se diferencian en RAs en la MTLE. Esta observación nos ayudó a reafirmar la teoría de que en el DG epiléptico se ve favorecida la astrogliogénesis en el nicho que normalmente es neurogénico, apoyando la idea de que las NSCs mismas pueden contribuir a la astrogliosis reactiva que es parte de la MTLE con esclerosis hipocampal.

Para descartar la posibilidad de que esta activación masiva de las NSCs y el cambio fenotípico de las NSCs a React-NSCs fueran atribuibles únicamente a la inflamación que produce el modelo de MTLE en el DG, inyectamos lipopolisacárico (LPS) intrahipocampalmente a ratones Nestin-GFP. El marcaje con BrdU reveló la ausencia de inducción de la proliferación celular y de la activación de las NSCs en ratones inyectados con LPS, por lo que concluimos que nuestras observaciones previas habían sido debidas a la hiperexcitación y las convulsiones.

Con estos resultados probamos que niveles diferentes de hiperexcitación neuronal disparan respuestas diferentes en las NSCs. Cuando el nivel de esta hiperexcitación es suficientemente alto para disparar convulsiones, las NSCs cambian completamente su programa de ciclo celular prácticamente aboliendo el destino neurogénico en favor de la astrogliogénesis reactiva. Tanto las NSCs como sus células hijas dejan de producir progenitores de destino neuronal sino que en lugar de eso se convierten en React-NSCs que se diferenciarán terminalmente en RAs. Se ha descrito que los RAs empeoran el desequilibrio eléctrico y son parcialmente responsables de las convulsiones espontáneas, por lo que la diferenciación de las React-NSCs podría contribuir a estas alteraciones y a la formación de la cicatriz glial que es parte de la esclerosis hipocampal, un rasgo distintivo de la mayoría de casos de MTLE.

A continuación nos interesamos en caracterizar estas React-NSCs y RAs derivados de React-NSCs, para lo cual necesitábamos una herramienta mejor que las líneas basadas en la expresión de nestina ya que los RAs, incluso los derivados de astrocitos parenquimales, expresan nestina y por esa razón aquellos RAs derivados de React-NSCs serían indistinguibles utilizando dicho marcador. Basándonos en la información disponible acerca del marcador de NSCs receptor 1 del ácido lisofosfatídico (*lysophosphatidic acid receptor 1*, LPA_1), hipotetizamos que **la expresión de LPA_1, y de LPA_1-GFP en un ratón transgénico, podría ser una herramienta única para identificar y analizar las NSCs mientras se convierten en React-NSCs** y que **LPA_1 podría tener un papel en la función de las NSCs**. Por tanto, nuestro **Objetivo 3** fue **validar el ratón transgénico LPA_1-GFP como herramienta para estudiar las React-NSCs**. Primeramente validamos mediante inmunotinción que el transgén se expresaba principalmente en NSCs y verificamos que la expresión del receptor LPA_1 podía ser observada en estas NSCs LPA_1-GFP^+.

A continuación, caracterizamos los efectos del tratamiento de MTLE en el nicho neurogénico de los ratones LPA_1-GFP. Realizamos un curso temporal sometiendo a los animales al mismo modelo de MTLE que en el objetivo anterior, inyectamos BrdU 2d después y sacrificamos a los animales en seis puntos temporales diferentes para llevar a cabo tinción inmunohistoquímica y análisis cuantitativo de imagen basado en la microscopía confocal. Al cuantificar las proporciones relativas de los tipos celulares marcados con BrdU en el DG, confirmamos el destino neurogénico predominante en los ratones Sal y el cambio completo hacia astrogliogénesis reactiva en los MTLE. También observamos que la expresión de LPA_1-GFP se mantenía en las React-NSCs mientras se activaban masivamente y perdían su morfología radial inicial en favor de una morfología multipolar típica de los RAs.

Por lo tanto, rastreamos la expresión de LPA_1-GFP a lo largo del tiempo en las React-NSCs y otros tipos celulares del nicho. Acerca de las primeras, seguimos su transformación en RAs empleando la expresión de S100β como indicador de maduración astroglial y observamos una clara tendencia al aumento en la proporción de células LPA_1-GFP^+ que colocalizaban S100β, sugiriendo considerablemente la diferenciación terminal en RAs. Además, cuando restamos la proporción de esta

población LPA_1-GFP^+ diferenciada de la población glial LPA_1-GFP^+ encontramos en animales MTLE una disminución significativa a lo largo del tiempo en la contribución de las React-NSCs no diferenciadas. Estos resultados fueron en la misma línea que aquellos obtenidos en ratones transgénicos Nestin-$CreER^{T2}$/R26R:YFP en los cuales la mayoría de células derivadas de React-NSCs se terminaban convirtiendo en RAs maduros.

Una nueva característica que descubrimos en estos ratones LPA_1-GFP fue la expresión *de novo* del transgén en neuronas de la GCL en animales MTLE varias semanas después de la inducción de MTLE. Dado que solo apareció en este grupo, aislamos los datos de los ratones MTLE y encontramos un aumento significativo en la proporción de neuronas que expresaban LPA_1-GFP a lo largo del tiempo. Esta es una peculiaridad para la cual las interpretaciones con complicadas debido a la escasez de trabajos previos, pero que podría ser debida a la respuesta a la neurotoxicidad inducida por la hiperexcitación neuronal y las convulsiones en el hipocampo.

Continuamos investigando la utilidad del ratón LPA_1-GFP para el análisis ultraestructural de las NSCs y React-NSCs. Con este propósito, realizamos inmunohistoquímica preinclusión contra GFP para microscopía electrónica de transmisión (*transmission electron microscopy*, TEM) y observamos el marcaje en el DG de ratones Sham y MTLE. Confirmamos la expresión específica del transgén en las NSCs y React-NSCs de la SGZ y su ausencia en astrocitos o RAs de áreas adyacentes. Recurriendo a esta aproximación para buscar diferencias ultraestructurales entre NSCs y React-NSCs observamos un incremento no significativo en el número de mitocondrias en las últimas. A pesar de que este aumento en el número de mitocondrias ha sido observado en RAs en otras condiciones patológicas, no observamos esta característica en los RAs en MTLE al compararlos con los astrocitos de las condiciones normales. Esto sugiere que, si este incremento en las React-NSCs es consistente, podría no ser debido a su fenotipo reactivo sino a la inducción masiva de su entrada en el ciclo celular.

A continuación nos preguntamos la implicación de LPA_1 en la activación de las NSCs y en su adquisición del fenotipo de React-NSCs en la MTLE. Para este objetivo, sometimos a ratones *knockout* del receptor, llamados $maLPA_1$, y a sus *wild-type* (WT) al tratamiento de MTLE e inyectamos BrdU 2d después para analizar la proliferación y la activación de las NSCs a los 3d y dos semanas. Encontramos un decremento en el segundo punto temporal en el número total de células $BrdU^+$ en el DG de los ratones $maLPA_1$ en comparación con los WT. Recurriendo a la tinción de nestina y otros marcadores celulares y a criterios morfológicos, evaluamos la activación y el fenotipo de las NSCs y encontramos también un decremento, tanto a 3d como a 2 semanas, en la proporción de React-NSCs activadas o derivadas de división en los animales $maLPA_1$. No observamos diferencias obvias en la morfología de las React-NSCs entre ratones WT y $maLPA_1$, por lo que concluimos que la expresión de LPA_1 está implicada en la proliferación celular y la activación de las NSCs en el DG epiléptico pero no parece afectar a la transformación de las NSCs en React-NSCs y más tarde en RAs.

Estos datos apoyan la noción de que las convulsiones provocan un cambio en el destino de la división de las NSCs hacia la generación de RAs. Además, el marcador LPA_1-GFP marca específicamente a las React-NSCs en su transformación en RAs y la expresión del transgén se mantiene incluso en una subpoblación de estos RAs derivados de React-NSCs. La diferencia funcional atribuible a esta expresión duradera debe aún ser estudiada, pero los resultados que obtuvimos acerca de la función de LPA_1 en la activación masiva de las NSCs tras el tratamiento MTLE sugiere que este receptor está implicado en la fracción de la gliosis que podría ser debida a la expansión inicial de las React-NSCs.

Por último, nos interesamos en analizar si los efectos en el nicho neurogénico de nuestro modelo de MTLE eran debidos a la hiperexcitación neuronal sola o a su combinación con otros efectos provocados por la administración local de KA. Hipotetizamos que **independientemente del modelo de inducción de MTLE las NSCs y el nicho neurogénico se verían afectados de manera similar**. Por tanto, nuestro **Objetivo 4 fue establecer un modelo alternativo de MTLE mediante la inyección intraamigdalar de KA**. Para conseguir este objetivo, optimizamos un protocolo para realizar consistentemente la inyección en la amígdala evitando la difusión potencial del KA al hipocampo.

Administramos BrdU 2d después de someter a ratones Nestin-GFP al modelo intraamigdalar de MTLE (MTLE-a) y sacrificamos a los animales una semana después para examinar el aspecto general del DG mediante análisis cuantitativo de imagen basado en la microscopía confocal. Al cuantificar el número total de células $BrdU^+$, obtuvimos un incremento significativo en los ratones MTLE-a en comparación con los inyectados con salino (Sal-a). Nos centramos en la división de las NSCs y también observamos un incremento en la proporción de NSCs activadas en los animales MTLE-a, en parte reproduciendo los resultados que habíamos obtenido con el modelo de MTLE intrahipocampal. Además, las NSCs muestran el fenotipo reactivo típico de las React-NSCs inducidas por MTLE. Por último, observamos astrocitos en división, aunque en números bajos, solo en ratones MTLE-a, sugiriendo que este tipo celular puede ser también afectado por la hiperexcitación neuronal provocada inicialmente en la amígdala.

Estos datos sugieren que las convulsiones inducidas en la amígdala son suficientes para provocar cambios en el DG en las mismas líneas que aquellos producidos en el modelo directo de inducción de MTLE. La MTLE-a aumenta la activación de las NSCs, tal y como ocurre en el modelo intrahipocampal de MTLE, y promueve la división astrocítica en el DG. Este modelo de MTLE es también útil porque nos permite desarrollar manipulaciones en el DG para estudiar las NSCs y el nicho neurogénico, como las inyecciones de vectores retro- o adenovirales o la inserción de electrodos que serían incompatibles con la inyección en el DG.

En conclusión, nuestros resultados prueban que, a nivel poblacional, cuando las NSCs se activan se dividen varias veces dando lugar a precursores neuronales y no vuelven a

la quiescencia tras ello. Si se favorece su activación mediante hiperexcitación neuronal suave (EA), se acelera la cascada neurogénica. Si esta actividad neuronal es lo suficientemente alta para provocar convulsiones (MTLE), sin embargo, cambian su fenotipo a la morfología de React-NSCs y salen del programa neurogénico. Las React-NSCs en expansión, en su lugar, se diferencian en RAs. Durante este proceso el marcador de NSCs LPA_1-GFP todavía se expresa en las React-NSCs y sirve como herramienta para rastrearlas y caracterizarlas ultraestructuralmente. Finalmente, el modelo de MTLE-a confirmó que más importante que el lugar epileptogénico, siempre que esté conectado con el hipocampo, es el nivel de hiperactividad neuronal que se dispara finalmente en el DG, y que puede ser capaz de manipular el destino de las NSCs hipocampales y alterar el nicho neurogénico.

3.2. Summary

Adult neurogenesis, the process of formation of new neurons in the adult brain, is preserved in two brain regions: the subventricular zone (SVZ) of the lateral ventricles, which generates interneurons destined to the olfactory bulb; and the subgranular zone (SGZ) of the dentate gyrus (DG), which generates granule cells (GCs) that are integrated into the hippocampal circuitry. Neurogenesis in the latter, called adult hippocampal neurogenesis (AHN), is involved in functions such as learning, spatial memory acquisition, fear conditioning, anxiety and responses to stress.

AHN exists thanks to a population of neural stem cells (NSCs) that remains in the SGZ of the DG. These NSCs are mainly quiescent, but when they are activated they most often divide asymmetrically giving rise to amplifying neural progenitors (ANPs) that, in turn, proliferate and originate the neuroblasts (NBs) that maturate and give rise to GCs, which integrate into the hippocampal circuitry. After several rounds of cell division, NSCs differentiate into astrocytes and exit the stem cell pool, being unable to generate more neuronal precursors. This activation-coupled NSC depletion is a mechanism that contributes to the age-related decline in neurogenesis, which makes more necessary the knowledge of NSC-activation regulation.

Partly due to the division-coupled NSC progressive exhaustion, the study of NSC multipotency and cell division properties has focused on the conditions in which NSCs become activated and the possibility of their return to quiescence. Wnts, BMPs and the proactivation protein Ascl1, among others, have been reported to be involved in their maintenance of quiescence, but data increasingly suggest that when NSCs are activated their return to quiescence in the long term is improbable. Thus, stimuli that induce their activation would ultimately favor their depletion.

In the complicated regulation that rules neurogenesis and the dynamics of NSC division, it has been reported that excitatory neuronal activity promotes NSC activation, whereas the inhibitory maintains their quiescence. Supporting this idea, models and brain alterations that increase electrical activity in the hippocampus have been shown to alter AHN and NSC recruitment. Along the same lines, in the most frequent type of epilepsy,

mesial temporal lobe epilepsy (MTLE), aberrant neurogenesis and a long-term decline in AHN have been observed. Moreover, in models of this neurological disorder an accumulation of newly-born astrocytes has been documented. In these pathological situations, astrocytes often transform into reactive astrocytes (RAs), a glial cell type that is thought to contribute to the electrical imbalance and the recurrent seizures that constitute a hallmark of MTLE.

Taking into account the division-coupled NSC progressive exhaustion, we proposed that **NSC activation is a single event that inevitably leads to their exhaustion, and that return to quiescence after initial activation and self-renewal are negligible at the population level**. To test this hypothesis, our **Objective 1** was **to evaluate division versus quiescence dynamics in the hippocampal neurogenic niche**. For this purpose, we subjected Nestin-GFP mice, in which NSCs and ANPs in the DG can be readily visualized, to the continuous administration of the thymidine analog bromodeoxyuridine (BrdU) in drinking water to label every dividing cell and performed confocal-based quantitative image analysis following immunohistochemical staining of specific cell markers. In a first proliferation analysis, we confirmed the predominant contribution of ANPs to dividing cells in the DG followed by low proportions of NSCs. In two different differentiation analyses, administering BrdU for either 1w or 1m, we reported a majority of neurons among division-derived cells and the generation of new astrocytes. Due to the uncommon mitotic capacity shown by astrocytes in the proliferation analysis, we concluded that newborn astrocytes observed in the long term were those derived from NSC differentiation.

Remarkably, BrdU-labeled NSCs and ANPs were almost absent in the long-term differentiation analyses. In addition, NSC reentry into the cell cycle was very high in the short term but inexistent in the long term, revealing that indeed NSC activation leads to their depletion as stem cells and that NSC return to quiescence is an extremely infrequent event.

Together, these results strongly suggested that the neurogenic cascade in the DG follow the same principles that have been proposed at the population level no matter the approach, obtaining similar results to those reported in studies that employed discrete pulses of BrdU. First, in a given moment few NSCs are dividing but, when they do, they reenter the cell cycle in a consecutive manner, being the 75% of them in division one week after the initial activation. Our results agree with the expected majority of NSC asymmetric divisions due to the decrease in the NSC contribution to BrdU-labeled cells that we report in both differentiation analyses. Most divisions in the DG render neuronal progenitors that ultimately give rise to neurons, but astrocytes are generated too. Since astrocytes showed a very limited proliferative capacity, newborn astrocytes were most probably generated through NSC terminal differentiation since ANPs only generate neurons. This differentiation is a long process in which the few remaining $BrdU^+$ NSCs could be thought to be in a quiescent state after initial activation, but a new activation during this period of time has never been reported whereas ultimate astrocytic conversion indeed has been documented.

We then hypothesized that **stimuli that promote NSC entry into the cell cycle such as neuronal hyperactivity would accelerate their depletion or even provoke a shift in their properties and disrupt the correct progress of the neurogenic cascade**. Our hypothesis-driven **Objective 2** was thus **to study the response to different levels of neuronal hyperexcitation of the neurogenic niche and specifically of NSCs**. With this aim, we injected two different doses of kainic acid (KA, a glutamate agonist) directly into the DG of Nestin-GFP mice to induce epileptiform activity (EA, discharges that do not generate seizures) and MTLE (in which seizures are indeed generated), respectively, and labeled proliferating cells with BrdU before analyzing the neurogenic niche following immunohistochemical staining of cell markers. We found increased cell proliferation and NSC activation in both models of neuronal hyperactivity but a qualitative change in the neurogenic cascade only in MTLE mice: whereas EA seemed an accelerated version of the normal asymmetric cell division-derived neurogenic output, in MTLE ANP division was decreased and NSCs acquired a reactive-like morphology (React-NSCs).

We therefore characterized the division type of NSCs in MTLE, for what we took advantage of inducible Nestin-CreER^{T2}/R26R:YFP transgenic mice to unequivocally trace NSCs and their progeny. In saline-injected (Sal) mice the asymmetric division (NSC+ANP) accounted for most observed NSCs; meanwhile, in MTLE React-NSCs divided symmetrically giving rise to more React-NSCs. Interested in this feature, we then studied the differentiation of YFP^{+} cells in these animals and discovered a new property of stem cells: React-NSCs differentiate into RAs in MTLE. This observation helped us rejoin the theory that proposed that astrogliosis is favored in the otherwise neurogenic niche of the epileptic DG, supporting the idea that NSCs themselves can contribute to the reactive astrogliosis that is part of MTLE with hippocampal sclerosis.

To rule out the possibility of this massive NSC activation and NSC-to-React-NSC phenotypical change being attributable to the inflammation the MTLE model produces in the DG, we injected lipopolysaccharide (LPS) intrahippocampally to Nestin-GFP mice. BrdU labeling revealed the absence of induction of cell proliferation and NSC activation in LPS-injected mice, so we concluded that our previous observations had been due to neuronal hyperexcitation and seizures.

With these results we proved that different levels of neuronal hyperexcitation trigger different responses from NSCs. When the level of this hyperexcitation is high enough to trigger seizures, NSCs completely change their cell-cycle program almost abolishing the neurogenic fate in favor of reactive astrogliogenesis. Both NSCs and their daughter cells no longer produce neuronal fate-committed precursors but instead become React-NSCs that will later differentiate into RAs. RAs have been reported to impair the electrical imbalance and be partially responsible of spontaneous seizures, thus React-NSC differentiation could contribute to these features and to the formation of the glial scar that is part of hippocampal sclerosis, a hallmark of most cases of MTLE.

We then became increasingly interested in characterizing these React-NSCs and React-NSC-derived RAs, for what we were in need of a better tool than nestin-based lines as every RA, even parenchymal astrocyte-derived ones, express nestin and for this reason those RAs derived from React-NSCs would be undistinguishable using that marker. Based on the information available on the NSC marker lysophosphatidic acid receptor 1 (LPA_1), we hypothesized that **expression of LPA_1, and LPA_1-GFP in a transgenic mouse line, could be a unique tool to identify and analyze NSCs as they convert into React-NSCs** and that **LPA_1 might play a role in NSC function**. Thus, our **Objective 3** was **to validate LPA_1-GFP transgenic mouse as a tool to study React-NSCs**. We firstly validated by immunolabeling that the transgene was mostly expressed in NSCs and verified that the expression of the receptor LPA_1 could be observed in these LPA_1-GFP^+ NSCs.

Next, we characterized the effects of MTLE treatment in the neurogenic niche of LPA_1-GFP mice. We performed a time course subjecting the animals to the same MTLE model as in the previous objective, injecting BrdU 2d later and sacrificing the animals at six different time points for immunohistochemical staining and confocal microscopy-based quantitative image analysis. By quantifying the relative proportions of cell types labeled with BrdU in the DG, we confirmed the predominant neurogenic fate in Sal mice and the complete shift to reactive astrogliogenesis in MTLE. We also observed that the LPA_1-GFP expression was maintained in React-NSCs as they became massively activated and lost their initial radial morphology in favor of a multipolar RA-like morphology.

Hence, we traced the expression of LPA_1-GFP over time in React-NSCs and other cell types in the niche. Regarding the first, we followed their transformation into RAs employing S100β expression as an indicator of astroglial maturation and observed a clear increasing trend in the proportion of LPA_1-GFP^+ cells that colocalized S100β, strongly suggesting a terminal differentiation into RAs. Furthermore, when subtracting the proportion of this differentiated LPA_1-GFP^+ population from the LPA_1-GFP^+ glial population we found in MTLE animals a significant decrease over time in the contribution of non-differentiated React-NSCs. These results were along the same lines as those from Nestin-$CreER^{T2}$/R26R:YFP transgenic mice in which most cells derived from React-NSCs ended up converting into mature RAs.

A novel feature we discovered in these LPA_1-GFP mice was the *de novo* expression of the transgene in neurons of the GCL in MTLE animals several weeks after MTLE induction. As it only appeared in this group, we isolated the data from MTLE mice and found a significant increase in the proportion of LPA_1-GFP-expressing neurons over time. This is a peculiarity for which interpretations are complicated due to the lack of previous works, but that could be due to the response to the neurotoxicity induced by neuronal hyperexcitation and seizures in the hippocampus.

We further investigated the usefulness of LPA_1-GFP transgenic mouse for the ultrastructural analysis of NSCs and React-NSCs. For this purpose, we performed pre-

embedding GFP immunohistochemistry for transmission electron microscopy (TEM) and observed the labeling in the DG of Sham and MTLE mice. We confirmed the specific expression of the transgene in NSCs and React-NSCs of the SGZ and its absence in astrocytes or RAs of adjacent areas. Moreover, taking advantage of this approach to search for ultrastructural differences between NSCs and React-NSCs we observed a non-significant increase in the number of mitochondria in the latter. Despite this rise in the number of mitochondria has been reported in RAs in other pathological conditions, we did not observe this characteristic in RAs in MTLE compared to astrocytes in normal conditions. This suggests that, if this increase in React-NSCs is consistent, it could be not due to their reactive phenotype but possibly to the massive induction of their entry into the cell cycle.

We next wondered the involvement of LPA_1 in the NSC activation and acquisition of the React-NSC phenotype in MTLE. Towards this aim, we subjected knockout mice of the receptor, called $maLPA_1$, and their wild-type (WT) counterparts to MTLE treatment and injected BrdU 2d later to analyze proliferation and NSC activation at 3d and 2w time points. We found a decrease in the second time point in the total number of $BrdU^+$ cells in the DG of $maLPA_1$ compared to WT mice. Resorting to nestin and other cell marker staining and morphological criteria, we evaluated NSC activation and phenotype and also found a decrease, at both 3d and 2w, in the proportion of activated or division-derived React-NSCs in $maLPA_1$ animals. We did not observe obvious differences in React-NSC morphology between WT and $maLPA_1$ mice, thus we concluded that LPA_1 expression is involved in cell proliferation and NSC activation in the epileptic DG but does not seem to affect NSC transformation into React-NSCs and later RAs.

These data strongly support the notion that seizures trigger a change in the fate of NSC divisions towards the generation of RAs. Furthermore, the NSC marker LPA_1-GFP specifically labels React-NSCs as they transform into RAs and the transgene expression is even maintained in a subpopulation of these React-NSC-derived RAs. The functional difference attributable to this long-lasting expression remains to be studied, but the results we obtained regarding the function of LPA_1 in the massive NSC activation after MTLE treatment suggest that this receptor is involved in the fraction of gliosis that could be due to the initial expansion of React-NSCs.

We were lastly interested in assessing whether the effects in the neurogenic niche of our MTLE model were due to neuronal hyperexcitation alone or its combination with other effects provoked by local KA administration. We hypothesized that **regardless of the model of induction of MTLE NSCs and the neurogenic niche would be affected in a similar manner**. Therefore, our **Objective 4** was **to establish an alternative model of MTLE by intraamigdalar injection of KA**. To accomplish this objective, we optimized a protocol to consistently perform the injection into the amygdala avoiding potential diffusion of KA to the hippocampus.

We administered BrdU 2d after subjecting Nestin-GFP mice to the intraamigdalar MTLE model (MTLE-a) and sacrificed the animals at 1w to examine the general

appearance and the cell proliferation in the DG via confocal microscopy-based quantitative image analysis. When we quantified the total $BrdU^+$ cells, we obtained a significant increase in MTLE-a mice compared to the saline-injected (Sal-a) ones. We focused on NSC division and also observed an increase in the proportion of activated NSCs in MTLE-a animals, partially reproducing the results we had obtained with the intrahippocampal MTLE model. In addition, NSCs seemed to be acquiring the reactive-like morphology that is typical of MTLE-induced React-NSCs. Lastly, dividing astrocytes, although in low numbers, were only observed in MTLE-a mice, suggesting that this cell type can also be affected by the neuronal hyperexcitation initially provoked in the amygdala.

These data suggest that seizures induced in the amygdala are enough to trigger changes in the DG along the same lines as those produced in the direct model of MTLE induction. MTLE-a increases NSC activation, just like occurs in the intrahippocampal MTLE model, and promotes astrocytic division in the DG. This model of MTLE is also useful because it allows us to develop manipulations in the DG to study NSCs and the neurogenic niche, such as retro- or adenoviral vector injections or electrode insertion that would be incompatible with the injection into the DG.

In conclusion, our results prove that, at the population level, when NSCs are activated they divide several times giving rise to neuronal precursors and do not return to quiescence after that. If their activation is favored by mild neuronal hyperexcitation (EA), the neurogenic cascade is accelerated. If this neuronal activity is high enough to trigger seizures (MTLE), however, they change their phenotype to the React-NSC morphology and exit the neurogenic program. The expanding React-NSCs, instead, differentiate into RAs. During this process the NSC marker LPA_1-GFP is still expressed in React-NSCs and serves as a tool to trace and ultrastructurally characterize them. Finally, the MTLE-a model confirmed that more important than the epileptogenic site, provided that it is connected to the hippocampus, is the level of neuronal hyperactivity which is ultimately triggered in the DG, and which can be able to manipulate the fate of the hippocampal NSCs and disrupt the neurogenic niche.

3.3. Acknowledgments

Roberto Valcárcel Martín has been a holder of a Basque Government predoctoral fellowship.

This project has been directly funded by the following **grants**:

- Plan Nacional de Investigación Fundamental No Orientada (National Plan for Basic Research) 2012. **Ref.#** SAF-2015-70866-R**. Project title:** Mechanisms and Blockage of the induction of Reactive Neural Stem Cells in the Epileptic Hippocampus. **Financing institution:** Spanish Ministry of Economy and Competitiveness. **Duration:** 4 years, 2016-2019. **Amount:** 275.880€. (50% FEDER).

- Ramón y Cajal Program. **Ref.#** RYC-2012-11137. **Project title:** Neural stem cells, and neurogenesis in Aging and Epilepsy. **Financing institution:** Spanish

Ministry of Economy and Competitiveness. **Institution:** Achucarro Basque Center for Neuroscience Fundazioa. **Duration:** 5 years **2014-2019**.

- Plan Nacional de Investigación Fundamental No Orientada (National Plan for Basic Research) 2012. **Ref.#** SAF2012-40085**. Project title:** Exhaustion of Neural Stem Cells and Neurogenesis by Neuronal Hyperexcitation in the adult Hippocampus. **Financing institution:** Spanish Ministry of Economy and Competitiveness. **Duration:** 3 years, **2013-2015**. **Amount:** 117.000€.

- SAIOTEK 2012. **Ref.#** S-PC12UN014. **Project title:** Mechanisms of the induction of Reactive neural stem cells in mesial temporal lobe epilepsy mouse model. **Financing institution:** Basque Government. **Duration:** 2 years, **2012-2013**. **Amount:** 50.417,25 €.

- III Convocatoria de Ayudas a la Investigación. **Ref.#** N/A. **Project title:** Impacto de la Neuroinflamación y la Gliosis en las Sinapsis y Circuitos Cerebrales en un Modelo del Síndrome de Dravet. **Financing institution:** Federación Española de Enfermedades Raras. **Institution:** Achucarro Basque Center for Neuroscience Fundazioa. **Duration:** 1 years, 2018-2019. **Amount:** 10.000€ (100%).

The following **publications** are directly derived from the candidate's work on this project:

Valcárcel-Martín R, Pastor-Alonso O, Martín-Suárez S, Chun J, Rodríguez de Fonseca F, Estivill-Torrús G, Encinas JM. LPA_1 labels and regulates the transformation of neural stem cells into reactive neural stem cells after seizures. In preparation.

4. Introduction

4. Introduction

4.1. Adult neurogenesis

Discovery, extent and controversy

The common certainty that, once embryonic development is complete, neuronal generation and integration in the brain is abolished has been a dogma during an important part of the history of neuroscience. This strong belief was supported by pioneers such as the discoverer of the neuron doctrine, Santiago Ramón y Cajal, who affirmed: "In the adult centers, the nerve paths are something fixed, ended, and immutable. Everything may die, nothing may be regenerated. It is for the science of the future to change, if possible, this harsh decree." (Ramón y Cajal, 1928). An increasing number of studies and the development of new techniques helped the field understand that this idea about impossibility of regeneration might be not so immutable.

When the dogma of "no new neurons in adulthood" was a hundred years old, evidence of newborn neurons could mean a challenge and be responded with fierce opposition. The term referring to this putative generation of new neurons in the adult brain is adult neurogenesis, a process that most often involves division steps by neural stem cells (NSCs) and other progenitors and maturation steps from the neuroblast (NB) stage to the fully integrated neuron.

The first evidence of adult neurogenesis was described by Joseph Altman. Employing [^{3}H]-thymidine autoradiography studies, he showed newborn neurons being formed postnatally in the rat dentate gyrus (DG) of the hippocampus (Altman and Das, 1965). A few years later, the same laboratory discovered persistent neurogenesis in the subependymal layer of the lateral ventricles, which would later be named the subventricular zone (SVZ), from where most newly-formed cells migrated via rostral migratory stream (RMS) to the olfactory bulb (OB) (Altman, 1969). Interestingly, they also showed postnatal neurogenesis in the Guinea pig, a precocial rodent in which younglings are born with more mature brains than those of rats and mice (Altman and Das, 1967). These results proved that neurogenesis was not only restricted to rodents with considerable brain growth after birth.

However, Altman's work was long time discredited and marginalized despite his data were not empirically refuted. Reference to his published evidence was omitted by textbooks and original publications and his group lost all its public funding in the mid-1980s, a sad reflection of what a group of influential scientists can do to bring down opposing evidence to a dogma (Altman, 2011). In the late 1970s, supporting evidence was found by Michael Kaplan. He added electron microscopic to the existing autoradiographic experiments and showed that indeed the radioactively labeled, newborn hippocampal and olfactory bulb GCs had axons, dendrites and synapses and

thus were neurons (Kaplan and Hinds, 1977). In spite of these efforts, the idea of adult neurogenesis remained marginal for years.

In the 1980s, Fernando Nottebohm and colleagues collected new evidence in favor of adult neurogenesis in vertebrates revealing the addition of new neurons in the song-controlling high vocal center of the forebrain in adult canaries (Goldman and Nottebohm, 1983; Paton and Nottebohm, 1984). This helped Altman introduce the hypothesis that postnatal experience could sculpt the fine wiring of circuits in the brain, an attractive but controversial idea. The requirement of adult-born neurons for mastering new skills, for example, does not explain neither why adult neurogenesis is much more common in birds than in mammals nor why some brain systems use "replaceable" neurons whereas others do not. Moreover, it would establish neurons, and not only synapses, as another mode of learning unit. These interesting questions still require empirically challenging work to be solved (Nottebohm, 2011).

In the same decade as the data provided by Nottebohm, Kaplan again gave insight into neurogenesis in adult rats, this time showing that newly-formed GCs were a result of NB division and that this process lasted at least during the first 11 months of a rat's life (Kaplan and Bell, 1984). These findings in rodents still contradicted previous observations such as Angevine's, who affirmed neurogenesis in the mouse DG ended by postnatal day 20 (Angevine, 1965); and the general dogma of "no-new-neurons in the adult brain". In an influential study, Pasko Rakic, although admitting the generation of neurons in some postnatal nonprimates, failed to find any "heavily" radiolabeled neurons in rhesus monkeys ranging from 6 months to 11 years of age (Rakic, 1985). He argued that the large mature brain of primates may not permit redistribution of new neurons, lacking this capacity to specialize in a more stable network of neurons. This piece of evidence made the concept of adult neurogenesis seem distant in species evolutionarily closer to humans.

It was not until the late 1990s that this almost unique feature of the DG, later named adult hippocampal neurogenesis (AHN), was extended to primates. Thanks to the increased use of bromodeoxyuridine (BrdU), a nonradioactive thymidine analog that can be detected by antibodies (Gratzner, 1982), and the introduction of several molecular markers to identify steps of neuronal maturation, the study of mammalian neurogenesis became once again popular. As opposed to what Rakic had described, Elizabeth Gould and colleagues observed BrdU-positive cells that expressed markers for GCs located in the DG of tree shrews, marmosets and even Old World monkeys (Gould *et al.*, 1997; Gould *et al.*, 1999; Gould *et al.*, 1998). Finally, Fred Gage and collaborators found proof of adult neurogenesis in humans. In postmortem tissue from patients previously treated with BrdU for cancer diagnostics purposes, BrdU-labeled cells colocalizing with neuronal markers were detected in the DG of the human hippocampus (Eriksson *et al.*, 1998).

The debate over adult neurogenesis in humans is still a hot topic and accounts for a scientific problem hard to solve, partly because of the difficulty in getting conclusive

quantitative results from postmortem or resected material. It is still in doubt, for example, whether or not neurogenesis in normal conditions exists in other adult brain areas such as the neocortex, the striatum or the amygdala (Gould, 2007). In an original paper by the laboratory of Jonas Frisén, researchers took advantage of the ^{14}C imprint in genomic DNA in humans before and after above-ground nuclear bomb testing. Comparing individual age to hippocampal neuronal age, this team revealed a cell turnover dynamics of 700 new neurons added in each hippocampus per day, with a modest decline during aging (Spalding *et al.*, 2013). To add more controversy, in the current year both evidence, and absence of evidence, of AHN in humans has been reported. In a recent article by Arturo Alvarez-Buylla and colleagues, no assumingly young neurons were detected in the human DG of postmortem brains and resected hippocampi after the first few years of life and similar results were observed in macaques (Sorrells *et al.*, 2018). As opposed to these data, Maura Boldrini and collaborators found putative progenitors and immature granule cells (GCs) in postmortem human hippocampi (Boldrini *et al.*, 2018). In agreement with the mentioned work authored by Spalding, they report a more constant presence of neurogenesis over time (Spalding *et al.*, 2013). In the most recent contribution regarding this feature, the authors found putative stem cells in DG samples from adult human brains, but their proliferative capacity was very limited and few immature neurons, shown as doublecortin (DCX)-positive cells, were detected (Cipriani *et al.*, 2018). These three research works employed similar methods but followed different criteria, what reveals the added trouble of choosing good markers and morphological features to define neurogenic populations in different species and ages.

Regarding the SVZ, the controversy is not over either. Since its discovery by Joseph Altman and additional work by Shirley Bayer (Bayer, 1985), the multipotency of dividing cells located in the walls of the lateral ventricle of adult mice was later confirmed *in vitro* (Lois and Alvarez-Buylla, 1993; Reynolds and Weiss, 1992). In addition, their migration through the RMS to the OB, where these cells differentiate into neurons, was assessed tracing grafted and endogenous SVZ cells (Lois and Alvarez-Buylla, 1994). After even describing a topographical model in the adult mouse (Doetsch *et al.*, 1997), the scientific community has not stopped questioning to what extent this phenomenon consistently occurs throughout evolution. Two studies in 2004 reached opposite conclusions on the generation of neurons in the human OB. One found dividing cells expressing markers of immature and of γ-aminobutyric acid (GABA)-ergic or dopaminergic neurons (Bedard and Parent, 2004), whereas the other found stem cells but not migrating NBs in the corresponding area (Sanai *et al.*, 2004). As recently as 2007, the laboratory of Peter S. Eriksson described the ventriculo-olfactory neurogenic system in humans, which contains the SVZ, the RMS, the olfactory tract, and the OB (Curtis *et al.*, 2007). However, their evidence supporting the presence of new neurons in the OB and that these were originated in the SVZ was still scarce (Sanai *et al.*, 2007). Most recent works seem to accept the SVZ neurogenic niche persists at least until adulthood in humans (Sanai *et al.*, 2011; Sorrells *et al.*, 2018; Wang *et al.*, 2011), but further work is necessary to elucidate its prevalence.

Main adult neurogenic niches in mammals

The two canonical brain regions where adult neurogenesis persists display similar neurogenic cascades (**Fig. 1**): NSCs divide asymmetrically originating amplifying precursors that, in turn, divide symmetrically giving rise to NBs, which will maturate into neurons. However, the architecture and cell fate of both niches are substantially different, thus will be discussed separately.

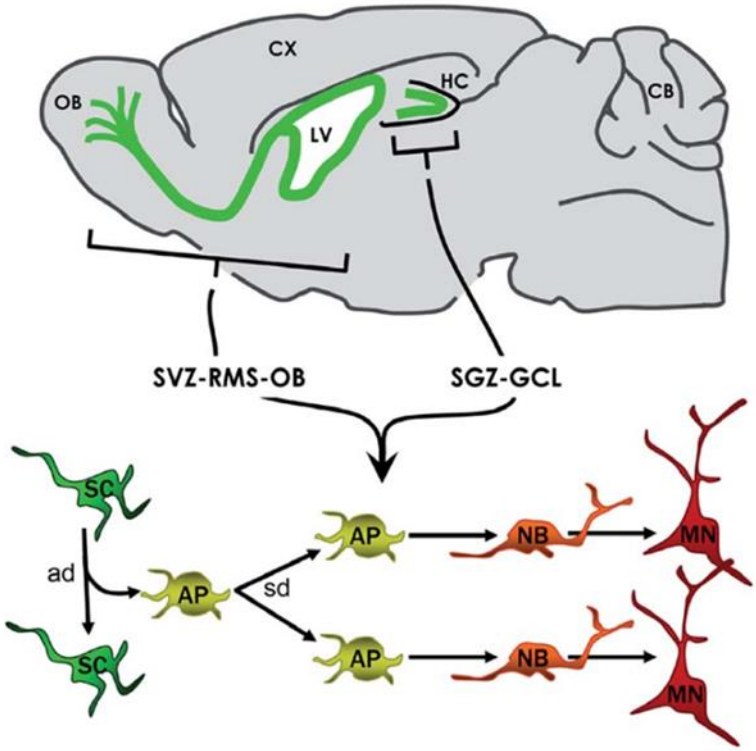

Figure 1. Adult neurogenesis persists in two areas of the adult brain. The SVZ of the lateral ventricles (LV) generates neuronal precursors that will migrate to the OB through the rostral migratory stream (RMS). The subgranular zone of (SGZ) of the DG generates neuronal precursors that will integrate locally in the granule cell layer (GCL). Both cases display a similar cascade of events, at the population level, to generate new neurons: neural progenitors with stem-cell capabilities (SC) divide asymmetrically (ad) giving rise to amplifying precursors (AP) that divide symmetrically (sd). Then, they exit the cell cycle and differentiate into neuroblasts (NBs) that will finally derive into mature neurons (MN). CX: cortex; HC: hippocampus; CB: cerebellum. Modified from (Encinas and Enikolopov, 2008).

SVZ

The periventricular germinal niche, or SVZ, is located in the walls of the lateral ventricles and consists of NSCs (B cells) and transient amplifying cells (C cells), which

give rise to NBs (A cells) that migrate through the RMS to the OB (Doetsch *et al.*, 1997). Lining the ventricle, a *bona fide* epithelium remains in the adult brain that is formed by a single layer of multiciliated ependymal cells (E cells), which are postmitotic (Spassky *et al.*, 2005). Both B cells (Merkle *et al.*, 2004) and E cells (Spassky *et al.*, 2005) have been proved to derive from developmental radial glia, what suggests a continuity between the embryonic and adult germinal niches.

B cells present astrocytic properties such as glial fibrillary acidic protein (GFAP) expression and have been subdivided in two populations: B1 and B2 cells. B1 cells are radial cells that extend their apical process towards the ventricle and a have a long basal process ending in the vascular network present in the SVZ, whereas B2 cells show a stellate morphology and are not in contact with the ventricular cavity (Doetsch *et al.*, 1997). Both populations express GFAP and can proliferate (Doetsch *et al.*, 1997; Ponti *et al.*, 2013), but only B1 cells have been described as the true NSCs. Their neurogenic potential was proved when labeled neurons in the OB were observed after intraventricular injection of an adenovirus targeting GFAP-expressing cells. These neurons were reported even in the contralateral OB, thus ensuring that only the ventricle-contacting B1 cells and their progeny would be labeled (Mirzadeh *et al.*, 2008). It is now well accepted that B1 cells provide a continuous supply of new neurons for the OB (Imayoshi *et al.*, 2008; Lazarini and Lledo, 2011; Petreanu and Alvarez-Buylla, 2002; Ponti *et al.*, 2013).

B1 cells contact the ventricle with a thin apical process that is interdigitated between E cells conforming a unique architecture in which, when the ventricular wall is viewed *en face*, these endings appear at the center of pinwheels formed by the apical surfaces of E cells (Mirzadeh *et al.*, 2008) (**Fig. 2**). This apical complex contains a primary non-motile cilium with functions involved in coupling intrinsic and extrinsic signaling, adapting B1 cells response to soluble factors present in the cerebrospinal fluid (CSF) (Lehtinen *et al.*, 2011). B1 cells can exist in either a quiescent or an activated state (Codega *et al.*, 2014; Mich *et al.*, 2014). Alterations in the CSF flow have been proved to promote their activated state via sodium and calcium signals in an epithelial sodium channel-dependent manner (Petrik *et al.*, 2018). Another interesting feature is that nestin, an intermediate filament known to be a marker of NSCs, is only expressed in activated B1 cells that will generate C cells (Codega *et al.*, 2014).

Type C cells divide symmetrically three to four times before giving rise to A cells that will divide one or two more times during their migration to the OB (Ponti *et al.*, 2013). These migrating NBs travel long distances through a glial network of interconnecting paths that converge at the anterior ventricle, forming the RMS that will carry A cells into the OB (Doetsch and Alvarez-Buylla, 1996). In the OB, they migrate radially and differentiate into up to ten different types of granule and periglomerular interneurons; interestingly, the location of the original NSC in the ventricular wall can predict the type of OB neuron that will be produced (Lim and Alvarez-Buylla, 2014; Merkle *et al.*, 2007). This postnatal inflow of new neurons has been described to be important for

flexible olfactory associative learning (Sakamoto *et al.*, 2014) and overall OB circuitry plasticity (Lepousez *et al.*, 2013).

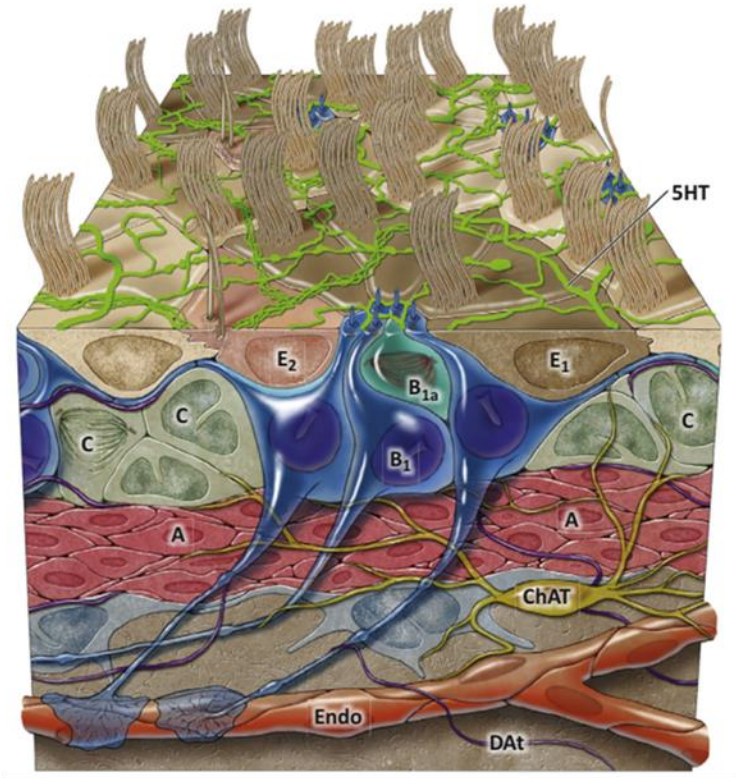

Figure 2. Schematic of the SVZ organization. B1 cells, which are the quiescent NSCs of the SVZ, become activated B1 cells (B1a) that actively divide. Activated B1 cells generate the amplifying precursor C cells which, after three rounds of divisions, give rise to A cells, the migrating neuronal-fate committed neuroblasts. Note that B1 cells contact the ventricle with an apical process surrounded by the apical surfaces of ependimal cells (E), forming together pinwheel structures on the surface. Coursing along this ventricular surface is a rich network of serotonergic axons (5HT). The basal processes of B1 cells have endings on blood vessels. Choline acetyltransferase (ChAT)-positive neurons present in the region have endings in the SVZ. Dopaminergic terminals (DAt) can be also observed. Modified from (Lim & Alvarez-Buylla, 2014).

SGZ of the DG

The hippocampal neurogenic niche, the SGZ of the DG, is located in the interphase between the GCL and the hilus. As opposed to the SVZ, the SGZ is not in contact with any ventricular cavity. See **Fig. 3** for a schematic representation of the neurogenic cascade in the DG (Bielefeld *et al.*, 2017; Encinas and Enikolopov, 2008).

NSCs have their triangular soma located in the narrow strip of tissue that constitutes the SGZ and extend a single apical process that crosses the GCL and arborizes in the molecular layer (ML), what gives them a typically radial morphology (Filippov *et al.*, 2003; Mignone *et al.*, 2004). Because of their astroglial properties such as GFAP expression, they have been often referred to as a subtype of astrocytes (Seri *et al.*, 2001), radial astrocytes (Seri *et al.*, 2004) or radial glia-like cells (Bonaguidi *et al.*, 2011). Because they represent the first step in the neurogenic cascade, they have also been named type-1 progenitors (Filippov *et al.*, 2003; Kronenberg *et al.*, 2003). Moreover, due to their scarce rate of cell division and quiescent state and before their multipotency was demonstrated they were also designated as quiescent neural progenitors (QNPs) (Encinas *et al.*, 2006).

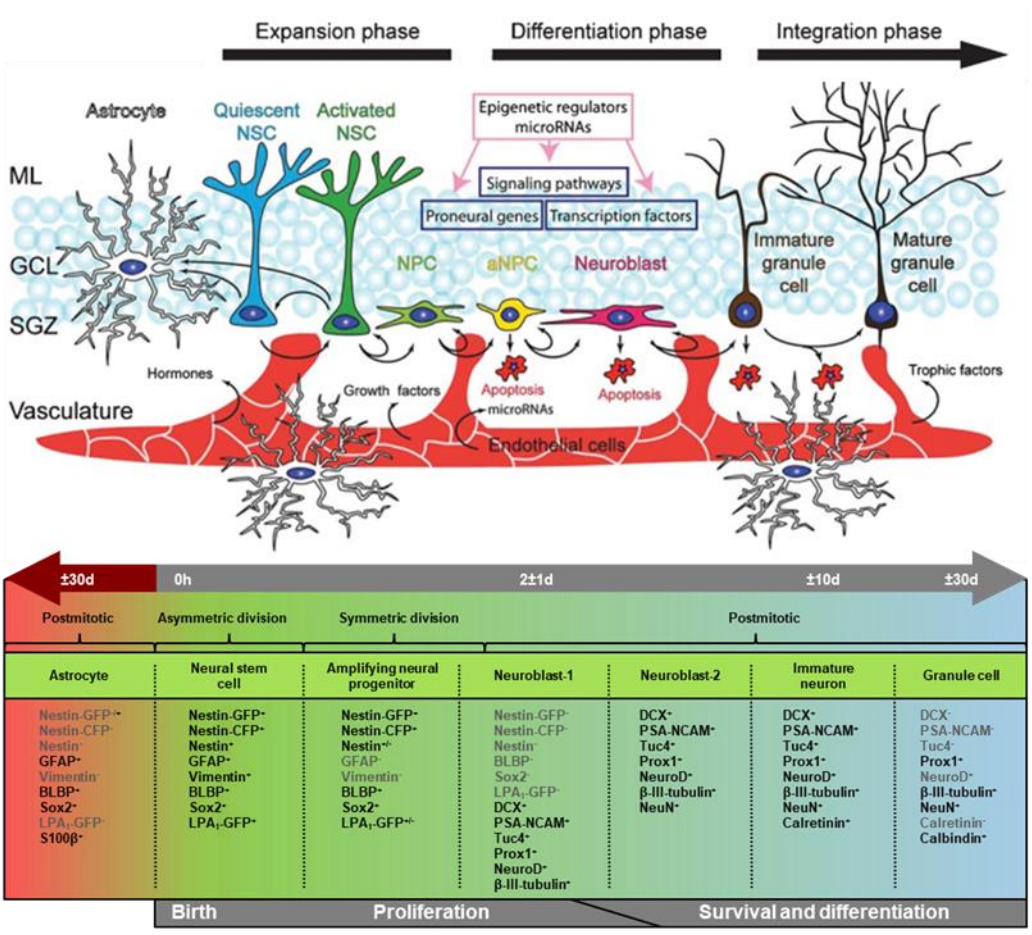

Figure 3. Schematic representation of the consecutive steps taken to generate a new GC in the adult DG. Different cell markers combined with morphological features and division possibility and type characterize each differentiation stage in the neurogenic cascade of the DG. The complexity of the neurogenic niche allows for both local and distant cell communication. aNPC: ANP. Modified from (Bielefeld et al, 2017) and from (Encinas and Enikolopov, 2008).

Hippocampal NSCs were first identified as cells with astrocytic properties (Seri *et al.*, 2001) combined with some of radial glia such as morphology and vimentin expression (Gould *et al.*, 1992). They also express brain lipid-binding protein (BLBP) and Sox2

(Encinas and Enikolopov, 2008). Nestin expression is particularly interesting because of its tissue pattern and the generation of transgenic strains. Nestin (from *ne*uroepithelial *st*em prote*in*) (Lendahl *et al.*, 1990) is an intermediate filament selectively expressed in NSCs and early progenitors of the nervous system and has been used for a while as one of the best markers for these populations. However, its presence has been reported in some other tissues such as pancreatic islets, tooth and myoblasts (Sejersen and Lendahl, 1993; Terling *et al.*, 1995; Zulewski *et al.*, 2001). This relatively extended nestin expression seems to be regulated by the presence of various regulatory elements, but the neural enhancer present in the second intron is strong and sufficient to direct the expression of an exogenous transgene to the developing neuroepithelium (Zimmerman *et al.*, 1994). Therefore, this is the regulatory element that has been widely used for the generation of a number of transgenic mouse lines (Encinas *et al.*, 2006; Imayoshi *et al.*, 2006; Kawaguchi *et al.*, 2001; Mignone *et al.*, 2004; Tronche *et al.*, 1999; Yamaguchi *et al.*, 2000).

Subgranular NSCs, as we have mentioned, are mostly quiescent and in a given moment a 2-5% are dividing (Encinas *et al.*, 2006; Kronenberg *et al.*, 2003). When they are activated, they divide three times asymmetrically at the population level (Encinas *et al.*, 2011b; Pilz *et al.*, 2018), in a horizontal plane parallel to the SGZ (Encinas and Enikolopov, 2008); giving rise to amplifying neural progenitors (ANPs) or type-2 cells (Kronenberg *et al.*, 2003).

ANPs are small round or oval cells which are devoid of GFAP and vimentin expression but maintain that of BLBP and, at lower level, nestin (Encinas *et al.*, 2006; Kempermann *et al.*, 2004). These cells have a higher mitotic activity, with 20-25% of them dividing as shown by a single injection of BrdU (Kronenberg *et al.*, 2003). ANPs usually group in clusters, with the division plane normally perpendicular to the SGZ such that the daughter cells extend horizontally along the SGZ (Encinas and Enikolopov, 2008). After dividing around 2.5 times in a symmetrical fashion (Encinas *et al.*, 2011b), they exit the cell cycle and start to differentiate into neuronal precursors.

During the transition from ANPs to NBs or type 3 cells (Kempermann *et al.*, 2004), most progenitors undergo apoptosis and are efficiently phagocytosed by microglia (Sierra *et al.*, 2010) such that only one third of the total of newborn cells will maturate into GCs. Surviving NBs start expressing markers of immature neurons, e.g. DCX, polysialylated neural cell adhesion molecule (PSA-NCAM) and Prox-1, and completely cease nestin expression. Most of these cells are larger and extend longer horizontal processes than ANPs and do not incorporate BrdU, thus are considered postmitotic neuronal precursors or type 1 NBs (NB1) (Encinas and Enikolopov, 2008).

Type 2 NBs (NB2) are larger than NB1 cells, remain in the SGZ and extend longer processes horizontally and obliquely to the plane of the SGZ. They express similar markers as NB1s but also start NeuN expression and do not divide (Encinas *et al.*, 2006).

Immature neurons (INs) are larger than the previous classes and their morphology becomes more similar to that of mature GCs. During this stage, cells present a single apical process crossing the GCL and branching in the ML that will become the apical dendrite (Encinas and Enikolopov, 2008; Kempermann *et al.*, 2004) and, apart from the markers that characterize NB2 cells, transiently express the calcium-binding protein calretinin (Brandt *et al.*, 2003). As early as one week of age, these new neurons start to extend their axon towards the hilus (Stanfield and Trice, 1988; Zhao *et al.*, 2006). Mostly coinciding in time, the onset of neurotransmitter receptor expression occurs. First, GABAergic inputs tonically activate newborn GCs due to their high cytoplasmic chloride ion content (Ge *et al.*, 2006); a response that coincides in time with POMC-EGFP transgene expression (Overstreet Wadiche *et al.*, 2005). Two to four weeks after neuronal birth, the response to GABA shifts from excitatory to inhibitory, the most typical in the mature brain, at the same time that they start to manifest responses to glutamate and integrate in the hippocampal circuitry (Esposito *et al.*, 2005; Ge *et al.*, 2007; Toni *et al.*, 2008; van Praag *et al.*, 2002). For a summary of this maturation process, see **Fig. 4** (Zhao *et al.*, 2008).

Newborn neurons in the DG show typical features of mature GCs by four weeks of age but continue to change its morphology and behavior for months until full maturation (Ge *et al.*, 2007; Toni *et al.*, 2007; Zhao *et al.*, 2006). Close to this age, calretinin expression is substituted by that of calbindin, marking a more mature state (Brandt *et al.*, 2003). During the period in which synaptic input is established, there is a selection process dependent upon NMDA (N-acetyl-D-aspartate) receptor expression (Ge *et al.*, 2007; Tashiro *et al.*, 2006); although this selection, in terms of cell loss, is much smaller (Sierra *et al.*, 2010).

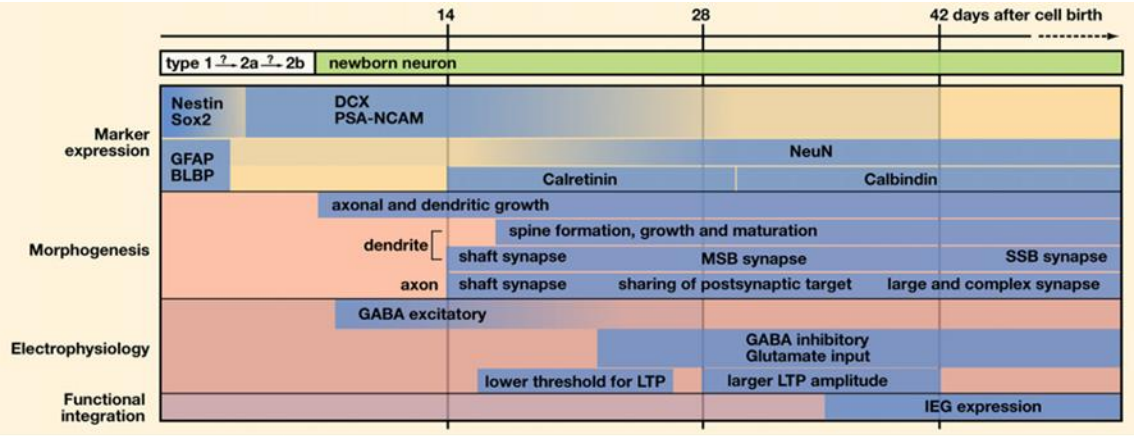

Figure 4. Development of newborn neurons in the SGZ. Different stages are characterized by expression of specific markers, morphogenesis, synapse formation, electrophysiological properties, and functional integration. MSB: multiple-synapse boutons; SSB: single-synapse boutons; LTP: long-term potentiation; IEG: immediate early gene. Modified from (Zhao et al., 2008).

The final stages in terms of integration in the hippocampal circuitry also involve functional changes. Even though calbindin is found in all mature GCs, it does not mark full maturation by itself. New neurons with ages from four to seven weeks are

electrophysiologically indistinguishable from preexisting GCs in the DG (Jessberger and Kempermann, 2003; van Praag *et al.*, 2002), but in the last maturation steps long-term potentiation (LTP) amplitude and threshold for LTP induction are different from neurons born during embryonic and postnatal neurogenesis (Ge *et al.*, 2007; Schmidt-Hieber *et al.*, 2004). The integration of new neurons can also be studied by evaluating the expression of immediate early genes (IEGs), whose levels reach those of preexistent GCs when the newborn cells are older than five weeks (Jessberger and Kempermann, 2003). However, other authors have reported that this difference in the recruitment of incorporating and preexisting neurons is maintained even when new GCs are five months old (Ramirez-Amaya *et al.*, 2006). A recent contribution by the laboratory of Linda Overstreet-Wadiche reported that an enhancement of adult neurogenesis translates into a reduction in excitatory postsynaptic currents and dendritic spine density in mature GCs, suggesting a redistribution of preexisting synapse to newborn neurons (Adlaf *et al.*, 2017). This piece of evidence strongly supports the idea that newly-generated GCs indeed modify the hippocampal circuits.

Functions dependent on hippocampal activity and inherent circuitry, such as episodic and spatial memory formation (van Strien *et al.*, 2009; Whitlock *et al.*, 2006), rely at least in part on remarkable anatomical features. One of these peculiarities involves a mostly unidirectional passage of information through its circuitry, in contrast to the reciprocal connectivity that is common in other cortical structures (Stepan *et al.*, 2015). The most prominent pathway in this passage, which also gives the DG a special relevance, is called the trisynaptic circuit. The trisynaptic circuit is comprised of three excitatory (glutamatergic) synapses between the entorhinal cortex (EC) and the region 1 of the hippocampal *Cornu Ammonis* (CA): EC layer II onto DG, DG onto CA3 and CA3 onto CA1. This circuit was already illustrated by Ramón y Cajal (**Fig. 5**) and was of great interest to him and one of his disciples, Rafael Lorente de Nó (Lorente de Nó, 1934; Ramón y Cajal, 1995). Neurons in layer II of the EC send their axons via the perforant path to the DG, where they synapse onto apical dendrites of GCs. These cells, in turn, give rise to mossy fibers that innervate the CA3 pyramidal neurons. Lastly, these cells synapse via the Schaffer collaterals onto CA1 pyramidal neurons completing the hippocampal trisynaptic circuit (Amaral and Witter, 1989; Witter *et al.*, 2000).

The EC is the origin of the main synaptic input the hippocampus receives and also acts as output region, allowing the origination of entorhinal-hippocampal loops (Witter *et al.*, 2000). This position as the first station of information processing in the hippocampal formation makes the EC an almost mandatory relay for afferences originating from other brain areas (Stepan *et al.*, 2015) and thus an influence on hippocampal LTP and cognitive functions (Basu and Siegelbaum, 2015).

The integration of new neurons into the existing hippocampal network suggests they must be involved in hippocampus-related brain functions. The computational modeling of AHN has been recently reviewed (Aimone, 2016), but some remarks regarding its functional contribution will be pointed out. It has been proved that the level of AHN correlates with acquisition of spatial memory shown as performance in the Morris water

maze (MWM) (Kempermann and Gage, 2002). Voluntary exercise increases progenitor proliferation in the SGZ and enhances LTP in the DG, which correlates with improved performance in the MWM (van Praag *et al.*, 1999). Causal evidence, however, has provided intriguing results depending on the approach used to ablate neurogenesis and the tests employed to evaluate learning tasks (Deng *et al.*, 2011). AHN has also been reported to have a role in some types of hippocampus-dependent conditioning (Saxe *et al.*, 2006; Shors *et al.*, 2001), anxiety-like behaviors (Bergami *et al.*, 2008), depression and stress responses (Snyder *et al.*, 2011). Interestingly, increasing AHN has been related to forgetting of established memories (Akers *et al.*, 2014). Nevertheless, limitations due to probable differences in animal species and strains, sensitivity of the methods and possible side effects of ablation of neurogenesis make it difficult to claim conclusions about the exact functions AHN has in cognition.

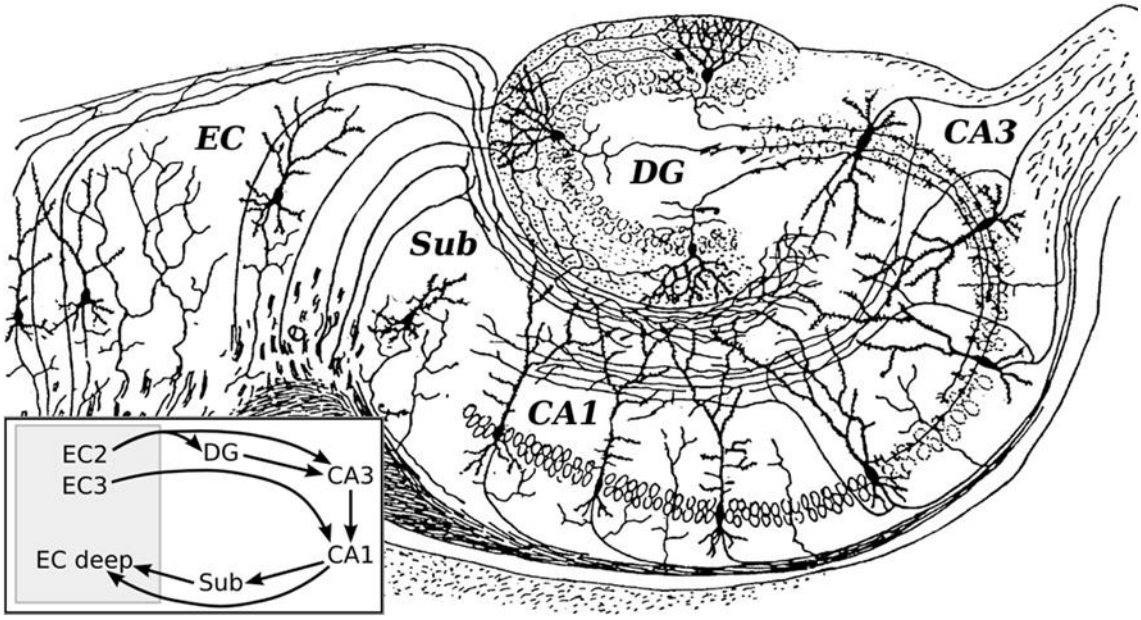

Figure 5. Schematic representation of the trisynaptic excitatory circuit based on the classic drawing by Santiago Ramón y Cajal. Neurons in layer II of the EC (EC2) project by way of the perforant path and synapse onto the DG. Axons of the GCs in the DG then form the mossy fibers that innervate the CA3 pyramidal neurons. These, in turn, send a collateral process of their axons called the Schaffer collateral to the CA1 pyramidal neurons. Other parallel and the inhibitory circuit are specified in the bottom left insert, although were not represented in the original drawing. Sub: subiculum. The drawing was downloaded from the public domain by way of the Wikipedia, but originally was published in (Ramón y Cajal, 1995).

4.2. Properties of the hippocampal NSCs

When NSCs were first identified, by means of chemical antimitotic treatment to ablate neurogenesis, as the primary precursors in the adult DG, they were described as subgranular astrocytes with mitotic potential and the capability of producing new GCs (Seri *et al.*, 2001). Even when this proliferative niche had been discovered, most cells derived from divisions were characterized by localization, morphology and markers as neurons (Altman and Das, 1965; Kaplan and Hinds, 1977). Years after the initial

surprise followed by confirmation and validation of this feature, however, these progenitors had been reported to render only neuronal progeny.

In the 1980s, several works performed by the team of Pasko Rakic in rhesus monkey tried to deepen in the knowledge on new cell formation in the postnatal and adult DG. When addition of newborn GCs was described to stop, shortly after birth in these studies, new GFAP-positive or non-neuronal cells were still being added and even the proportion of glial cells increased during postnatal age (Eckenhoff and Rakic, 1984; Rakic and Nowakowski, 1981). This could be interpreted as an increase in astrocyte production in the neurogenic niche of the DG. Nevertheless, this possible turnover was only speculation and adult neurogenesis in primates had not been confirmed yet (Rakic, 1985). New methods and studies provided new data to work on, and the proof of existence of AHN in Old World monkeys and humans (Eriksson *et al.*, 1998; Gould *et al.*, 1999; Kornack and Rakic, 1999) could make the study of the origin and fate of the neurogenic cascade more appealing.

Multipotency and self-renewal are two features that *bona fide* stem cells must fulfill, what has maintained the interest in solving the question on whether or not adult NSCs present these properties. In spite of the specifically radial morphology and location in the SGZ (Garcia *et al.*, 2004; Kosaka and Hama, 1986), their astroglial properties made the scientific community wonder if hippocampal NSCs could give rise to not only neurons but also astrocytes. Tracing cells labeled during proliferation, it was soon reported that markers of the neuronal lineage and one of mature astrocytes, S100β, did not coexist in the same division-derived cells. This indicated that the existence of a late common progenitor for neurogenesis and gliogenesis in the DG was improbable, but still astrogliogenesis was taking place in this neurogenic niche (Steiner *et al.*, 2004).

The identification of the SGZ astrocyte-like population as the true NSCs (Garcia *et al.*, 2004; Seri *et al.*, 2004; Seri *et al.*, 2001) narrowed the targets of the methods suitable for studying their divisions. Using a retroviral approach to label only dividing precursors, it was soon reported that NSCs could be multipotent at a single-cell level and could self-renew; and employing lentiviruses plus proliferation markers it was observed that at the population level they could originate both astrocytes and neurons, with a marked bias towards the latter cell type (Suh *et al.*, 2007). From this point on, different analyses utilizing nestin-based reporter lines recapitulated this property and confirmed the production of mature astrocytes from subgranular NSCs (Bonaguidi *et al.*, 2011; Encinas *et al.*, 2011b).

The debate over multipotency and the type of divisions NSCs can undergo has recently been another mystery to solve. In a report that resorted to genetic labeling and lineage-tracing approaches, J. M. Encinas and colleagues proposed a coupling between NSC activation followed by asymmetric division and the subsequent appearance of newborn astrocytes derived from NSC differentiation (Encinas *et al.*, 2011b). This programmed order-dependent kind of multipotency is a possible explanation for the preference NSCs present for generating neurons, as the existence of intermediate progenitors necessarily

increases the proportion of neurons produced over astrocytes, which would only be originated by final differentiation. In addition, this "disposable stem cell" concept offers an explanation for the observed age-related progenitor loss, since the few NSCs that enter the cell cycle get depleted in favor of transformation into postmitotic astrocytes (Encinas *et al.*, 2011b; Lugert and Taylor, 2011). This eventual differentiation is supported by previous observations in which the majority of BrdU/GFAP-double positive cells also presented S100β expression, a marker of mature astrocytes, when evaluated four weeks after BrdU injection (Steiner *et al.*, 2004).

Nevertheless, another research work published the same year challenged in a way the idea that this asymmetric mode of cell division is the only manner in which NSCs can behave. This time using *in vivo* clonal analysis, the authors revealed that NSCs can divide symmetrically giving rise to two copies of themselves, although with low probability (Bonaguidi *et al.*, 2011). Also, the majority of the labeled clones containing a NSC were multilineage and a 7-10% of the total clones contained at least one neuron and one astrocyte. Still, a high proportion of the labeled clones, especially the ones analyzed one or two months after labeling, were quiescent; and NSC depletion accounted for more than a 65% of the clones when evaluated at twelve months (Bonaguidi *et al.*, 2011; Taylor, 2011). This is consistent with the previous finding that, when NSCs get activated, they lose their stem cell capabilities in the end. Furthermore, part of the symmetric division that this work reported can be attributed to the fact that NSCs tend to locate in clusters in the DG (Mineyeva *et al.*, 2018). The conclusion that two NSCs formed a clone originated through symmetric division of one of them was made by quantifying how close the two labeled NSCs were (Bonaguidi *et al.*, 2011), but the bias towards a paired distribution already exists in the general NSC population meaning that part of the assumed clones of NSCs could be just clusters of unrelated cells (Mineyeva *et al.*, 2018).

These apparently opposed theories have been tried to be unified in comments and other original works, being called the "pessimist's and optimist's" views of adult neurogenesis (**Fig. 6**). The variety of tools chosen, such as the reporter constructs and general genetic manipulations, and the difference in scale, from clonal to population level, could be partially blamed for the differing conclusions; but do not solve the specific problem on whether NSC symmetric division is improbable or does not occur at all (Kempermann, 2011a). Precursor heterogeneity has also been proposed as, ironically, a unifying hypothesis, based on divergences in morphology and properties found between the different progenitor types in experimental approaches (Bonaguidi *et al.*, 2012; Lugert *et al.*, 2010; Suh *et al.*, 2007).

In a recent and interesting report, mathematical modeling and experimental data may help us understand NSC dynamics and the reasons behind their age-related depletion (Ziebell *et al.*, 2018). The authors suggest the existence of a "resilient stem cell population", quiescent NSCs that neither get activated nor depleted, as a possible subpopulation necessary to fit the clonal data. However, for their model to fit clonal data they also need to assume that dividing NSCs return to quiescence after division, a

behavior that, along with the resilient stem cells, was not observed in the "disposable stem cell" population model (Encinas *et al.*, 2011b) or that is infrequent and short-timed (Pilz *et al.*, 2018). The most plausible scenario they predict in order to also fit the observed decline of NSC population is one in which aged cells exit quiescence through activation with a higher probability than through depletion, with half of this depletion explicable by astrocytic transformation and the rest explained by cell death/apoptosis (Ziebell *et al.*, 2018); although this phenomenon has never been observed and if it exists is extremely uncommon (Sierra *et al.*, 2015).

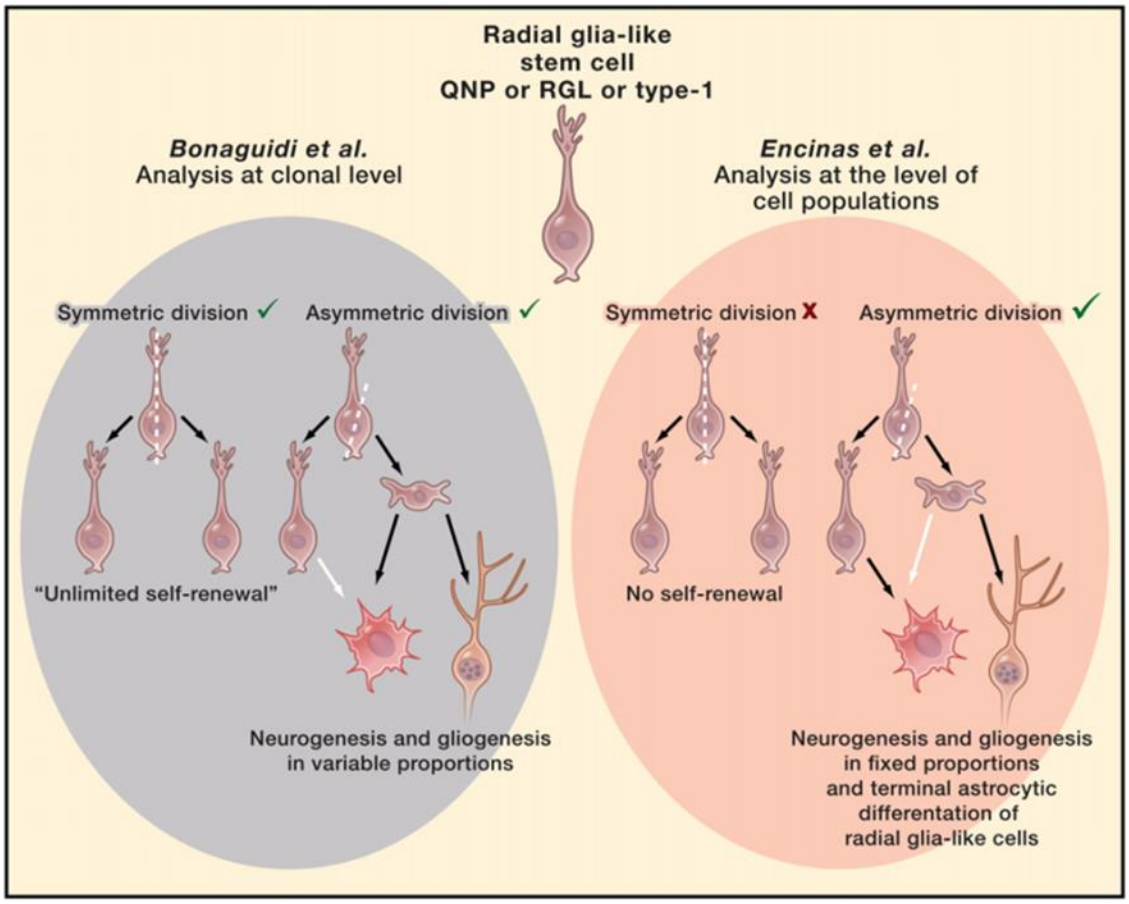

Figure 6. Two views of adult neurogenesis in the DG. In principle, radial glia-like stem cells of the hippocampus might divide symmetrically or asymmetrically, which would have different consequences for the maintenance of self-renewing stem cells in the long term. Bonaguidi et al. proposed that hippocampal stem cells at the clonal level do manifest the possibility of symmetric division (Bonaguidi et al., 2011). Thus, the NSC population could be regenerated and neurogenesis sustained or recovered over time. Encinas et al., on the other side, evaluating precursor cells at the population level found little evidence for such option (Encinas et al., 2011b) and instead observed that stem cells eventually deplete irreversibly mostly by differentiating into astrocytes. Modified from (Kempermann, 2011a).

With this full variety of possible situations, multipotency has been proved but frequencies and modes of division must be further explored. Frequency of the progeny obtained has been evaluated in a meticulous *in vivo* live imaging analysis (Pilz *et al.*, 2018), in which apart from confirming previously mentioned properties (Bonaguidi *et*

al., 2011; Encinas *et al.*, 2011b) the authors observed other possible direct transformations or kinds of division that give rise to neurons and astrocytes. Some of the contributors to this work had published only three years before how genetic manipulation can differentiate hippocampal adult NSCs into oligodendrocytes that enhance remyelination in a model of a demyelinating disease (Braun *et al.*, 2015). This, although artificially induced, extends NSC multipotency and should lead to more exhaustive studies on properties of NSCs and progenitors.

4.3. Regulation of neurogenesis and NSC dynamics

As it has been mentioned, NSCs are in baseline conditions a predominantly quiescent cell type at the population level. Whether or not their exhaustion is provoked either by astrocytic conversion or by cell death, age-related loss of NSCs and neurogenesis has extensively been proved in animal models since the discovery of the latter (Altman and Das, 1965; Andersen *et al.*, 2014; Bonaguidi *et al.*, 2011; Encinas *et al.*, 2011b; Encinas and Sierra, 2012; Kuhn *et al.*, 1996; Walter *et al.*, 2011). Taking into account the functional significance of the addition of new neurons, it has been hypothesized that decreased neurogenesis could be partially responsible for age-related cognitive impairment (Cameron and McKay, 1999; Leuner *et al.*, 2007). In conclusion, NSC entry into the cell cycle is a mechanism, if not the only, that contributes to their decline through a process of finite divisions and final differentiation into astrocytes (Encinas *et al.*, 2011b) or might be cell death. In any case, although possible, the symmetric mode of division that could counterbalance NSC loss seems to occur with a low probability (Bonaguidi *et al.*, 2011; Suh *et al.*, 2007).

Due to the described activation-coupled NSC gradual but steady depletion, stimuli that induced NSC exit from quiescence would accelerate the decline of their population (Pascual-Brazo *et al.*, 2014). This notion has been supported by the fact that disruption of some quiescence signals can lead to a short increase in neurogenesis followed by a long-term decrease and suppression caused by a loss of NSCs (Ehm *et al.*, 2010; Mira *et al.*, 2010). Speaking in terms of saving resources, if the recruitment of more newborn neurons becomes necessary it seems “wiser” to regulate neurogenesis at a later stage, in more neuronal fate-committed precursors, thus sparing the NSC population. This is a possible interpretation from data gathered about how exercise, enriched environment, fluoxetine and deep brain stimulation, for example, promote ANP proliferation or recruitment of newborn neurons (Encinas *et al.*, 2011a; Encinas *et al.*, 2006; Hodge *et al.*, 2008; Kronenberg *et al.*, 2003). However, changes in the mitotic capability of NSCs seem restricted to some stimuli in which injury or high increases in neuronal activity participate (Gao *et al.*, 2009; Huttmann *et al.*, 2003).

Although direct connection between signaling pathways and external stimuli that regulate AHN is still lacking, some mechanisms involving extracellular cues have been described, such as those downstream to bone morphogenetic proteins (BMPs), Notch, Wnts, GABA, insulin growth factors (IGFs) and Sonic hedgehog (Shh) (Faigle and Song, 2013; Ming and Song, 2011; Urban and Guillemot, 2014). For example, BMPs

are necessary for the maturation and integration of GCs, possibly via activation of the BMPR-Ib present in NBs and neurons (Mira *et al.*, 2010).

In this complicated regulation, other cell types of the hippocampal niche that are not strictly involved in the neurogenic cascade also have a function (Aimone *et al.*, 2014). To begin with, astrocytes can secrete Wnt3a and ephrin-B2, which have been proved to regulate neurogenesis possibly via β-catenin signaling (Ashton *et al.*, 2012; Lie *et al.*, 2005). Astrocytes can also release interleukins (ILs) IL-1 and IL-6, proinflammatory cytokines that, combined with other factors, can increase neuronal differentiation from neural progenitors (Barkho *et al.*, 2006). Microglia, for its part, is required to respond to fractalkine for AHN to occur normally, what suggests that a balance between pro- and anti-inflammatory cytokines and chemokines is necessary (Bachstetter *et al.*, 2011). Importantly, microglia also shapes neurogenesis by phagocytosis of apoptotic newborn cells that failed to survive their first weeks (Sierra *et al.*, 2010).

At the exclusive level of NSCs, the signaling involved in their switch from quiescence to an activated state and overall cell cycle dynamics are not fully understood but remarkable steps have recently been taken. The interest in these characteristics is double: first, we need to ascertain whether NSC activation/depletion is actually advantageous for neurogenesis or detrimental in the long term; second, the notions about regulation of NSC cell cycle are vital to be able to take advantage of their regenerative potential. For example, it is known that aging is marked by a decrease in the number of newborn neurons in the DG but it is not clear if the reason behind is either the increase in quiescence of aged NSCs, the diminished capability of ANPs to proliferate, the loss of NSCs over time or all of them.

The thymidine analog BrdU has been extensively employed in the study of adult neurogenesis (Eriksson *et al.*, 1998; Gould *et al.*, 1997) since every dividing cell incorporates it in their DNA and daughter cells are readily observable by detection with antibodies (Gratzner, 1982). Most typically, pulse-and-chase experiments have been carried out to label dividing cells in a specific time point, but continuous administration paradigms have been rarely used for this purpose. The fact that only a 1-5% of hippocampal NSCs are dividing in a given moment (Kronenberg *et al.*, 2003) makes them harder to "capture" and in turn observe their progeny and activation-quiescence behavior. Resorting to a two-marker paradigm, it was observed that, after dividing three times in a row at the population level, NSCs do not return to quiescence but exit the stem cell pool (Encinas *et al.*, 2011b). This behavior somehow goes against what was observed in the mentioned clonal analysis, in which some activated NSC-derived clones maintained a NSC or even two (Bonaguidi *et al.*, 2011). More recent observations have described the participation of the E3-ubiquin ligase Huwe1 destabilizing the proactivation protein Ascl1 as a mechanism that promotes NSC return to quiescence and prevents their exhaustion, although long-term analyses of quiescence were not performed (Urban *et al.*, 2016). Precisely employing Ascl1 as a target gene to label NSCs, an *in vivo* two-photon imaging approach managed to follow their division modes and progeny over time and reported no symmetrical NSC divisions after the more

typical asymmetrical ones and a progressive depletion of NSC-containing clones after three divisions (Pilz *et al.*, 2018), thus confirming the previously reported data at the population level obtained by Encinas *et al.* (Encinas *et al.*, 2011b).

Regulation of quiescence has been addressed in a number of other papers lately, trying to overcome at least the difficulty in telling activated from dormant NSCs. BMP signaling, this time through BMP-Ia receptor activation, has been described to be necessary for NSCs to maintain their quiescent stage, and its deletion leads to an over-activation of adult NSCs that ultimately depletes their population (Mira *et al.*, 2010). Inhibitors of BMPs such as noggin are present in the DG and promote NSC activation, self-renewal and multipotency, an effect that seems specific for hippocampal NSCs (Bonaguidi *et al.*, 2008).

It has been reported that EGFR-expressing NSCs in the SVZ are more proliferative and neurogenic whereas $EGFR^-$ ones are more quiescent, suggesting EGFR as an identity marker to distinguish the activated state (Codega *et al.*, 2014; Pastrana *et al.*, 2009). This strategy was successfully reproduced in the DG, where $EGFR^+$ NSCs were able to generate more neurospheres than the respective population devoid of this receptor (Walker *et al.*, 2016).

Wnts also have a role in regulation of quiescence. They are secreted by astrocytes and NSCs, thus they are thought to act both in a paracrine and an autocrine manner (Okamoto *et al.*, 2011; Qu *et al.*, 2010), and through their canonical pathway they can directly promote NSC proliferation and induce neurogenesis *in vitro* (Lie *et al.*, 2005). There is also *in vivo* evidence suggesting that the Wnt inhibitor secreted Frizzled-related protein 3 (sFRP3), secreted by GCs, participates in NSC quiescence maintenance and neurogenesis, as in its absence NSCs proliferate more and newborn neuron maturation is promoted (Jang *et al.*, 2013). Expression of another Wnt inhibitor, Dickkopf 1 (Dkk1), increases with age and its deletion from the brain was also able to restore neurogenesis in aged mice, what supports the idea of increased NSC quiescence as a process involved in the decline of AHN with age (Seib *et al.*, 2013). The mechanisms by which the Wnt pathways are thought to regulate AHN were summarized in a comment on these two papers and are shown in **Fig. 7** (Wu and Hen, 2013).

Notch signaling is also important for NSC quiescence and adult neurogenesis, although differences in receptors and neurogenic niches could lead to divergent conclusions. Particularly, deletion of Notch1 receptor from $nestin^+$ hippocampal NSCs and their progeny translated into a premature loss of stem cells and transient progenitors, suggesting again that increased NSC activation provokes a decline in their population (Ables *et al.*, 2010). Nevertheless, this effect seems different in the SVZ, where a similar Notch1 selective ablation affected the activated population by promoting its division and ultimate depletion but was not enough to make the quiescent NSCs exit the dormant stage and their population remained unchanged (Basak *et al.*, 2012). In zebrafish, different Notch receptors seem to regulate different properties of NSCs (Alunni *et al.*, 2013), a feature that could partly explain these differences between SGZ

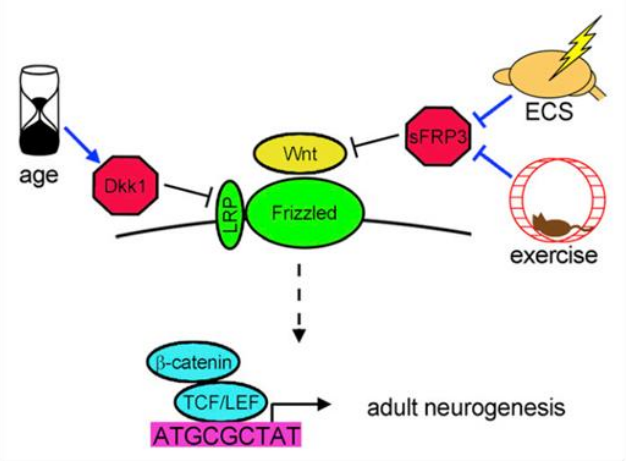

Figure 7. Wnt antagonists inhibit AHN. Wnt protein binding to the Frizzled/LRP heteromeric receptor and downstream formation of the β-catenin TCF/LEF complex leads to subsequent transcriptional activation of target genes. Inhibition by Dickkopf 1 (Dkk1) and secreted Frizzled-related protein 3 (sFRP3) of Wnt signaling downregulates NSC division and neuronal maturation. Exercise or electroconvulsive shock (ECS)-mediated neuronal activity inhibit sFRP3 expression, allowing Wnt-Frizzled/LRP binding and activating adult NSCs. Dkk1 expression is upregulated with age, deriving in suppression of AHN due to, presumably, increased NSC quiescence. Modified from (Wu and Hen, 2013).

and SVZ adult NSCs or even contribute to the population heterogeneity present in the SVZ (Codega *et al.*, 2014) and proposed for the SGZ (Giachino and Taylor, 2014).

An interesting hypothesis that could explain the effect of Notch signaling pathways on stem cell quiescence involves Hes proteins and one of their targets, the already mentioned Ascl1 (Urban and Guillemot, 2014). Hes proteins are transcription factors induced by Notch activity which act as gene expression inhibitors and have oscillating levels, due to their own gene repression and their short half-life, that regulate quiescence of neural progenitors in the embryonic brain (Imayoshi and Kageyama, 2014; Imayoshi *et al.*, 2010; Shimojo *et al.*, 2008). Their oscillation, although not confirmed yet in adult NSCs, is opposite to the one of their targets, including Ascl1. Ascl1 is another transcription factor whose expression is induced by activating signals received by adult NSCs and promotes their exit from quiescence. Indeed, its expression is specific in proliferative NSCs, although not always present in them (Andersen *et al.*, 2014). Ascl1 destabilization by Huwe1 has been proved to be necessary for the hippocampal stem cells to return to quiescence after activation, and if they fail this return the proliferative NSC pool gets depleted (Urban *et al.*, 2016). These sets of data further support the idea that stimuli or pathways which favor NSC entry into the cell cycle also derive in a more rapid depletion of their population.

A specific gene whose function has been linked to several steps of the neurogenic process is the lysophosphatidic receptor 1 (LPA_1) (Matas-Rico *et al.*, 2008). During cortical development, LPA_1 is expressed in neuronal precursors suggesting a regulatory function in neurogenesis (Hecht *et al.*, 1996). Traditionally, postnatal expression of this gene has been reported in oligodendrocytes during the progress of myelination (Weiner

et al., 1998), but this receptor has recently been proposed as a good marker for hippocampal adult NSCs (Walker *et al.*, 2016) (**Fig. 8**). In a recent single-cell RNA sequencing analysis that followed the different neurogenic populations from development to adult stages, this receptor was one of the few markers found to be specifically enriched in NSCs even in their quiescent state (Hochgerner *et al.*, 2018). Given this specificity and enrichment in NSCs, we could expect defects in neurogenesis in its absence. However, a mouse strain lacking LPA_1 did not show apparent abnormalities in the hippocampal formation or differences in DG volume (Matas-Rico *et al.*, 2008); whereas defects in cortical layer width in adults had been previously described (Estivill-Torrus *et al.*, 2008). In addition, around a 50% perinatal lethality due to defective suckling behavior and brain metabolism alterations had been reported in a formerly-generated null mouse strain (Contos *et al.*, 2000; Harrison *et al.*, 2003).

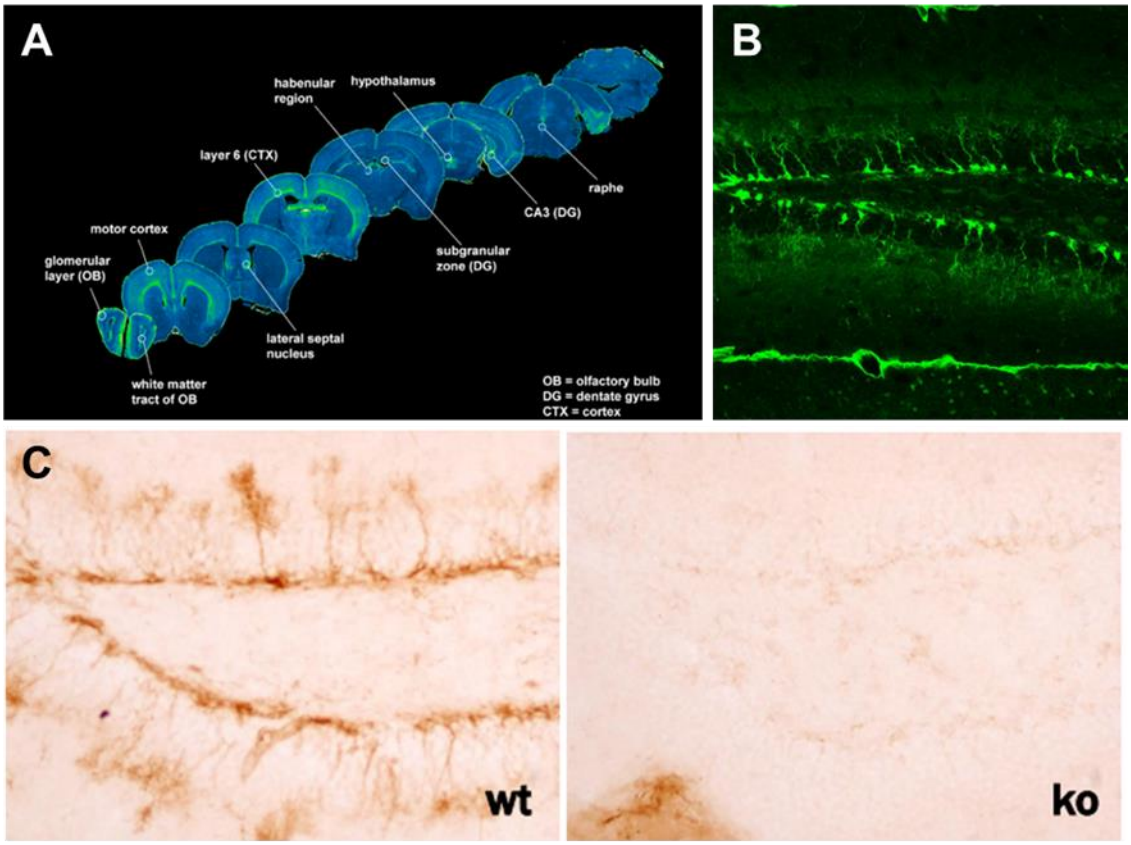

Figure 8. LPA_1-GFP and LPA_1 are expressed in adult NSCs in the DG. GFP^+ cells in the adult brain were detected in several brain regions (**A**) including the SGZ of the adult DG (**B**), where fluorescence is especially remarkable in radial NSCs. Note that GFP expression was not very conspicuous in the SVZ. (**C**) Immunohistochemical staining for LPA_1 revealed the specific labeling in radial NSCs in the DG of WT (left) and its absence in the DG of the knockout $maLPA_1$-null mice (right). (**A**) was taken from GenSat database at www.gensat.org; (**B**) was modified from (Walker et al., 2016); (**C**) was kindly provided by Guillermo Estivill-Torrús at IBIMA, Málaga.

In the paper regarding hippocampal features of the Málaga variant of LPA_1-null ($maLPA_1$), the authors indeed found defects in proliferation in the DG and adult neurogenesis based on a reduction in PSA-NCAM and DCX expression. These deficits

were still present after exposure to environmental enrichment and voluntary exercise to increase newborn neuron generation (Matas-Rico *et al.*, 2008). Nevertheless, conclusions on the contribution of the constitutive deletion of this gene to the effects of enrichment should be taken cautiously as it seems to affect baseline neurogenesis (Kempermann, 2011b). More evidence on the participation of LPA_1 in AHN, however, was found in the fact that its endogenous ligand LPA induced net neurogenesis by enhancing precursor survival without changing proliferation *in vivo* (Walker *et al.*, 2016). Works on the function of this relatively new adult NSC marker are lacking and future research on this topic should improve our knowledge on the possibilities and properties of SGZ stem cells and overall neurogenic niche.

Accumulating data suggest a relationship between neuronal activity and NSC activation. In fact, some of the mentioned mechanisms have been proposed as mediator pathways for activity-dependent NSC recruitment. Secretion of the Wnt inhibitor sFRP3 by GCs, for example, seems to decrease with neuronal activity and in its absence quiescent NSCs get activated and newborn neuron maturation is favored (Jang *et al.*, 2013). For its part, a single injection of kainic acid (KA), an agonist of ionotropic glutamate receptors that mimics neuronal hyperactivity, increased Ascl1 expression in quiescent NSCs and promoted their division (Andersen *et al.*, 2014). On the contrary, tonic release of the typically inhibitory neurotransmitter GABA by parvalbumin (PV)-expressing interneurons maintains NSCs in their quiescent state and the deletion of a subunit of the ionotropic $GABA_A$ receptor is enough to activate a symmetric mode of NSC division (Song *et al.*, 2012). These PV^+ neurons are depolarized by GABAergic projections coming from the medial septum, which have been proved to regulate stem cell quiescence too (Bao *et al.*, 2017). Moreover, inhibition of the metabotropic $GABA_B$ receptor and deletion of its subunit $GABA_{B1}$ stimulated NSC proliferation (Giachino *et al.*, 2014). Therefore, evidence increasingly suggests that excitatory neuronal activity in the DG drives NSCs towards their activation state, whereas the inhibitory maintains their quiescence. A schematic summary of the different proposed mechanisms of regulation is shown in **Fig. 9**.

The fact that neuronal excitation affects hippocampal stem cell division is in addition supported by several reports in which manipulations or brain alterations that affect electrical activity have been observed to alter AHN (Pineda and Encinas, 2016). Seizures increase NSC recruitment and activation (Huttmann *et al.*, 2003; Indulekha *et al.*, 2010), a feature that has been also proved in the animal model for electroconvulsive therapy (ECT), electroconvulsive shock (ECS) (Jun *et al.*, 2015; Segi-Nishida *et al.*, 2008). Studies on long-term effects of the NSC division enhancement, their fate choices and overall neurogenesis are still lacking, thus will be partly addressed in this work.

4.4. Neurogenesis and epilepsy

Mesial temporal lobe epilepsy (MTLE), the most frequent form of human epilepsy, is a chronic neurological disorder characterized by spontaneous recurrent motor seizures generated in the mesial temporal lobe. It is thought that, in most patients, MTLE is

initiated by lesions or functional alterations triggered by events such as febrile seizures, encephalitis or traumatisms which, after a latency period of 5-10 years, originate these convulsions (Engel, 1993; O'Dell *et al.*, 2012; Sharma *et al.*, 2007). This pathology is associated with histological changes in the hippocampus that involve neuronal loss, dispersion of the GCL and lesions in CA (Bae *et al.*, 2010; de Lanerolle *et al.*, 2003; Sharma *et al.*, 2007), as well as gliosis with reactive astrocytes (RAs) (O'Dell *et al.*, 2012; Sierra *et al.*, 2015). This series of alterations is known as hippocampal sclerosis and its severity usually correlates with an increased loss of the cognitive functions related to the hippocampus (**Fig. 10**) (Wieser, 2004).

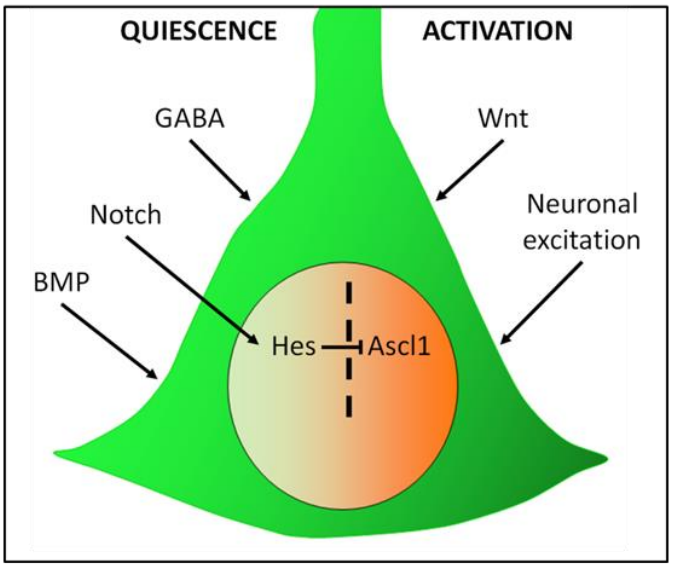

Figure 9. Schematic summary of NSC quiescence (left) and activation (right) regulation. BMPs, a group of growth factors, are considered to be necessary for NSCs to remain quiescent, a state that is also favored by GABA signaling. Notch ligands induce quiescence possibly through Hes proteins, a kind of inhibitory transcription factors, inhibiting the proactivation protein Ascl1. Wnts, a major family of signaling proteins, can directly promote NSC division through their canonical pathway. As opposed to the action of GABA, excitatory neuronal activity favors NSC activation. Modified from (Urban and Guillemot, 2014).

Neuronal alterations such as aberrant GC mossy fiber growth towards the GCL and even inner ML of the DG are also present in MTLE (Buckmaster *et al.*, 2002; Nadler *et al.*, 1980; Okazaki *et al.*, 1999; Tauck and Nadler, 1985). This axonal sprouting could contribute to epileptogenesis, possibly through the excitatory synapses with other GCs that have been reported and that would result in a predominantly excitatory circuit deriving in recurrent excitation and seizures (Scharfman *et al.*, 2003; Sharma *et al.*, 2007).

Adult neurogenesis is also affected in MTLE. In experimental models of this disorder such as the pilocarpine model in rat, it has been observed that there is an initial boost in newborn neuron generation (Cha *et al.*, 2004) with development of aberrant axonal projections (Parent *et al.*, 1997). This could be due to the mentioned increase in NSC activation that follows systemic KA injection-induced seizures (Huttmann *et al.*, 2003),

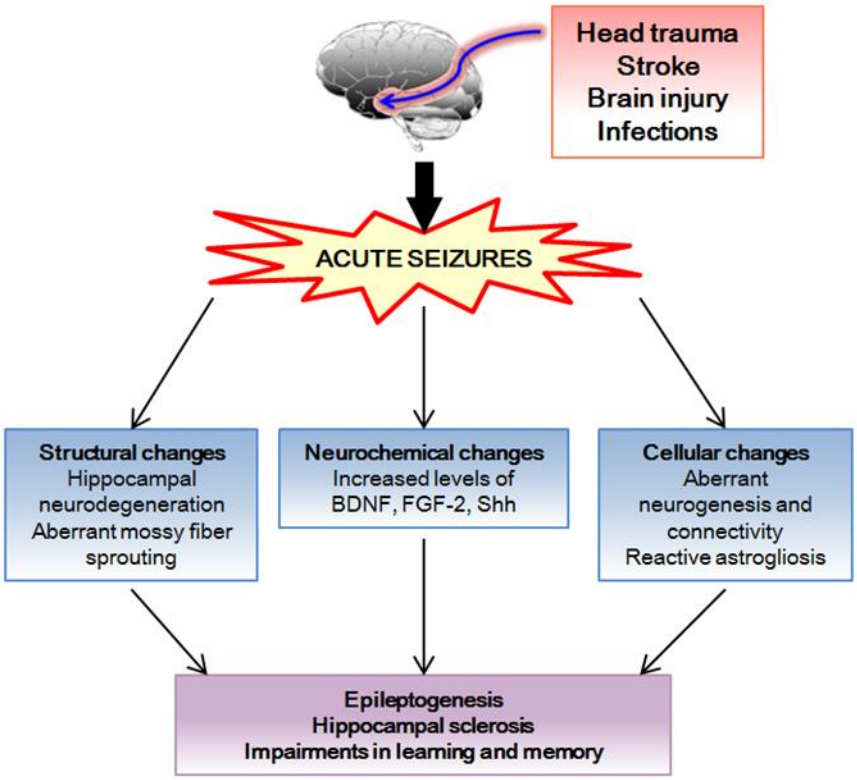

Figure 10. Schematic of the different changes that follow acute seizures. Acute seizures or *status epilepticus* typically occur following head trauma, stroke, brain injury or brain infections. Acute seizures induce multiple structural alterations in the brain particularly the hippocampus. The major hippocampal changes include degeneration of dentate and CA1-CA3 neurons and aberrant sprouting of mossy fibers. Acute seizures also transiently upregulate multiple factors in the hippocampus such as BDNF, FGF-2 and Shh. Cellular changes in the hippocampus comprise aberrant neurogenesis in the hilus, occurrence of hilar basal dendrites in newly added GCs and reactive astrogliosis. All these changes are believed to contribute to the formation of aberrant circuitry and epileptogenesis in the hippocampus, hippocampal sclerosis (of which reactive gliosis is part), and learning and memory impairments. Modified from (Kuruba et al., 2009).

but as we will see NSCs in epilepsy models do not seem to behave normally in terms of newborn neuron generation. This short-term stimulation of neurogenesis might contribute to the epileptogenic process favoring recurrent hyperexcitation; indeed, this idea is supported by the decrease in convulsive activity observed after infusion with cytosine β-D-arabinofuranoside (Ara-C), an antimitotic agent which inhibits AHN (Jung *et al.*, 2004). Inhibition performed by means of brain irradiation, though, was not enough to prevent mossy fiber reorganization in the ML, suggesting that the major contribution belongs to preexistent GCs (Parent *et al.*, 1999).

Nevertheless, the neurogenic boost would be transitory, as other studies suggest that neurogenesis is abolished as a long-term consequence in chronic epilepsy developed after KA- or flurothyl-induced seizures (Hattiangady *et al.*, 2004; Hattiangady and Shetty, 2010; McCabe *et al.*, 2001). One possibility to explain this impairment is the

reported generation of new GABAergic interneurons as a fraction of the product of AHN (Liu *et al.*, 2003). If no new inhibitory neurons can be incorporated into the circuitry, this could derive in an increased neuronal excitability. However, this possibility does not seem probable since GCs still account for the majority if not all of neurons produced in the neurogenic cascade; and especially because SGZ NSCs generate and differentiate into RAs following intrahippocampal KA injection at the expense of neurogenesis (Sierra *et al.*, 2015). This shift from the predominant neurogenic fate towards an almost pure reactive astrogliogenesis would indeed be a plausible explanation for the ablation of neurogenesis observed in the mentioned chronic MTLE models.

Another common feature in experimental models of MTLE and human samples is aberrant neurogenesis, the generation of abnormal neurons in the DG. The aberrations include ectopic location (mostly in the hilus), abnormal morphology with mossy fiber sprouting (Parent *et al.*, 1997), and altered electrophysiological properties (Scharfman, 2000; Scharfman *et al.*, 2003). The contribution of this aberrant neurogenesis to MTLE is not completely understood, but a positive correlation between some of these peculiarities and the frequency of seizures was found in a model of mouse epilepsy (Hester and Danzer, 2013). Although causality cannot be claimed from that study, it has also been observed that reducing overall neurogenesis by triggering apoptosis in dividing nestin-expressing cells reduced aberrant neurogenesis and the frequency of chronic seizures (Cho *et al.*, 2015). This ectopic location of newborn neurons can also occur when seizures are induced in other brain areas connected to the DG such as in the amygdala via kindling (Fournier *et al.*, 2010; Fournier *et al.*, 2013). The amygdalar region is connected to the DG via EC synapses (Finch *et al.*, 1986) and its involvement is not trivial in hippocampal excitatory loops as it has been shown to modulate hippocampal-mediated memory processes (Packard *et al.*, 1994) and synaptic plasticity (Nakao *et al.*, 2004).

The ultimate neurogenic decline in MTLE fits with the division-coupled astrocytic differentiation of adult NSCs once they are activated. The increase in neuronal activity would translate into NSC recruitment for cell division and, in turn, NSCs would finally transform into astrocytes (Encinas *et al.*, 2011b). This hypothesis was supported by the fact that, in animal models of the disorder, an accumulation of newly-born astrocytes is observed in the long term (Kralic *et al.*, 2005; Nitta *et al.*, 2008).

In human tissue, putative NSCs defined as nestin-positive radial cells were found in hippocampi from young TLE patients but none was found in those of adult patients, suggesting that the NSC pool is depleted after chronic seizure activity in humans (Blumcke *et al.*, 2001). Moreover, neural progenitors were absent in an ex vivo study of epilepsy patients with hippocampal sclerosis (Paradisi *et al.*, 2010).

The data and especially the conclusions obtained from postmortem or ex vivo tissue, however, have not been proved to be really reproducible and sometimes seem contradictory. Until further exploration and even confirmation of the presence of NSCs

in the adult human DG, the general consensus might be that an initial boost in proliferation is followed by decreased cell division and neurogenesis (Pineda and Encinas, 2016).

Some of the mechanisms involved in the relationship between excitability and NSC activation, such as GABA activity, have been commented but others are noteworthy. The levels of brain-derived neurotrophic factor (BDNF) are acutely upregulated after seizure generation (Shetty *et al.*, 2003) and when locally synthesized in dendrites of GCs it promotes differentiation and maturation of progenitors in the SGZ via GABA release from PV^+ interneurons (Waterhouse *et al.*, 2012), suggesting another mechanism of excitation-dependent NSC regulation. Neuronal activity can also upregulate the expression of growth factors such as basic fibroblast growth factor (bFGF, FGF-2) (Riva *et al.*, 1992). FGF-2 is acutely overexpressed after seizures (Indulekha *et al.*, 2010) and has been related to astrocyte hypertrophy after inflammatory insult (Kang *et al.*, 2014) and to cell proliferation in the hippocampus in response to KA injection (Yoshimura *et al.*, 2001). Nevertheless, in chronic epilepsy its expression decreases (Hattiangady *et al.*, 2004) as well as the number of FGF-2-positive RAs (Erkanli *et al.*, 2007), so its role in the chronification of the disease and the reactive astrogliosis is still unclear. Lastly, Shh not only regulates neurogenesis but also directly induces stem cell properties in the reactive astroglia found after brain injury (Sirko *et al.*, 2013). In addition, the hedgehog signaling that Shh activates was observed to be enhanced following both acute and chronic ECS treatment (Banerjee *et al.*, 2005). The regulation of the downstream protein Smo and its mRNA are not well understood, however, and further research is necessary to unveil the mechanisms involved in the relationship between Shh and the astrocyte and NSC responses to neuronal activity.

Not only increased neuronal activity recruits NSC for division and, potentially, eventual differentiation into astrocytes, it has been reported that neuronal hyperexcitation in the DG favors astrogliogenesis at the expense of neurogenesis (Kralic *et al.*, 2005). Indeed, although epileptiform activity (EA) acts like an accelerated form of aging impairing neurogenesis through NSC depletion, MTLE qualitatively changes the fate of NSC division towards reactive astrogliogenesis (Sierra *et al.*, 2015). RAs, on their part, have impaired glutamate buffering and produce proinflammatory cytokines with proepileptogenic potential such as IL-1β, which could participate in the development of secondary recurrent seizures (Devinsky *et al.*, 2013).

Interestingly, reactive astrogliosis induced by adenoviral infection of hippocampal astrocytes impaired the excitation/inhibition balance of network activity, what translated in neuronal hyperexcitability (Ortinski *et al.*, 2010). Furthermore, widespread chronic astrogliosis caused by β1-integrin conditional deletion in radial glia and its progeny led to the development of spontaneous seizures *in vivo* and neuronal hyperexcitability in acute brain slices, supporting the hypothesis that reactive astrogliosis is sufficient to trigger epileptic seizures (Robel *et al.*, 2015).

Given the probable exacerbation of MTLE by the presence of RAs, the newly-formed ones would contribute to this imbalance in neuronal activity that could act in favor of the chronification of this neurological disorder. The apparent benefit of increasing neurogenesis in epileptic patients due to the long-lasting loss of this capacity, therefore, meets opposition in the fact that stimulating NSC activation in this condition, if any is left spared, promotes reactive astrogliogenesis instead (Sierra *et al.*, 2015). Studying this new possibility of adult NSCs of transforming into reactive NSCs (React-NSCs) that ultimately derive in RAs, as well as establishing markers and differential functionalities for these versus those of parenchymal astrocytes-derived RAs, should open new perspectives to interpret the "virtues" and "failures" this stem cell population is capable of.

5. Hypothesis and Objectives

5. Hypothesis and Objectives

Effective AHN depends large- and primarily on the cell output of NSCs. These cells act as a finite and non-renewable resource and thus preserving their population and properties is desirable to counteract the progressive depletion of neurogenesis that associates with aging or some pathological conditions. Many of the properties that characterize NSCs are still not fully understood as essential experiments and appropriate tools are still missing in the literature. In our attempt to generate new knowledge about NSCs and AHN we have generated the following hypotheses and objectives:

- We hypothesize that **NSC activation is a single event that inevitably leads to their exhaustion and return to quiescence after initial activation and self-renewal are negligible at the population level.**

Objective 1. To evaluate division versus quiescence dynamics in the hippocampal neurogenic niche.

Objective 1.1. To assess proliferation and NSC activation in the normal DG employing a continuous BrdU-administration paradigm. For this purpose, we will take advantage of BrdU administration in drinking water for 1w, sacrificing the animals 1d later to stain and visualize specific markers of dividing populations and quantify their relative proportions by means of confocal microscopy-based quantitative image analysis.

Objective 1.2. To analyze the differentiation output of the cell division-derived populations in the DG after prolonged exposure to BrdU labeling. Towards this aim, we will administer BrdU in drinking water for 1w, or 1m, and wait for 1m after BrdU withdrawal to study the division-derived differentiated populations in the DG by means of confocal microscopy-based quantitative image analysis.

Objective 1.3. To study the reentry into the cell cycle versus quiescence or differentiation of cells that have already experimented division in the DG during continuous BrdU administration. We will evaluate the reentry into the cell cycle in all three paradigms of BrdU administration utilizing Ki67as a marker of cell division in already BrdU-labeled cells. Specifically, we will also focus on the possibility of reentry of NSCs.

- We hypothesize that **stimuli that promote NSC entry into the cell cycle such as neuronal hyperactivity would accelerate their depletion or even provoke a shift in their properties and disrupt the correct progress of the neurogenic cascade**.

Objective 2. To study the response to different levels of neuronal hyperexcitation of the neurogenic niche and specifically of NSCs.

Objective 2.1. To study cell proliferation and NSC activation in the DG following two models of neuronal hyperexcitation: EA and MTLE. For this purpose, we will inject two different doses of KA into the DG that induce neuronal hyperexcitation in the form of spike discharges (EA) or seizures (MTLE) and acutely label proliferating cells with BrdU at 2 or 6d postinjection. We will then analyze the overall cell division and that of NSCs, ANPs and astrocytes with the help of cell markers and confocal microscopy-based quantitative image analysis.

Objective 2.2. To evaluate the symmetric versus asymmetric mode of cell division of NSCs after seizures. For this objective, we will perform clonal analysis of dividing cells resorting to inducible Nestin-CreER^{T2}/R26R:YFP transgenic mice in control and MTLE conditions by means of confocal microscopy-based quantitative image analysis.

Objective 2.3. To study the differentiation output of NSCs after seizures. With this aim, we will perform a long-term analysis in inducible Nestin-CreER^{T2}/R26R:YFP transgenic mice and quantify the cell types derived from NSC division following EA and MTLE by means of confocal microscopy-based quantitative image analysis.

Objective 2.4. To assess the effect on cell proliferation and NSC activation of an inflammatory stimulus. For this purpose, we will inject lipopolysaccharide (LPS) directly into the DG and administer BrdU 2d later to perform at 3d a short-term analysis by means of confocal microscopy-based quantitative image analysis.

- We hypothesize that **expression of LPA$_1$, and LPA$_1$-GFP in a transgenic mouse line, can be a unique tool to identify and analyze NSCs as they convert into React-NSCs** and that **LPA$_1$ might play a role in NSC function**.

Objective 3. To validate LPA$_1$-GFP transgenic mouse as a tool to study React-NSCs.

Objective 3.1. To validate the expression of LPA$_1$ in hippocampal NSCs. For this purpose, we will quantify the contribution of NSCs to LPA$_1$-GFP$^+$ cells in the neurogenic niche of the DG and perform immunolabeling of LPA$_1$ to verify that the receptor is indeed expressed in LPA$_1$-GFP$^+$ NSCs.

Objective 3.2. To characterize the effects of MTLE in the DG of LPA$_1$-GFP mice. For this objective, we will perform a time course sacrificing the animals at six different time points after MTLE induction. Employing BrdU labeling and specific markers, we will evaluate the changes provoked in the neurogenic capacity of the DG and in LPA$_1$-GFP$^+$ NSCs by means of confocal microscopy-based quantitative image analysis.

Objective 3.3. To trace the expression of LPA$_1$-GFP in React-NSCs until their ultimate transformation into RAs. For this goal, we will follow the transformation of LPA$_1$-GFP$^+$ NSCs in the time course after seizure induction with the

help of BrdU labeling and specific cell markers and assess the expression of the transgene during NSC transformation and the potential expression in other cell types in the DG.

Objective 3.4. To validate the usefulness of LPA_1-GFP transgenic mice for ultrastructural studies. For this purpose, we will validate LPA_1-GFP specific expression in NSCs and React-NSCs in the DG of Sham and MTLE mice and search for putative ultrastructural particularities of these cell types via GFP pre-embedding immunohistochemistry for transmission electron microscopy (TEM).

Objective 3.5. To study the involvement of LPA_1 in the seizure-induced NSC activation. For this objective, we will resort to knockout (KO) mice of the receptor called maLPA_1, and their wild-type (WT) counterparts, to evaluate how the absence of LPA_1 affects cell proliferation and NSC activation after MTLE.

- We hypothesize that **regardless of the model of induction of MTLE NSCs and the neurogenic niche will be affected in a similar manner**.

Objective 4. To establish an alternative model of MTLE by intraamygdalar injection of KA.

Objective 4.1. Characterize cell proliferation and NSC activation in the DG of mice injected with KA into the amygdala. For this goal, we will optimize a protocol to consistently inject KA into the amygdalar region and study the changes induced in the DG of Nestin-GFP mice with the help of BrdU labeling and specific immunolabeling for confocal microscopy-based quantitative image analysis.

6. Materials and Methods

6. Materials and Methods

6.1. Animals

All the animals were housed with ad libitum food and water access, in 12:12h light cycle, and were 2 months old at the time of the start of the experiments. All procedures were approved by the University of the Basque Country EHU/UPV Ethics Committees (Leioa, Spain) and Diputación foral de Bizkaia under protocol M20/2015/236. All procedures followed the European directive 2010/63/UE and NIH guidelines.

Nestin-GFP transgenic mice, generated in the laboratory of Dr. Grigori Enikolopov at Cold Spring Harbor Laboratory (Cold Spring Harbor, NY, USA) (Mignone *et al.*, 2004), who also kindly provided the strain, were crossbred with C57BL/6 mice for at least 10 generations.

Nestin-CreER^{T2}/R26R:YFP mice, from Dr. Amelia J. Eisch laboratory (University of Texas Southwestern Medical Center, Dallas, TX, USA), were crossbred with C57BL/6-Tyr^{c-2J}/J (Jax labs, stock no. 000058), creating white furred albino mice in a C57BL/6 genetic background (Lagace *et al.*, 2007). A batch of these mice was hosted at the Catholic University of Leuven (Katholieke Universiteit Leuven, Leuven, Belgium), given tamoxifen and then subjected to the saline, EA and MTLE models at the Research Group for Neurobiology and Gene Therapy headed by Dr. Veerle Baekelandt. After that, the fixed brains were sent to us for analysis. Another batch of mice was sent to our laboratory at the Achucarro Basque Center for Neuroscience, subjected to tamoxifen injection and the saline, EA and MTLE models and further processed here.

LPA$_1$-GFP transgenic mice, generated by the GENSAT project at Howard Hughes Medical Institute (The Rockefeller University, NY, USA) (Gong *et al.*, 2003), were provided by Dr. Gerd Kempermann at the Center for Regenerative Therapies Dresden (Technische Universität Dresden, Dresden, Germany) and crossbred with C57BL/6 mice for at least 10 generations.

For the studies regarding absence of LPA$_1$, mice of the spontaneous variant maLPA$_1$-null (Estivill-Torrus *et al.*, 2008), derived from previously reported LPA$_1$-null (Contos *et al.*, 2000); and their WT counterparts (on a mixed background C57BL/6 x 3129SW) were kindly provided by Guillermo Estivill-Torrús at the Instituto de Investigación Biomédica de Málaga (IBIMA, Hospital Regional de Málaga, Málaga, Spain).

6.2. Tamoxifen injection

To induce YFP expression in the Nestin-CreER^{T2}/R26R-YFP mice, 1mg of tamoxifen (dissolved at 20mg/ml in corn oil) was administered intraperitoneally twice a day for 5 consecutive days. This experimental paradigm assures that upregulation of nestin in astrocytes following insult does not contaminate our results. The inducible expression

of GFP by tamoxifen was several days prior to the KA injection. Therefore, nestin upregulation in astrocytes due to KA injection could not translate into expression of YFP as nestin expression would start days after tamoxifen administration stopped.

6.3. Stereotaxic intrahippocampal injection

Mice were anesthetized with intraperitoneal ketamine (Dechra Veterinary Products, Barcelona, Spain)/medetomidine (Braun VetCare, Tuttlingen, Germany) (75:1 mg/kg) and received a single dose of the analgesic buprenorphine (1mg/kg) (Animalcare, York, United Kingdom) subcutaneously. After positioning in the stereotaxic apparatus, a 0.6mm hole was drilled at coordinates taken from Bregma to target the DG (based on (Franklin and Paxinos, 1997)): anteroposterior (AP) -1.8mm, laterolateral (LL) -1.6mm. A pulled glass microcapillary was inserted at -1.9mm dorsoventral (DV), and 50nl of saline (NaCl 0.9%, Sal group), KA (Sigma-Aldrich, St Louis, MO, USA) 0.74mM (0.037nmol, EA group) or KA 20mM (1nmol, MTLE group); or 500nl of LPS (4µg of lipopolysaccharides from *Salmonella enterica* serotype *typhimurium*, Sigma-Aldrich, St Louis, MO, USA) were delivered into the right hippocampus using a microinjector (Nanoject II, Drummond Scientific, Broomal, PA, USA). After 2min, the microcapillary was retracted, and the mice sutured and maintained on a thermal blanket until recovered from anesthesia. The animals were continuously monitored during the first hours following the procedure and once or twice daily after the first 24h.

6.4. Stereotaxic intraamigdalar injection

Mice were subjected to similar procedures as in the intrahippocampal KA injection except for the specifications that follow. A dose of 100nl of KA 12.96mM (1.3nmol) was injected to induce *status epilepticus* (SE) following previous literature (Alves *et al.*, 2017; Engel *et al.*, 2017), but coordinates taken from Bregma to target the right amygdalar complex were adapted to improve reproducibility and avoid crossing or contacting the lateral ventricle or the most lateral region of the hippocampus (Franklin and Paxinos, 1997): AP -1.4mm, LL -3.1mm and DV -4.7mm.

6.5. BrdU administration

For the NSC fate-chase experiments, the thymidine analog BrdU (Sigma-Aldrich, St Louis, MO, USA) was diluted in drinking water with 1% (w/v) sucrose at 1mg/ml concentration. For the proliferation analysis, BrdU was administered for 1w and animals were sacrificed 1d after BrdU removal from water (1w+1d). For differentiation analyses, animals were sacrificed 1m after either 1w- (1w+1m) or 1m-long (1m+1m) BrdU administrations in drinking water.

For the rest of experiments, BrdU was diluted in sterile phosphate-buffered saline (PBS) with 0.01N sodium hidroxyde and administered through intraperitoneal injections at 150mg/kg concentration. Nestin-GFP, LPA_1-GFP e and maLPA_1-null/WT mice were given four injections separated by 2-h intervals on the second or the sixth day (only for

the Nestin-GFP 7dpKAi analysis) after intrahippocampal injection of KA or Sal. Animals were sacrificed at different time points specified in each set of experiments.

6.6. Immunohistochemistry

Immunohistochemical techniques were performed essentially as described before following methods optimized for the use in transgenic mice (Encinas and Enikolopov, 2008; Encinas *et al.*, 2011b). Animals were subjected to transcardial perfusion with 30ml of PBS followed by 30ml of 4% (w/v) paraformaldehyde (PFA) in PBS, pH 7.4. The brains were removed and postfixed, with the same fixative, for 3h at room temperature, then transferred to PBS and kept at 4ºC.

Due to antigen sensitivity, mice whose brain sections were destined to LPA_1 immunostaining were perfused with periodate lysine PFA (PLP) fixative consistent of 0.01M sodium metaperiodate, 0.075M lysine and 4% PFA in 0.1M phosphate buffer (PB) (McLean and Nakane, 1974). The same fixative was used for overnight postfixation.

Serial 50µm-thick sagittal sections were cut using a Leica VT 1200S vibratome (Leica Microsystems GmbH, Wetzlar, Germany). Immunostaining was carried out following a standard procedure: the sections were incubated with blocking and permeabilization solution containing 0.25% Triton-X100 and 3% bovine serum albumin (BSA) in PBS for 3h at room temperature, and then incubated overnight with the primary antibodies (diluted in the same solution) at 4ºC. After thorough washing with PBS, the sections were incubated with fluorochrome-conjugated secondary antibodies diluted in the permeabilization and blocking solution for 3h at room temperature. After washing with PBS, the sections were mounted on slides with Dako fluorescent mounting medium (Dako, Carpinteria, CA). Those sections destined to the analysis of BrdU incorporation were treated, before the immunostaining procedure, with 2M HCl for 20min at 37ºC, rinsed with PBS, incubated with 0.1M sodium tetraborate for 10 min at room temperature, and then rinsed with PBS. The GFP signal from the transgenic mice was detected with an antibody against GFP for enhancement and better visualization.

The following primary antibodies were used: chicken anti-GFP (Aves laboratories, GFP-1020, 1:1,000), rat anti-BrdU (Bio-Rad, MCA2060, 1:400), rabbit anti-GFAP (Dako, Z0334, 1:1,500), goat anti-GFAP (Abcam, Ab53554, 1:1,000), rabbit anti-NeuN (Abcam, Ab177487, 1:500), rabbit anti-Iba1 (Wako, 019-19741, 1:1,000), rabbit anti-S100 (Dako, Z0311, 1:500), and rabbit anti-LPA_1 (EDG2, ThermoFisher Scientific, PA1-1041, 1:100). The secondary antibodies used, all in 1:500 concentration, were: goat anti-chicken Alexa Fluor 488 (ThermoFisher Scientific, A11039), donkey anti-chicken FITC (Rockland, 603-702-C37), donkey anti-rabbit Alexa Fluor 488 (ThermoFisher Scientific, A21206), donkey anti-rabbit Alexa Fluor 568 (ThermoFisher Scientific, A10043), donkey anti-rat Alexa Fluor 594 (ThermoFisher Scientific, A21209), donkey anti-rabbit Alexa Fluor 680 (ThermoFisher Scientific, A10043), and donkey anti-goat Alexa Fluor 680 (ThermoFisher Scientific, A21084). 4′,6-diamidino-

2-phenylindole (DAPI, Sigma-Aldrich), at 1:1,000, was also added to the sections during the incubation with the secondary antibodies to counterstain cell nuclei.

6.7. Pre-embedding immunohistochemistry for TEM

Mice destined to immunogold TEM study were perfused with saline followed by 4% PFA-0.5% glutaraldehyde. Brains were postfixed overnight at 4ºC in 4% PFA and then washed in 0.1M PB, after what they were sent to the Laboratory of Comparative Neurobiology, headed by Dr. José Manuel García Verdugo, at the Instituto Cavanilles de Biodiversidad y Biología Evolutiva (Universidad de Valencia, Paterna, Spain) where the samples were processed by Dr. Arantxa Cebrián Silla.

The immunogold-labeling protocol was performed as described (Sirerol-Piquer *et al.*, 2012). 50µm-thick coronal sections were obtained employing a VT 1000M vibratome (Leica) and incubated in 0.1% sodium borohydride to eliminate glutaraldehyde crosslinks. In order to permeabilize the tissue without damaging membranes, sections were cryoprotected in 25% sucrose for 30min and were subjected to 5 freeze-thaw cycles in methylbutane at -60ºC. Next, sections were incubated in blocking solution with acetylated bovine seroalbumin (BSAc, Aurion, Wageningen, The Netherlands) and the primary antibody chicken anti-GFP (Aves laboratories) for 72h at 4ºC. Sections were then washed with PB and blocked with 0.5% BSAc and 0.15% fish gelatin for 1h. After that, they were incubated with the 0.8nm-colloidal gold-conjugated secondary antibody (1:50) overnight at room temperature. To increase the size of colloidal gold particles and make them visible for TEM, samples were washed with 0.1M PB and 2% sodium acetate and incubated with silver intensification kit (Aurion) for 10-30min. To stabilize silver particles and avoid their loss, sections were incubated with 0.05% gold chloride and fixed with 0.3% sodium thiosulfate. Last, samples were postfixed with 2% glutaraldehyde and processed for TEM.

Sections were treated with 1% osmium tetroxide with 7% glucose for 30min, then dehydrated with increasing alcohol concentrations and contrasted with 2% uranyl acetate for 2h, after which they were included in epoxy resin (Durcupan, Sigma-Aldrich). Once polymerized (2d later), SGZ-containing samples were selected and 1.5µm-thick semithin sections were obtained with a diamond blade. These sections were stained with toluidin blue and analyzed with an Eclipse E800 (Nikon, Tokio, Japan) optic microscope. For TEM ultrastructural study with a Tecnai G2 Spirit (FEI, Hillsboro, OR, USA) electron microscope, 60-70nm-thick ultrathin sections were obtained. Images were acquired with a Morada digital camera (Olympus Soft Imaging Solutions, Münster, Germany).

6.8. Image capture

All fluorescence immunostaining images were collected employing a Leica SP8 (Leica, Wetzlar, Germany) laser scanning microscope and LAS X software. Brightness, contrast, and background were adjusted equally for the entire image using the "histogram" set of tools without any further modification. All images shown are

projections from z-stacks ranging from 3 to 20µm of thickness, typically 10µm for individual cell images.

6.9. Cell quantification

Quantitative analysis of cell populations in constitutive transgenic mice was performed by design-based (assumption free, unbiased) stereology using a modified optical fractionator sampling scheme as previously described (Encinas and Enikolopov, 2008; Encinas *et al.*, 2011b). Slices were collected using systematic-random sampling. Hemispheres were sliced sagittally in a lateral-to-medial direction including the entire DG. The 50-µm slices were collected in 6 parallel sets, each set consisting of approximately 12 slices, each slice 250 µm apart from the next.

For proportion quantifications, representative numbers ranging from 50 to 300 cells of interest were quantified and classified in randomly-selected confocal z-stacks from 30µm below to 30µm above the GCL using a 63x oil immersion objective.

Cells were categorized as NSCs, ANPs, neurons, astrocytes, oligodendrocyte progenitor cells (OPCs) or microglia following the criteria described previously (Encinas and Enikolopov, 2008; Encinas *et al.*, 2011b). NSCs were defined as radial glia-like cells positive for Nestin-GFP, YFP or LPA_1-GFP and GFAP with the cell body located in the SGZ or the lower third of the GCL and with an apical process extending from the SGZ towards the ML through the GCL. ANPs were defined as Nestin-GFP-positive cells devoid of GFAP immunostaining with the cell body located in the SGZ or the lower third of the GCL and with none or short horizontal processes. Neurons were defined as $NeuN^+$ cells with round big nucleus located in the GCL. Astrocytes were identified as GFAP- or S100β-positive cells with stellate morphology. OPCs were identified as Nestin-GFP-positive cells negative for GFAP with arborizing processes in every possible direction. Microglia was identified by Iba1 immunostaining. Reentry into the cell cycle was evaluated as proportion of Ki67-positive among BrdU-positive cells.

In the LPA_1-GFP time course, React-NSC-derived RAs were defined as LPA_1-GFP-positive cells with GFAP and S100β immunostaining, hypertrophic soma, thickened processes and stellate morphology, whereas their LPA_1-GFP-negative counterparts were considered parenchymal astrocyte-derived RAs.

In the maLPA_1-null/WT mice experiments, NSCs were defined as $nestin^+GFAP^+$ cells with an apical process extending from the SGZ towards the ML through the GCL. At the 2w-time point, though, we did not take into account the radial morphology due to the expected morphological change induced by seizures.

For total numbers of BrdU-positive cells, all $BrdU^+$-nuclei in the SGZ and the GCL were counted following bias-free stereology employing a Zeiss ApoTome2 (Carl Zeiss, Jena, Germany) microscope with a 40x oil immersion objective.

For the type of NSC division, the analysis was carried out in flat projections from 20-25µm-thick z-stacks. Only those pairs of cells whose nuclei were clearly still in contact

were scored. Asymmetric cell division was defined as the daughter cell of the NSC bearing none or short (less than 10µm) and thin (less that 1µm) processes, and lacking GFAP expression. Symmetric division was defined when the daughter cell presented clearly defined prolongations of at least 10µm in length and 1µm in thickness immunostained for GFAP.

6.10.Statistical analysis

SigmaPlot (San Jose, CA, USA) was used for statistical analysis. For analysis of pairs of groups, a Student´s t test was performed. For analyses involving more than two groups, a one-way ANOVA was performed. When evaluating the time x treatment interaction in the LPA_1-GFP time course a two-way ANOVA was employed, and analyses only continued when normality assumptions were fulfilled.

In all cases, all pairwise multiple comparisons (Holm-Sidak method or Dunn's) were used as a posthoc test to determine the significance between groups in each factor. Only $p<0.05$ is reported to be significant. Data are shown as mean ± standard error of the mean (SEM).

7. Results

7. Results

7.1. NSC-fate chase with continuous exposure to BrdU confirms they follow a "disposable"-stem cell model

Proliferation in the short term originates mostly neuronal fate-committed ANPs

One of the main issues regarding NSC biology is whether they can go back and forth between division and quiescence or not. Although the evidence points at that they do not do it, the lack of observation of this behavior could be due to a very long cell cycle or too sporadic entry (and reentry) into the cell cycle easy to miss by the normal division markers and BrdU pulse-and-chase experiments. For this purpose, we resorted to a continuous labeling protocol to guarantee that every cycling cell was "captured" and thus observable, along with its progeny, at posterior time points.

To firstly evaluate the initial proliferative potential of DG populations, a short-term analysis of dividing cells in the neurogenic niche was performed. With the objective of labeling proliferating cells, we took advantage of the thymidine analog BrdU, that is incorporated during the S phase of the cell cycle and can be detected with specific antibodies (Gratzner, 1982). BrdU was administered in drinking water to 2-month-old Nestin-GFP mice for 7d (1w) and animals were sacrificed 1d after BrdU removal (1w+1d group, **Fig. 11A**). This initial paradigm serves us to assess which cell types are more proliferative in the normal DG and help us interpret the data in longer-term experiments.

The proliferation analysis showed a great majority of Nestin-GFP$^+$ ANPs (more than a 70%) among the BrdU-labeled cell population, with a low proportion of Nestin-GFP$^+$GFAP$^+$ NSCs (Fig. **11B** and **C**). In agreement with the fact that NSCs are a predominantly quiescent cell type but constitute an approximate 2-5% of dividing cells in a given moment (Encinas *et al.*, 2006; Kronenberg *et al.*, 2003), they accounted for a 6% of cells that had experimented division. A slightly less frequent type of BrdU-positive cells was classified as OPCs, although most of them were found in the ML adjacent to the GCL or below the SGZ (**Fig. 11B** and **C**). A proportion of a 1% of BrdU-immunopositive cells was identified as microglia, mostly also in the ML or the hilus but within the limits of quantification (**Fig. 11B** and **D**). Similarly, a 1% of BrdU$^+$ cells was classified as neurons. Conservative criteria were considered for this category and not only NeuN immunostaining was taken into account but also round or slightly oval nuclear morphology, GCL location and absence of Nestin-GFP labeling. Thus, early NBs with Nestin-GFP expression were classified as ANPs in our quantifications. Another 1% of BrdU-labeled cells was represented by astrocytes.

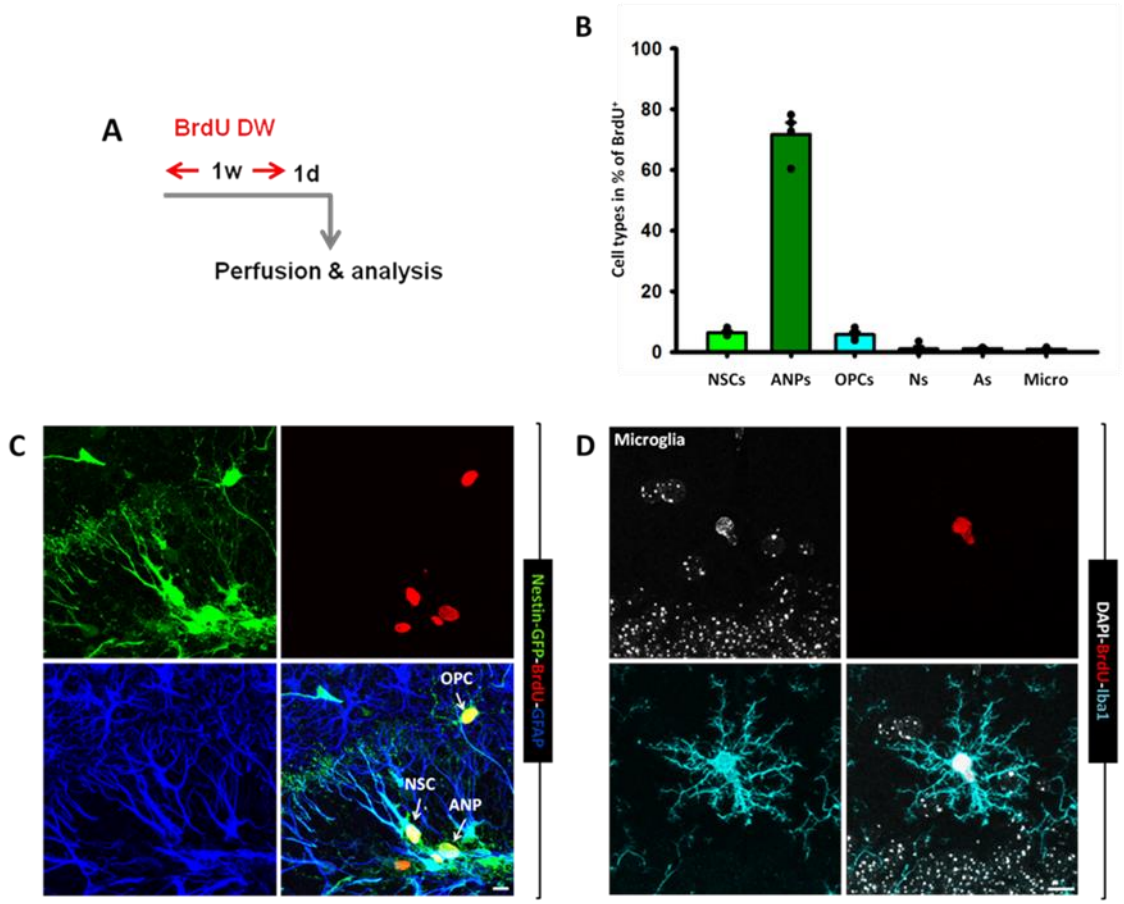

Figure 11. Proliferation analysis reveal the early stages of the neurogenic cascade. (**A**) In a proliferation paradigm, BrdU was administered to mice in drinking water for 1w and animals were sacrificed 1d after removing BrdU from water. (**B**) Quantifications showing the proportion of each cell type among the BrdU⁺ population in the neurogenic niche based on immunohistochemical markers and morphology. As the graph shows, most cells immunoreactive to BrdU were ANPs followed by NSCs (and OPCs). (**C** and **D**) Confocal microscopy images showing BrdU-positive cells observed in the proliferation analysis. (**C**) Both a NSC and an ANP in the SGZ are immunopositive for BrdU; a BrdU⁺ OPC is also observable adjacent to the GCL. (**D**) One of the few instances in which a microglial cell, located right above the GCL, was found positive for BrdU. Images correspond to maximum projections from approximately 10µm-thick z-stacks. Bars show mean ± SEM. Dots show individual data. Scale bars are 10µm. Ns: neurons. As: astrocytes. Micro: microglia.

Differentiation of dividing cells originates predominantly a neuronal fate in the DG

Using the same 1w-long BrdU-administration paradigm but sacrificing the animals 30d (1m) later (1w+1m group, **Fig. 12A**), we aimed to analyze the differentiation spectrum in the DG neurogenic niche. Waiting for a whole month should assure that every initially-dividing cell has reached its final fate, even those with long maturing processes such as GCs or astrocytes (Encinas and Enikolopov, 2008; Encinas *et al.*, 2011b; Encinas *et al.*, 2006). As expected, BrdU-positive cells in the DG were mainly identified as neurons located in the GCL (**Fig. 12B** and **C**). This cell type accounted for almost a 70% of the cells derived from division in the first week. A proportion of a 13% of BrdU-labeled cells was again classified as OPCs, what shows this cell type continues dividing in normal conditions (**Fig. 12B** and **D**). A noticeable 10% of newly-born cells

was represented by astrocytes, despite their negligible mitotic potential found in the proliferation analysis and therefore suggesting their origination from NSCs after division. An approximate 2.5% was classified as microglia cells (**Fig. 12B** and **E**). ANPs and NSCs, on their part, represented only a 1.6 and 1%, respectively, of BrdU-labeled cells.

In an additional differentiation experiment, we performed a long-term administration of the BrdU protocol. This was done with the purpose of maximizing the cell populations that incorporate BrdU and avoiding missing divisions of cells which enter the cell cycle with very low probability. The long-term-administration protocol consisted of BrdU administration in drinking water during 1m and sacrificing the mice after another 1m (1m+1m group, **Fig. 13A**). The overall result of this experiment was similar to the previous one but the obtained proportions were slightly different. Almost an 85% of BrdU-positive cells were categorized as neurons, confirming the data in the previous protocol in which neurons accounted for most division-derived cells (**Fig. 13B** and **C**). We observed a proportion of a 6% of astrocytes among cells immunopositive for BrdU (**Fig. 13B** and **D**). OPCs and microglia cells were also found among the BrdU-labeled population representing, respectively, a 3.6 and 1.1% (**Fig. 13B**).

In both differentiation analyses the proportions of $BrdU^+$ cells that were classified as NSCs or ANPs were extremely low, reaching the lowest points in the 1m+1m paradigm in which they represented together less than a 1% (**Fig. 13B**). Therefore, dividing NSCs or ANPs do not remain for a long period of time without transforming into another cell type (or dying) in the DG neurogenic niche.

Reentry into the cell cycle only occurs in the short term

We were especially interested in evaluating the reentry capacity of cells that have already divided. In all three performed paradigms, we quantified the proportion of BrdU-positive cells that expressed Ki67, a marker of cell division (Scholzen and Gerdes, 2000), and took it as frequency of reentry into a new round of cell division. In 1w+1d animals, a proportion of more than a 41% of cells was reentering the cell cycle (**Fig. 14A** and **C**), whereas in both differentiation analyses (1w+1m and 1m+1m) the levels of reentry were below a 1.5% or not even detected in some animals (**Fig. 14A**).

With the purpose of analyzing the potential NSC return to quiescence, we specifically focused on NSC reentry. We quantified the percentage of $BrdU^+$ NSCs that colocalized with Ki67 as a token for reentry frequency. Even though as high as a 75% of BrdU-labeled NSCs were also immunopositive for Ki67 in the proliferation assay (1w+1d), not a single NSC was observed with expression of the proliferation marker Ki67 1m after BrdU removal from drinking water (**Fig. 14B**). Not a NSC with BrdU incorporated that remained as a NSC 1m later, although very few were found, was detected reentering the cell cycle.

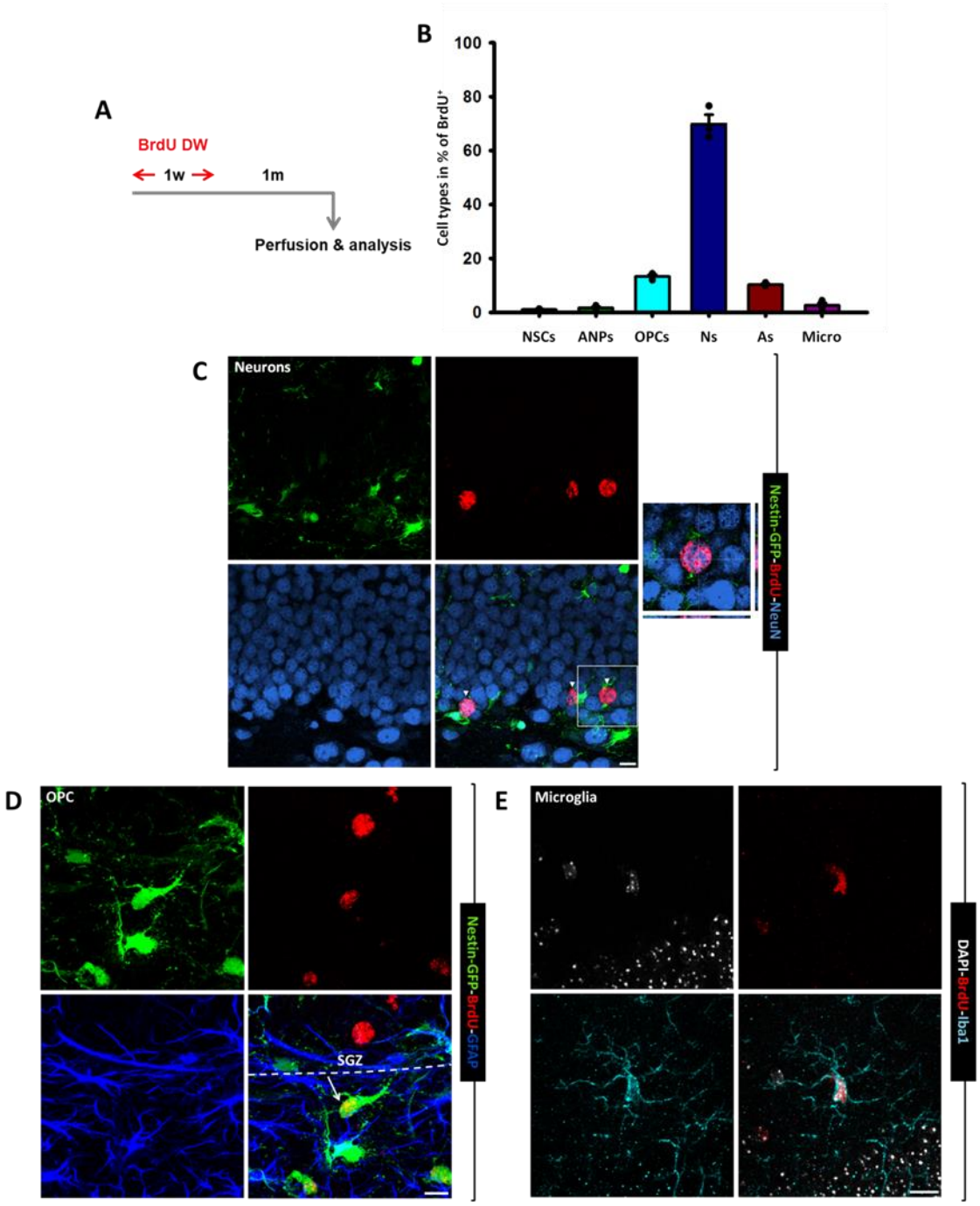

Figure 12. Differentiation analysis shows the predominant neurogenic fate in the DG. (**A**) In the 1w+1m differentiation analysis, animals were sacrificed 1m after 1w-long BrdU administration in drinking water. (**B**) Quantifications showing the proportion of each cell type among the BrdU⁺ population in the neurogenic niche. Most BrdU-positive cells were neurons (**C**). Astrocytes represented an approximate 10% of the cells immunoreactive to BrdU. OPCs also were a prominent proliferative cell type, although they were especially found either above the GCL or below (**D**) the SGZ. (**C-E**) Confocal microscopy images showing representative BrdU-positive cells found in the DG of these animals. (**C**) Several BrdU⁺NeuN⁺ neurons (arrowheads) can be observed in the GCL. The insert to the right is a single-plane close-up of the square in the bottom right image. (**D**) A Nestin-GFP-positive GFAP-negative OPC that also incorporated BrdU is observed 1m after 1w-long BrdU administration. (**E**) An Iba1⁺BrdU⁺ microglia cell found in contact with the GCL. Images correspond to maximum projections from approximately 10µm-thick z-stacks. Bars show mean ± SEM. Dots show individual data. Scale bars are 10µm. Ns: neurons. As: astrocytes. Micro: microglia.

Together, these results strongly suggest that the neurogenic cascade in the DG follow the same principles that have been proposed at the population level no matter the approach. First, in a given moment few NSCs are dividing but, when they do, they reenter the cell cycle shortly after the initial activation. Although no direct proof was provided, our results agree with the expected majority of NSC asymmetric divisions due to the decrease in the NSC contribution to BrdU-labeled cells that we report in both differentiation analyses. Most divisions in the DG render neuronal progenitors that ultimately give rise to neurons, but astrocytes are generated too. Since astrocytes showed a very limited proliferative capacity, our data support the notion that newborn astrocytes are generated through NSC terminal differentiation.

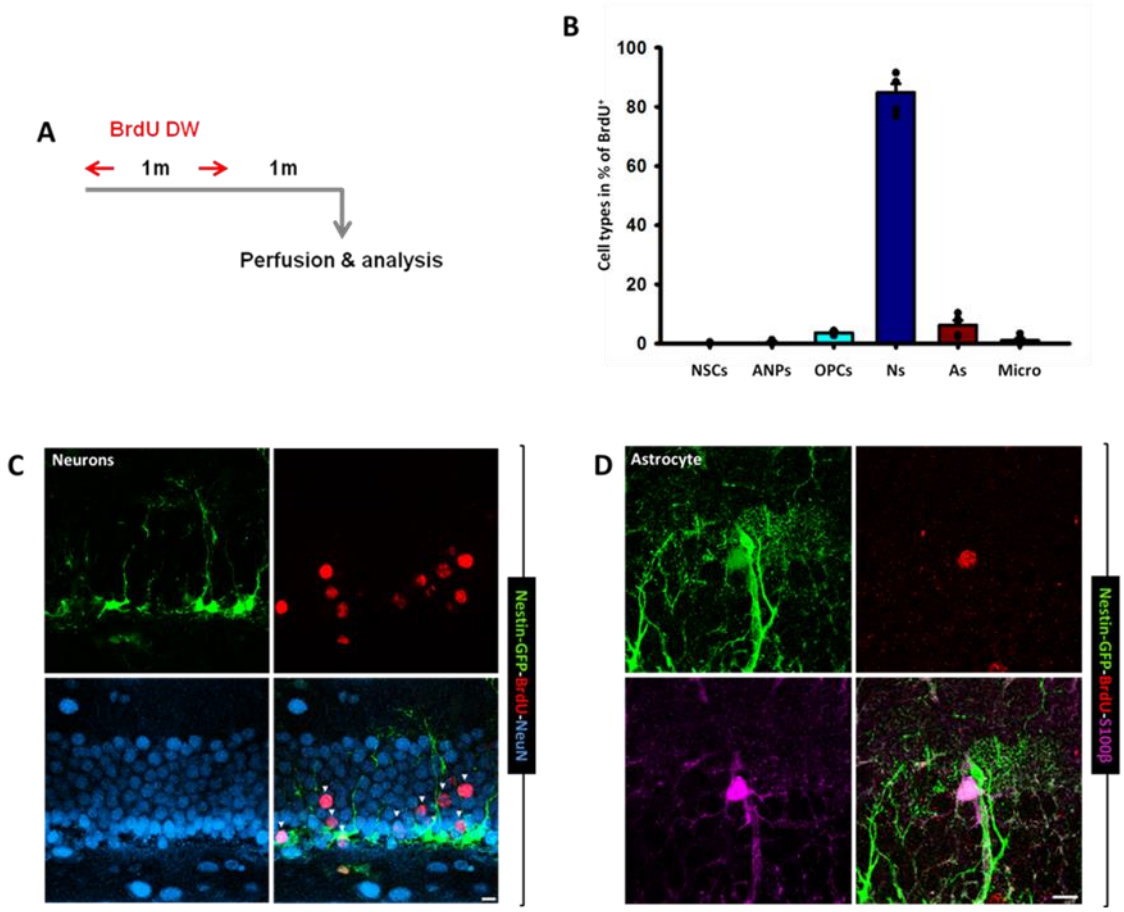

Figure 13. Long-term exposure to BrdU does not alter the neurogenic/astrocytic cell fate. (**A**) In the 1m+1m differentiation analysis, animals were sacrificed 1m after 1m-long BrdU administration in drinking water. (**B**) Quantifications showing the proportion of each cell type among the BrdU⁺ population in the neurogenic niche showing the neurogenic fate of most newborn cells (**C**) followed by astrocytes (**D**). (**C** and **D**) Confocal microscopy images showing representative BrdU⁺ cells found in the DG of these animals. (**C**) A number of BrdU⁺NeuN⁺ neurons (arrowheads) can be observed in the GCL. (**D**) An S100β-positive astrocyte with BrdU incorporated is situated in the upper part of the GCL. Note that it presents a dim Nestin-GFP expression, possibly showing the recent NSC differentiation. Images correspond to maximum projections from approximately 10µm- (**C**) and 3µm-thick (**D**) z-stacks. Bars show mean ± SEM. Dots show individual data. Scale bars are 10µm. Ns: neurons. As: astrocytes. Micro: microglia.

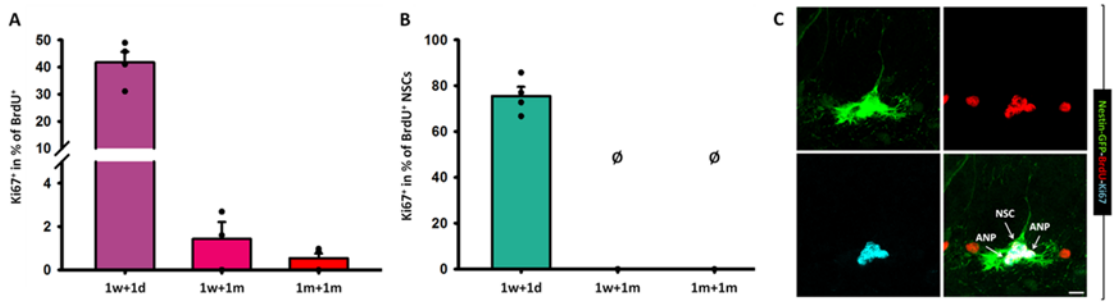

Figure 14. Reentry into the cell cycle and NSC reactivation are low-probability events in the long term. (**A**) Quantifications of reentry into the cell cycle, evaluated as percentage of Ki67-positive among BrdU-positive cells. Reentry into the cell cycle was high only in the proliferation experiment (1w+1m), representing divisions of both NSCs and ANPs following NSC activation. In the differentiation analyses (1w+1m and 1m+1m groups) very few cells were found reentering into the cell cycle. (**B**) Quantifications of specifically NSC reentry. A high percentage of BrdU⁺ NSCs were dividing again 1 day after 1w-long BrdU administration but not a single instance of this capacity was found when waiting 1 month after BrdU withdrawal from drinking water. (**C**) Confocal microscopy image showing a cluster formed by a NSC and two ANPs immunopositive for both BrdU and Ki67. Images correspond to maximum projections from approximately 10µm-thick z-stacks. Bars show mean ± SEM. Dots show individual data. Scale bar is 10µm.

7.2. MTLE provoked by KA injection into the DG causes a shift in NSC division towards reactive astrogliogenesis

Neuronal activity increases cell division in the short term and activates NSCs

As mentioned, NSC activation has been related to neuronal excitability (Pineda and Encinas, 2016), which is maximized in some neurological disorders that involve seizures such as MTLE (Huttmann *et al.*, 2003). Additionally, it is still unclear whether MTLE increases or decreases neurogenesis and at which steps seizures exert their effect. Thus, we are interested in testing how neuronal activity affects NSC behavior in terms of activation and fate.

To evaluate the hypothesis that different levels of neuronal activity lead to different NSC responses, we subjected Nestin-GFP animals to two models of neuronal hyperexcitation. For these models we chose a local administration of KA into the DG. Intrahippocampal KA injection has been largely employed to reproduce the pathophysiological features of human MTLE: spontaneous seizures and hippocampal sclerosis (Babb *et al.*, 1995; Bouilleret *et al.*, 1999; Kralic *et al.*, 2005; Nitta *et al.*, 2008); and for that model we injected 1nmol of KA in 50nl of saline. In addition, we wanted to mimic EA that occurs between seizures without triggering these seizures, for which we resorted to a 1/27 dilution of the previous KA dose: 0.037nmol in 50nl of saline. No seizures were detected in Sal or EA animals.

To determine cell proliferation in the DG after acute KA injection, we administered BrdU intraperitoneally to these Sal-, EA-, or MTLE-treated mice at 2 or 6 days post-KA injection (dpKAi) and sacrificed them 1d later. Overall proliferation, measured by total number of $BrdU^+$ cells, expectedly increased in KA-injected animals at 3dpKAi, with a 45% of rise in EA and a 150% in MTLE compared to Sal animals (**Fig. 15A**). This increase, however, only persisted, and even grew to a 160%, in EA mice at 7dpKAi (**Fig. 15B**). The total number of $BrdU^+$ NSCs was significantly higher in MTLE mice at both time points (over a 500% increase at 3dpKAi and 240% at 7dpKAi compared to Sal mice), but ANP proliferation was not increased (**Fig. 15A-D**). In fact, the number of dividing ANPs was reduced almost a 70% compared to Sal animals and more than an 80% compared to EA animals at 7dpKAi (**Fig. 15A** and **B**).

EA, however, not only promoted NSC activation at 3 and 7dpKAi (100% and 250% increase, respectively) but also ANP division at both time points (about a 45% at 3dpKAi and a 100% at 7dpKAi) (**Fig. 15A** and **B**). Dividing astrocytes ($BrdU^+GFAP^+$ cells with stellate morphology) were rare and their number was not affected after EA or MTLE (**Fig. 15A** and **B**). $BrdU^+$ cells found were almost completely restricted to the SGZ in Sal and EA animals, but in MTLE animals these cells were also found in the hilus and the ML (although $BrdU^+$ cells in these areas were excluded from the quantifications, **Fig. 15 E**).

To summarize, MTLE induced a rapid and massive activation of NSCs whereas EA induction of NSC activation was milder but also promoted ANP proliferation.

NSCs become reactive in MTLE

Importantly, MTLE not only activated NSCs in higher numbers but triggered in them the acquisition of a characteristic morphology that could answer to a "reactive phenotype". These NSCs, which will be called React-NSCs from this point forward, displayed after seizures obvious radial process thickening, multibranching with basal processes and Nestin-GFP and GFAP overexpression (**Fig. 15D**), very similar criteria to those used to describe RAs. The mentioned morphological changes, in addition to the migration in some cases from the SGZ to the GCL, led to the loss of the radial morphology in favor of a ramified one and contributed to the disruption of the neurogenic niche.

Remarkably, this React-NSC phenotype spread to almost every NSC including those that had experimented cell division as shown by BrdU immunolabeling (**Fig. 15D**). This made us wonder whether the massive NSC activation induced by MTLE could also have provoked a change in their cell-cycle program that derived in the generation of a different cascade in the DG.

React-NSCs divide symmetrically

As we have introduced, we observed that in MTLE animals most of the daughter cells of NSCs (also positive for BrdU labeling) presented a similar phenotype to that of the mother cell, suggesting a switch from the typical asymmetric division in normal conditions (Encinas *et al.*, 2011b) to a symmetric mode. If this were true, seizures might induce a switch in the differentiation of activated React-NSCs possibly leading to reactive astrogliogenesis.

To test this hypothesis, we resorted to inducible Nestin-Cre-ER^{T2}/R26R:YFP transgenic mice and performed genetic fate-mapping after tamoxifen injection (Lagace *et al.*, 2007). Nestin-Cre-ER^{T2}/R26R:YFP is a double transgenic mouse in which expression of the mutant recombinase Cre-ER^{T2} is regulated by the expression of nestin and can only access the genomic DNA upon tamoxifen administration, being the target in this case a floxed stop sequence that prevents the expression of the YFP reporter. Therefore, tamoxifen induces a recombination in nestin-expressing cells, mostly NSCs in our case, (see below) that leads to YFP expression in them and their progeny.

First, we analyzed the cell types in which YFP expression was activated 3d after tamoxifen induction. As expected, most YFP-positive cells were NSCs, with over an 85% representation, and proportions of an approximate 8% of ANPs and a 5% of NBs were found (**Fig. 16A** and **B**).

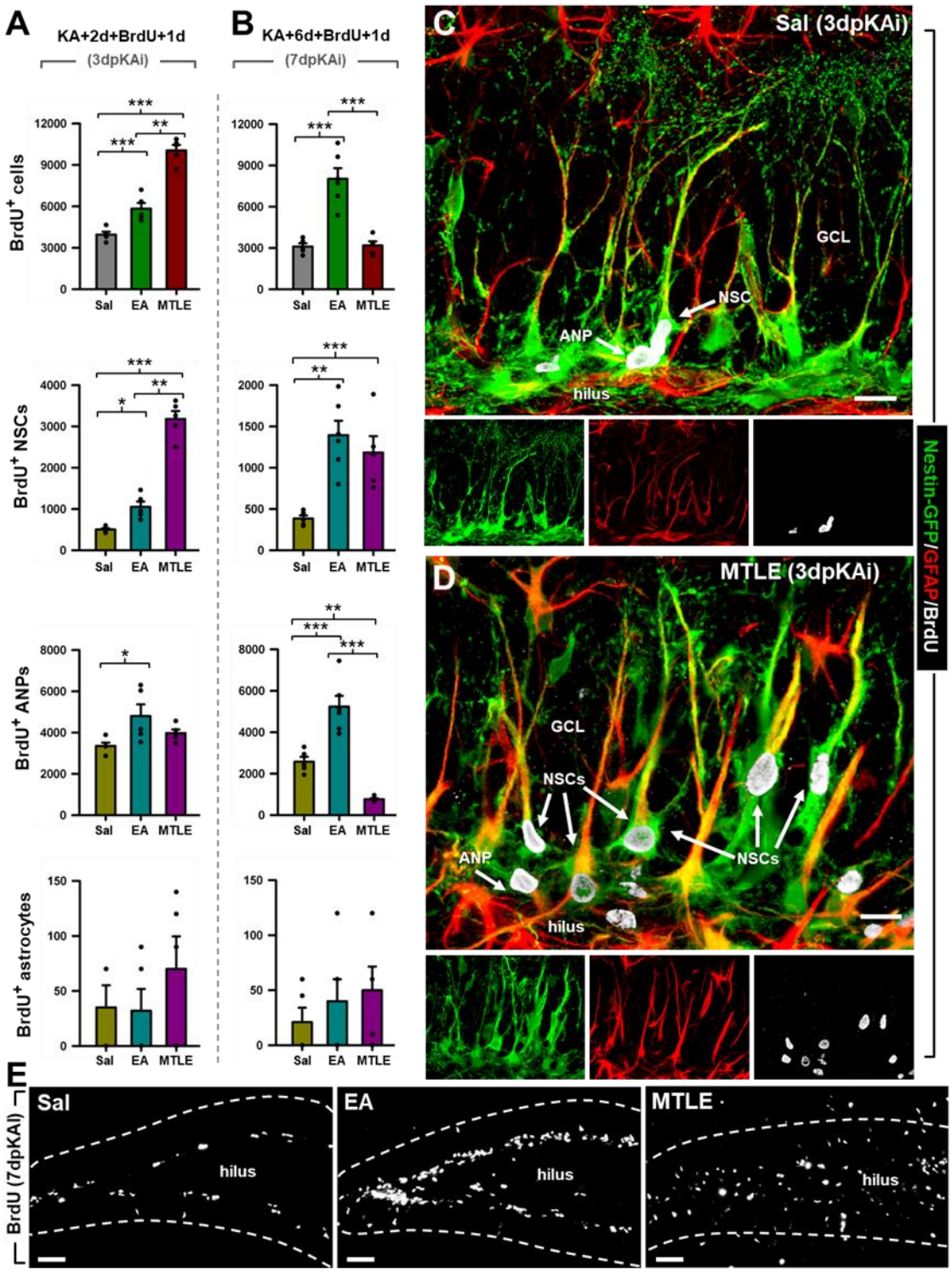

Figure 15. EA and MTLE promote cell proliferation and NSCs activation. (**A** and **B**) Quantification at 3 (**A**) and 7dpKAi (**B**) of the absolute number of BrdU⁺ cells and BrdU⁺ NSCs (Nestin-GFP-positive, GFAP-immunopositive cells with radial morphology located in the SGZ), ANPs (Nestin-GFP-positive, GFAP-negative cells located in the SGZ with short processes), and astrocytes (GFAP-positive with stellate morphology). *p < 0.05, **p < 0.01, ***p < 0.001 by all pairwise multiple comparison by Holm-Sidak post hoc test. Bars show mean ± SEM. Dots show individual data. (**C** and **D**) Representative confocal microscopy images showing the DG from Sal (**C**) and MTLE (**D**) Nestin-GFP mice after staining for GFP, BrdU, and GFAP at 3dpKAi. (**E**) Representative images showing cell proliferation in the DG of Sal (left), EA (middle), and MTLE (right) mice at 7dpKAi. Scale bar is 15µm in (**C**) and (**D**) and 50µm in (**E**).

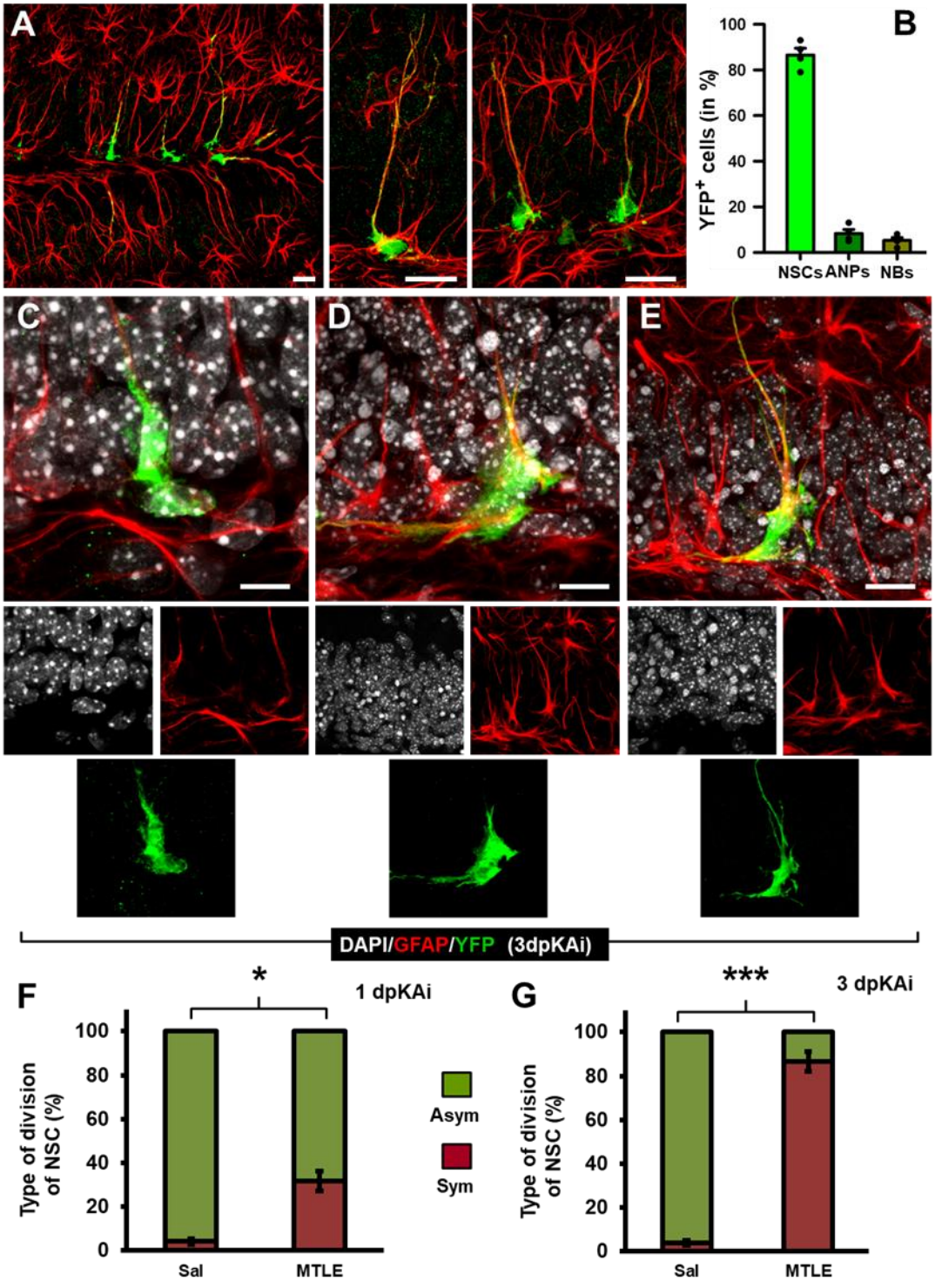

We next performed a short-term lineage analysis of YFP-expressing cells in inducible Sal and MTLE mice at 1 and 3dpKAi. We searched for pairs of YFP^+ cells, joined by the cytoplasm, whose nuclei could be unequivocally identified less than 5µm apart so that there was no doubt that the pairs of cells had been originated from cell division (**Fig. 16C-E**). To meet with our criteria, one of the cells had to be $GFAP^+$ and with NSC morphology so that the clones contained at least one NSC. In Sal mice, most of these clones contained a NSC and an ANP and thus derived from an asymmetric division (**Fig. 16C**, **F** and **G**). In contrast, in MTLE mice as soon as 1dpKAi we found a

Figure 16. React-NSCs divide symmetrically. (**A**) Confocal microscopy images (projection from z-stacks) showing activation of YFP expression in NSCs in the DG of inducible Nestin-CreER^{T2}/R26R:YFP transgenic mice. The animals received an injection of tamoxifen twice a day for 5d and were sacrificed 1d after the last injection. (**B**) Quantification of YFP-expressing cells 1d after the last injection of tamoxifen. (**C-E**) Confocal microscopy images of pairs of cells undergoing cell division (note that the cytoplasm is still united) in Sal (**C**) and MTLE mice at 1 (**D**) and 3dpKAi (**E**). Sal/KA was injected 3 days after tamoxifen treatment was finished to avoid potential *de novo* expression of nestin (and YFP) in reactive parenchymal astrocytes, which would interfere with the results. The asterisks indicate the nuclei of the YFP$^+$ cells. (**F** and **G**) Quantification of the type of cell division of YFP-expressing NSCs at 1 (**F**) and 3dpKAi (**G**) time points. The "asymmetric" category was assigned when the daughter cell had no processes, or short (less than 10µm) and thin (less that 1µm) processes lacking GFAP expression, as in (**C**). The "symmetric" category was assigned when the daughter cell expressed GFAP and had at least one long (more than 20µm) cytoplasmic process. Scale bars are 20µm in (**A**), 10µm in (**C**) and (**D**), and 15µm in (**E**). *$p < 0.05$ and ***$p < 0.001$ by Student's t test. Bars show mean ± SEM.

significantly increased proportion of NSC-derived clones formed by a NSC and a GFAP-expressing cell with long processes (**Fig. 16D** and **F**). At 3dpKAi the majority of the clones belonged to this symmetric-division category (**Fig. 16E** and **G**).

MTLE-induced React-NSCs differentiate into RAs

The observed switch in NSC division and change in morphology towards React-NSCs made us wonder whether the differentiation of these cells after MTLE treatment would lead to reactive astrogliogenesis. To test this, we subjected tamoxifen-treated Nestin-Cre-ER^{T2}/R26R:YFP transgenic mice to Sal, EA, or MTLE treatments (**Fig. 16**) and evaluated the fate of NSC-derived cells at 3, 14, and 30dpKAi (**Fig. 17** and **18**). Firstly, we observed an increase, sustained in time, in the total number of YFP-expressing cells with neuronal hyperactivity, *i.e.*, in EA and MTLE groups, compared to Sal mice (**Fig. 17A** and **18**). This increase was statistically significant only between MTLE and Sal groups at 3dpKAi (**Fig. 18A**) but between both KA-treated groups and Sal mice at 14 (**Fig. 18B**) and 30dpKAi (**Fig. 18C**).

Regarding the cell fate of the NSC-derived cells, we found no changes at 3dpKAi (**Fig. 18A**). At later time points, we observed that most NSC-derived cells were neurons in Sal and EA mice (**Fig. 17B** and **18B** and **C**). However, in MTLE mice the neuronal population was a minority among the total YFP-expressing population and the vast majority corresponded to RAs unambiguously distinguished by their multibranched hypertrophic morphology (**Fig. 17A**) and expression of GFAP and S100β (**Fig. 17C** and **D**). We avoided interference with our results due to the possible upregulation of nestin in parenchymal astrocytes by inducing the expression of YFP with tamoxifen several days prior to the KA injection. Therefore, nestin upregulation in astrocytes following KA injection could not lead to YFP expression as that of nestin would start days after tamoxifen administration stopped. The confirmation that this strategy worked is that we did not find YFP$^+$ astrocytes anywhere but in the SGZ or the GCL or regions in contact with them.

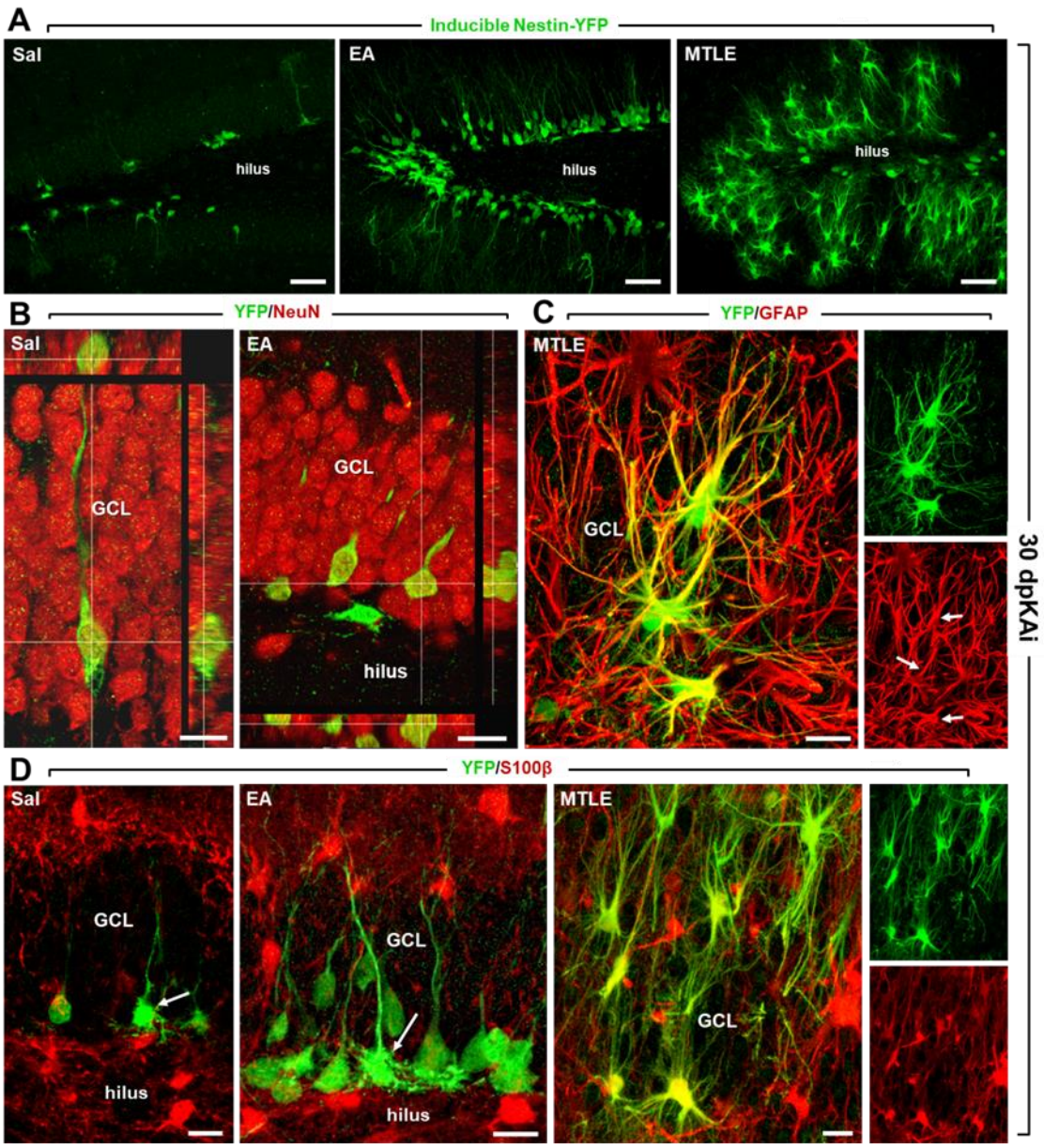

Figure 17. Neurogenesis and astrogliogenesis in inducible Nestin-CreER^{T2}/R26R:YFP transgenic mice. (**A**) Confocal microscopy images of the DG after staining for YFP show the neurogenic effect of EA and the reactive astrogliogenic effect of MTLE at 30dpKAi. (**B**) Examples of NSC-derived newborn neurons (YFP$^+$NeuN$^+$) in Sal (left) and EA (right) mice. Both images are single focal planes extracted from 20µm-thick z-stacks. (**C**) Example of NSC-derived newborn reactive astrocytes (YFP$^+$GFAP$^+$) in MTLE mice. The image corresponds to a projection from a 20µm-thick z-stack. Arrows in the red (GFAP) panel point at the processes colocalizing with YFP. (**D**) Examples of YFP$^+$ NSCs (arrows) and neurons lacking S100β in Sal (left) and EA (middle). In these two groups, most NSC-derived cells were neurons. In MTLE (right), S100β-expressing RAs unambiguously distinguished by their multibranched hypertrophic morphology constituted the vast majority of YFP$^+$ cells. Images are single focal planes extracted from 20µm-thick z-stacks. Scale bar is 40µm in (**A**), 15µm in (**B**), and 10µm in (**C**) and (**D**).

Inflammatory response alone does not increase NSC activation

Lastly, we wondered whether NSCs become React-NSCs not because of neuronal hyperactivity *per se* after MTLE, but because of secondary inflammation following

seizures. Hyperexcitation leads to excitoxicity-derived loss of neurons, a known hallmark of MTLE (Sharma *et al.*, 2007), which triggers an inflammatory response that could be partly responsible of the phenotypical changes we observed. To test this possibility, we injected LPS intrahippocampally to Nestin-GFP mice and compared NSC activation and phenotype with those observed in Sal, EA and MTLE animals. To

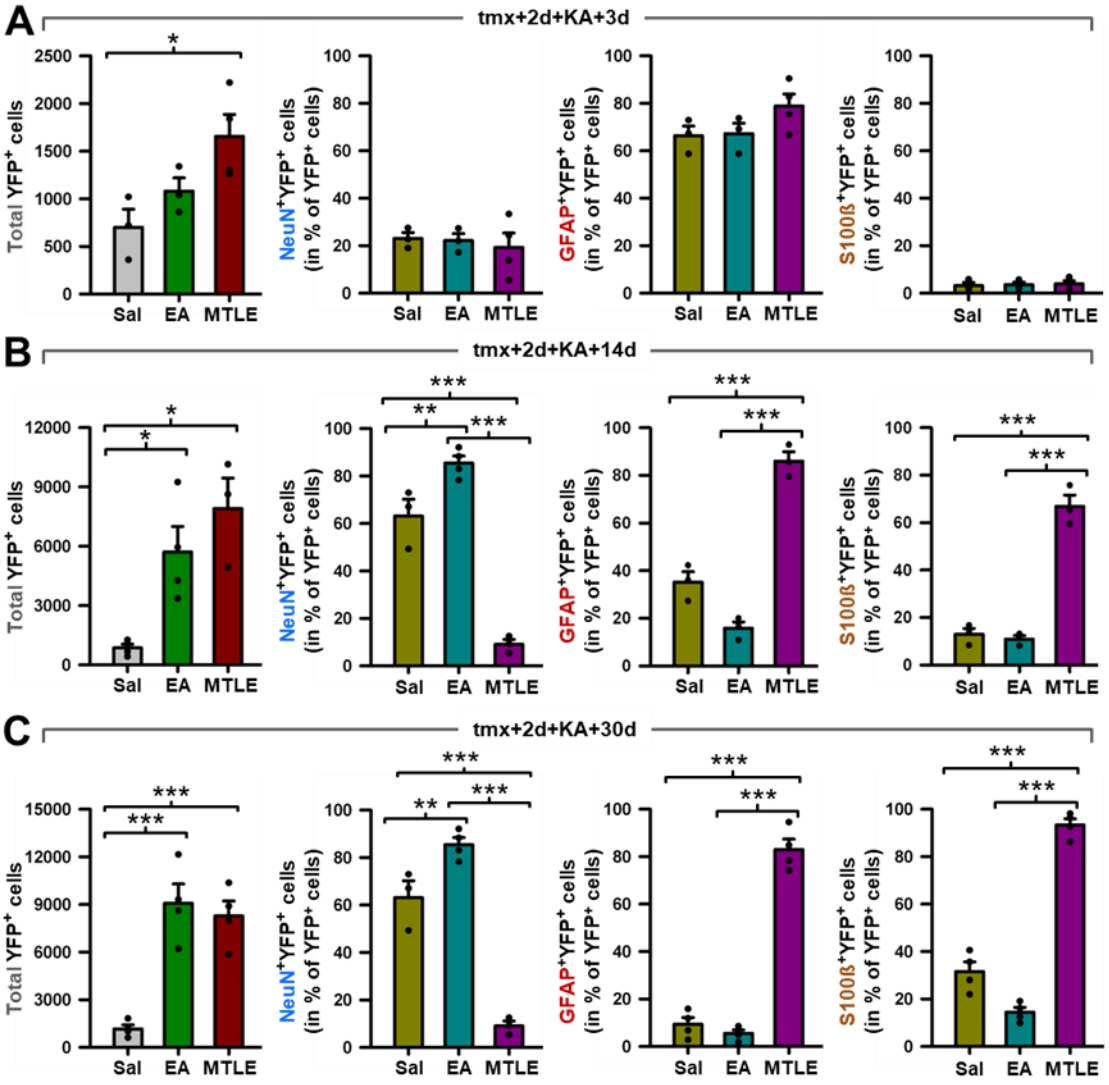

Figure 18. Lineage tracing in inducible Nestin-CreER^{T2}/R26R:YFP transgenic mice reveals that neurogenesis is promoted in EA whereas astrogliogenesis is favored in MTLE. (**A-C**) Quantification of the absolute number of YFP$^+$ cells and the relative number of YFP$^+$ cell types at 3 (**A**), 14 (**B**), and 30dpKAi (**C**). The total number of YFP-positive cells increased significantly in the EA and MTLE mice in comparison to the Sal group. At 3dpKAi (**A**), no differences in the proportion of YFP$^+$ cell types was found between groups. At 14 (**B**) and 30dpKAi (**C**), however, the neuronal fate of YFP$^+$ cells (number of NeuN$^+$YFP$^+$ cells) was significantly promoted in EA mice, although it already represented the majority in Sal mice. Remarkably, in MTLE mice the neuronal population was a minority of YFP$^+$ cells and the astroglial fate (GFAP$^+$YFP$^+$ or S100β$^+$YFP$^+$) was favored compared to Sal and EA mice. *p < 0.05, **p < 0.01, ***p < 0.001 by all pairwise multiple comparisons by Holm-Sidak post hoc test. Bars show mean ± SEM. Dots show individual data.

assess overall cell proliferation, we injected BrdU 2d after injection and quantified the total number of $BrdU^+$ cells 1d later in the SGZ and GCL. Cell proliferation in the neurogenic niche of the DG was decreased in LPS mice compared to both groups injected with KA (**Fig. 19A-C**). The proportion of activated NSCs was also significantly lower than that of EA and MTLE mice (**Fig. 19D-F**). No obvious morphological particularities were observed in the NSCs of LPS-injected animals. Thus, these results indicate that inflammation alone is not sufficient to provoke the NSC response to seizures in terms of activation and morphology.

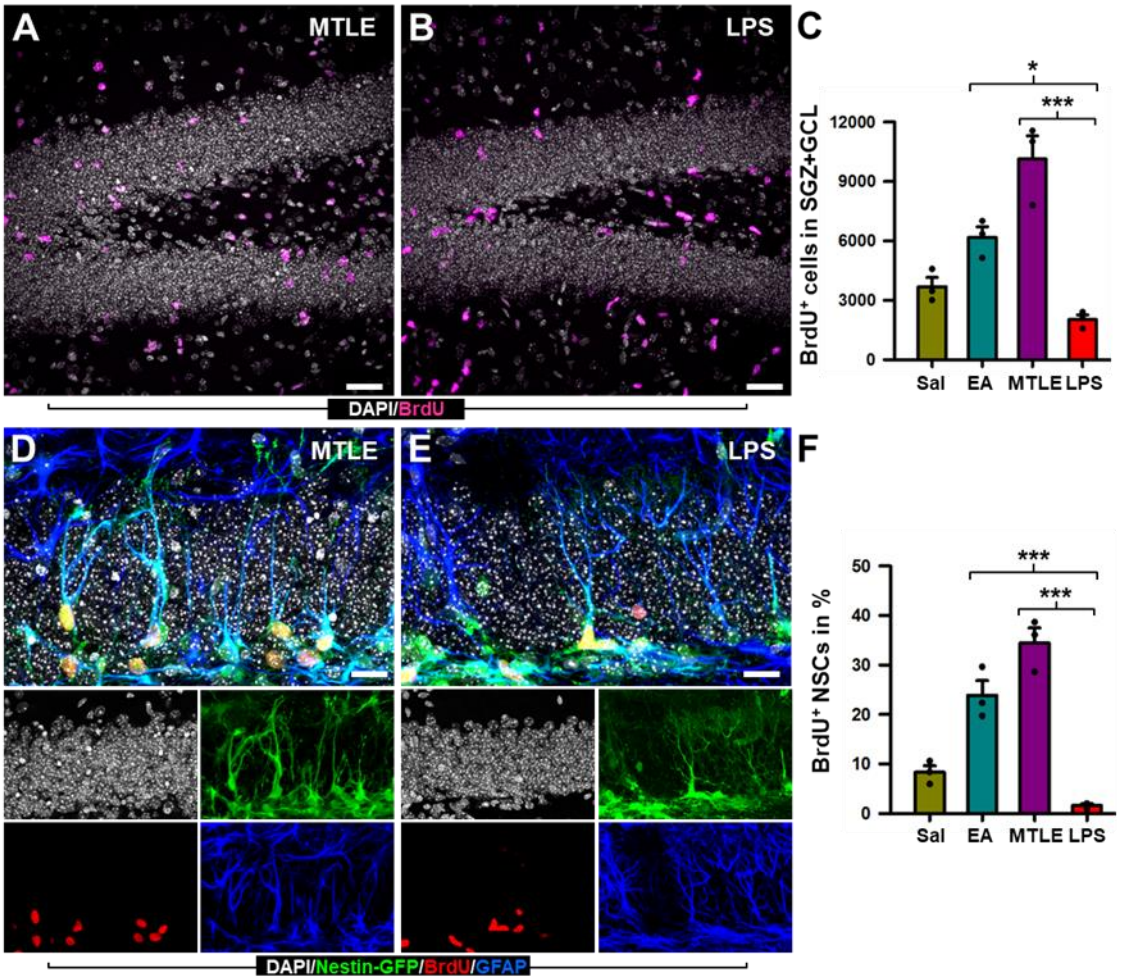

Figure 19. LPS decreases cell proliferation and NSC activation in the neurogenic niche. Intrahippocampal injection of LPS to trigger an inflammatory response increased cell proliferation in the whole DG but reduced it in the neurogenic niche (SGZ+GCL), in comparison to the KA-injected groups. (**A** and **B**) Confocal microscopy images showing $BrdU^+$ cells in an MTLE (**A**) and an LPS (**B**) mouse. (**C**) Quantification of $BrdU^+$ cells in the SGZ and GCL. Proliferation in the LPS group is significantly lower than the EA and MTLE groups. (**D** and **E**) Confocal microscopy images showing activated NSCs in an MTLE (**D**) and an LPS (**E**) mouse. (**F**) Quantification of the proportion of activated NSCs among the NSC population. In the LPS group the percentage of $BrdU^+$ NSCs is significantly reduced compared to the EA and MTLE groups. For easier visualization only the comparison to MTLE is shown. *$p < 0.05$, ***$p < 0.001$ by all pairwise multiple comparison by Holm-Sidak post hoc test. Bars show mean ± SEM. Dots show individual data. Scale bar is 50µm in A and B; and 20µm in (**D**) and (**E**).

Overall, these results prove that different levels of neuronal hyperexcitation trigger different responses from NSCs. When the level of this hyperexcitation is high enough to trigger seizures, NSCs completely change their cell-cycle program almost abolishing the neurogenic fate in favor of reactive astrogliogenesis. Both NSCs and their daughter cells no longer produce neuronal fate-committed precursors but instead become React-NSCs that will later differentiate into RAs.

7.3. LPA_1 labels NSCs during their transformation into RAs and participates in their massive activation after seizures

LPA_1 is a specific marker for adult NSCs in the DG

Having revealed the new facet of NSC multipotency, we aimed to characterize the transformation process from NSCs to RAs through React-NSCs. For this purpose, we were in need of a new tool that selectively labeled this lineage. There are not really good markers that are exclusively expressed in hippocampal NSCs, what constitutes one of the reasons why they avoided unambiguous detection for decades after AHN had been discovered. Additionally, the suitability of the widely-employed nestin-based transgenic lines gets deeply weakened in our case, since nestin is also expressed in RAs whichever their origin is. This makes the work of distinguishing between parenchymal astrocyte-derived RAs and React-NSC-derived RAs impossible due to *de novo* nestin expression in the former.

Thus, we resorted to a new transgenic mouse line: LPA_1-GFP. This transgenic mouse was employed and described for the first time by the group of Kempermann (Walker *et al.*, 2016), but prior to our MTLE experiments we performed two more simple validation methods.

First, we quantified in the neurogenic niche of the DG (SGZ+GCL), based on GFAP labeling and morphology, the proportion of cell types among the LPA_1-GFP-expressing population. More than an 85% of this population was classified as $GFAP^+$ NSCs with radial morphology, being the rest most often cluster-forming ANPs still in contact with presumably their mother NSC (**Fig. 20A** and **B**). This suggests transgene expression is downregulated as neural progenitors get more committed for the neuronal lineage and confirms the NSC-specific labeling as described before (Walker *et al.*, 2016).

Second, we performed an immunohistochemical staining for LPA_1 protein. We observed good colocalization between LPA_1 and LPA_1-GFP in hippocampal NSCs, including their radial apical projection despite the LPA_1 puncta-like staining (**Fig. 20C**). Immunohistochemical techniques for the receptor required a specific fixative (PLP, see Materials and Methods), thus were only performed for this validation experiment.

These results show LPA_1-GFP is a good tool to label NSCs in the DG. Even though GFP expression is dimmer, especially in the radial processes, than in Nestin-GFP animals, its narrower expression in the cells participant of the neurogenic cascade suited it well as a good candidate for our purposes of visualizing React-NSCs.

LPA_1-GFP recapitulates the abolition of neurogenesis and the majority generation of RAs after MTLE

Our next goal was to assess whether the React-NSCs originated following MTLE treatment maintain LPA_1-GFP expression or not. More importantly, we were interested

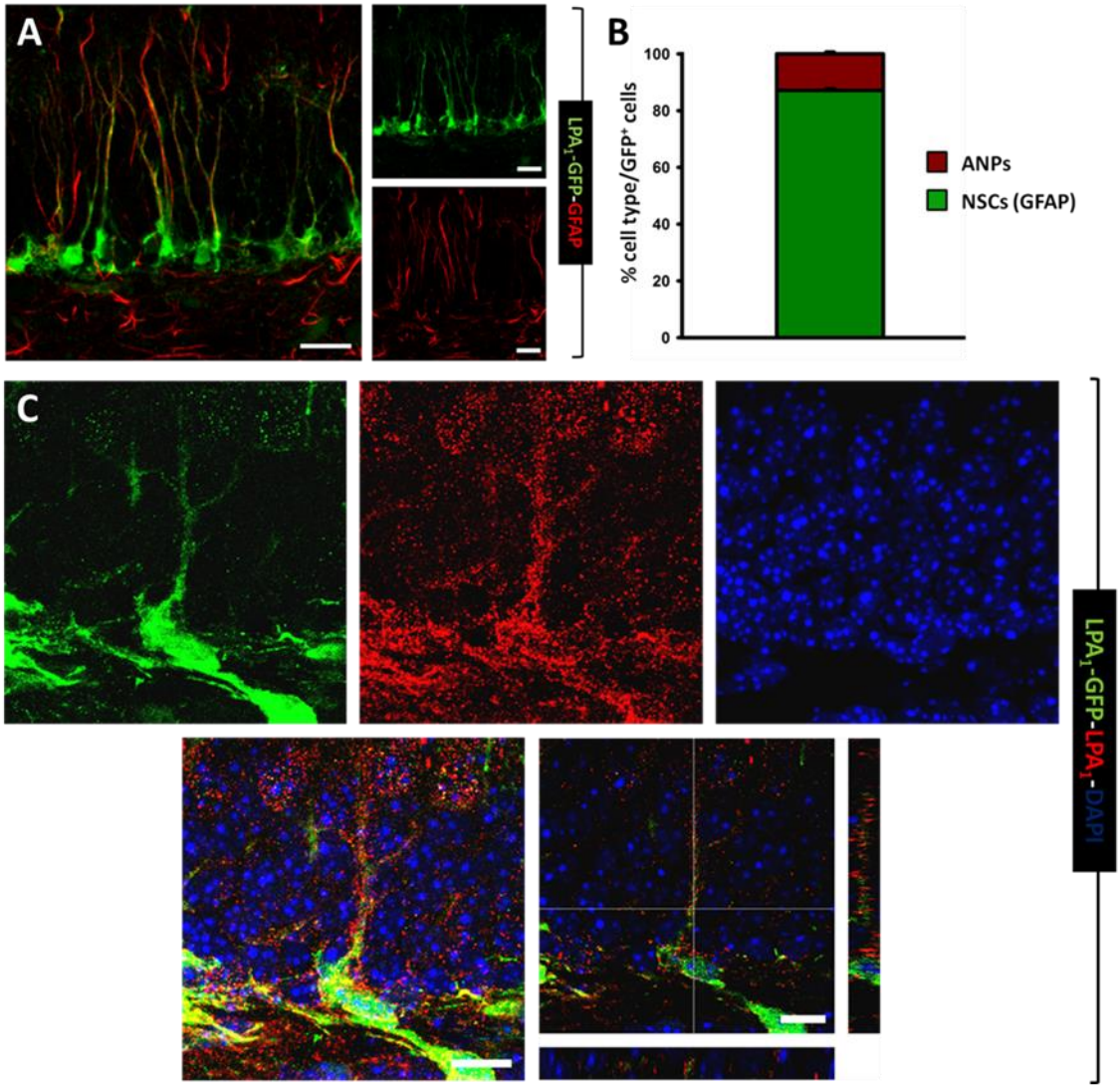

Figure 20. LPA_1 and LPA_1-GFP are specific markers for adult NSCs. (**A**) Confocal microscopy images showing GFP fluorescence in the DG of an LPA_1-GFP transgenic mouse stained for GFP and GFAP. Note the colocalization in the $GFAP^+$ NSC radial processes. (**B**) Quantification of the proportion of cell types, based on GFAP expression and morphology, among the GFP-positive population found in the hippocampal neurogenic niche of LPA_1-GFP transgenic mice. Radial NSCs account for more than an 80% of the cells immunopositive for GFP. (**C**) Confocal images showing an LPA_1-GFP^+ NSC colocalizing LPA_1 immunoreactivity. Note the remarkable colocalization, but not full dot overlapping that could be a sign of spectral leaking, in the radial projection (bottom right panel, cross section) that crosses the GCL and arborizes in its upper part reaching the ML. Scale bars are 30µm in (**A**) and 10µm in (**C**). Bars show mean ± SEM.

in finding out if this expression extended through the complete transformation from React-NSCs into React-NSC-derived RAs. It was also critical for us to rule out the transgene expression in other cell types in the epileptic DG, especially in parenchymal astrocyte-derived RAs, to be able to unequivocally trace those RAs differentiated from React-NSCs.

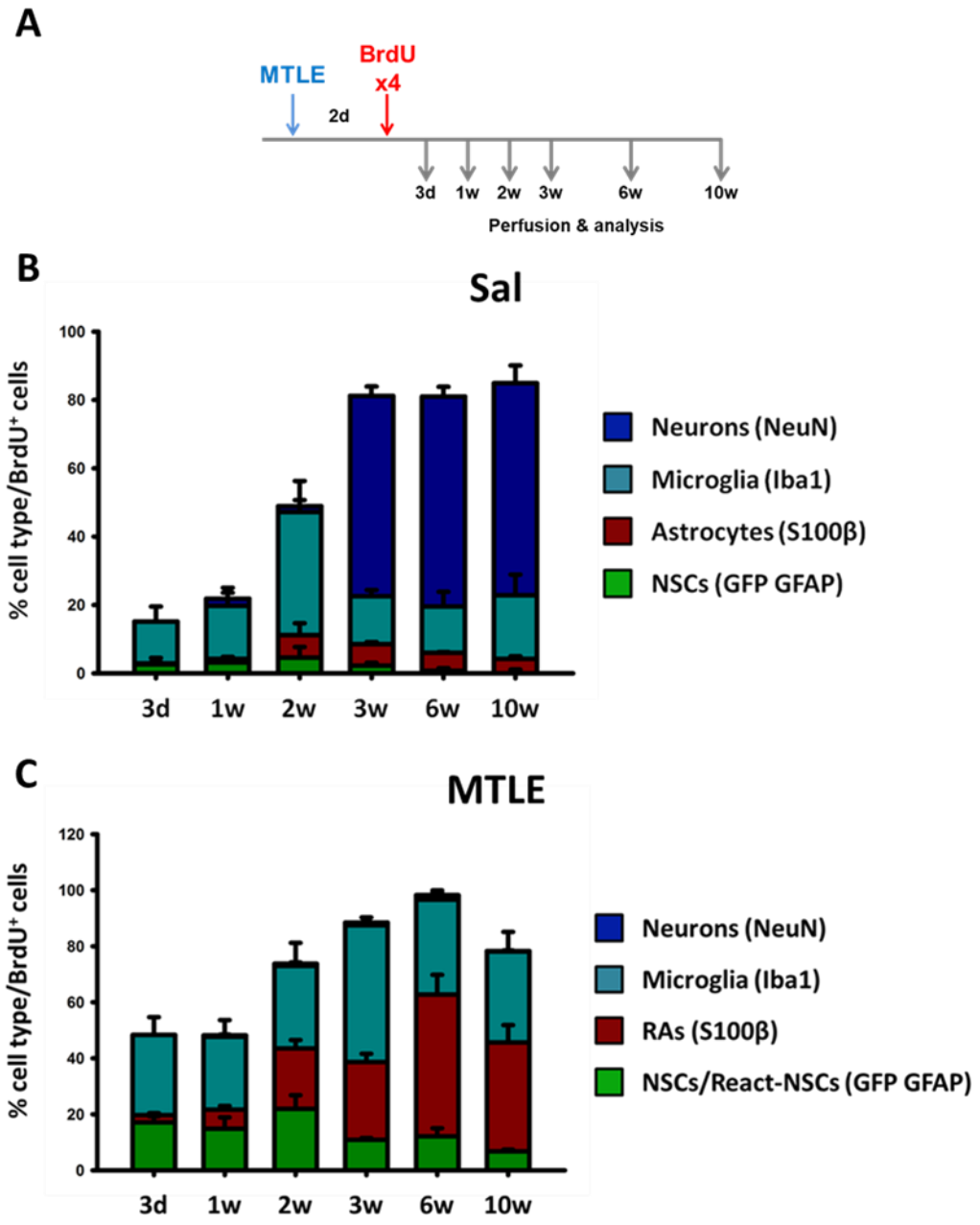

Figure 21. MTLE shifts the normal neurogenic niche towards reactive astrogliogenesis also in LPA$_1$-GFP transgenic mice. (**A**) Experimental paradigm for the MTLE/Sal time course performed in LPA$_1$-GFP transgenic mice. BrdU injections were given 2h apart one from another. (**B** and **C**) Quantifications of the proportion of cell types among the BrdU$^+$ population in Sal (**B**) or MTLE (**C**) based on the expression of markers and morphological criteria. In Sal mice (**B**), the great majority of BrdU-positive cells from the 3w-time point on were NeuN$^+$ cells devoid of LPA$_1$-GFP expression with round soma and located in the GCL and thus were categorized as neurons. Note that, apart from the proliferating cell type microglia, division-derived astrocytes were also observed after 2w. In MTLE mice (**C**), however, neurogenesis was ablated in favor of the generation of React-NSCs and RAs. Microglial proliferation was also prominent. Bars show mean ± SEM.

Firstly, we aimed to confirm the previously described changes in the DG following MTLE in LPA$_1$-GFP transgenic mice, for what we performed a time course with six different analysis time points after Sal or MTLE treatment. To label division-derived

cells, we also administered BrdU in a similar fashion as in the in the Nestin-GFP animals (**Fig. 21A**).

To evaluate the predicted ablation of neurogenesis in favor of reactive astrogliogenesis, we quantified the contribution, expressed in percentage, of known proliferative populations and their progeny to the total $BrdU^+$ cells found in the neurogenic niche of the DG. As expected, most cells derived from division were classified as neurons from the 3w-time point on in Sal mice, accounting for an approximate 60%. A mild maintained astrogliogenesis of around a 5% was observed too (**Fig. 21B**). Microglia also proliferated profusely in the short term, but its proportion among the $BrdU^+$ cells stabilized close to a 15% 3w after surgery. The proportion of NSCs decayed over time, as expected by their usual division-coupled-astrocytic-differentiation dynamics (Encinas *et al.*, 2011b), representing less than a 1% from the 6w-time point on.

Nevertheless, in MTLE animals neurogenesis was abolished. Neurons were a minority, with a 1.6% contribution at its maximum point, or even inexistent among the labeled division-derived cells (**Fig. 21C**). Reactive astrocytes, on the contrary, were generated in important numbers after only 2w following MTLE treatment, representing over a 35% of division-derived cells in the latest two time points. An approximate 30% of $BrdU^+$ cells was represented by microglia. Remarkably, React-NSCs still recognizable by their persistent LPA_1-GFP expression were also an appreciable proportion of $BrdU^+$ cells in the DG, with its minimum being below 7% at 10w.

In order to appreciate changes in the stem cell population, we quantified the total number of NSCs and React-NSCs in Sal and MTLE mice, the total number of those which colocalized with BrdU and expressed the latter as a proportion (**Fig. 24A-C**). Even though normality was not achieved for two-way ANOVA to be performed, there seems to be an expansion of the React-NSC population in the short term (**Fig. 22** and **24A**) followed by a decrease in the long term (**Fig. 23** and **24A**). The number of $BrdU^+$ React-NSCs in MTLE animals was much higher than that of $BrdU^+$ NSCs in Sal animals (**Fig. 22**, **23** and **24B**), and when these numbers were expressed as a percentage of BrdU-labeled among the NSC or React-NSC population a similar increase was observed (**Fig. 24C**). This increase in the proportion of division-derived React-NSCs was more obvious in the 6w and 10w time points, being $BrdU^+$ NSCs in Sal animals in those time points almost inexistent.

These results confirmed the shift from neurogenesis to reactive astrogliogenesis that appears after seizures provoked by a model of MTLE and that we first observed in Nestin-GFP mice. Furthermore, LPA_1-GFP^+ NSCs preserve the transgene expression as they become React-NSCs. We next sought to analyze for how long the expression of GFP continued and whether it appeared in other cell types over time.

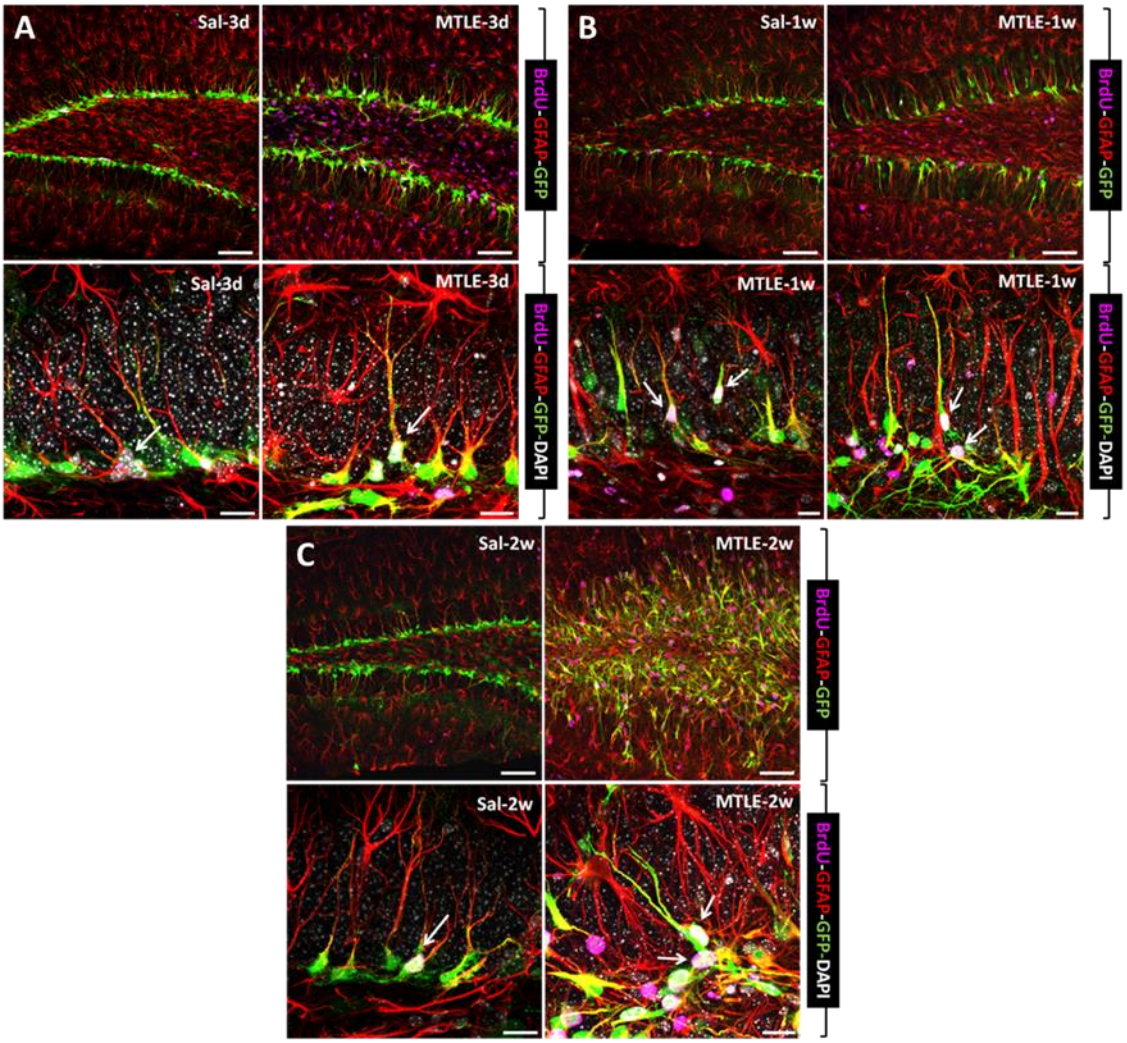

Figure 22. LPA_1-GFP expression shows in the short term the disruption of the neurogenic niche and the massive NSC activation and induction of the React-NSC-phenotype. (**A**-**C**) Confocal microscopy images showing the appearance of the general DG (top panels) and NSCs (bottom panels) in LPA_1-GFP transgenic mice subjected to Sal or MTLE treatments and analyzed after 3d (**A**), 1w (**B**), or 2w (**C**). Note the normal radial morphology and low proliferation rate ($BrdU^+$ nuclei in magenta, arrows) of NSCs in Sal mice (**A** and **C**, bottom left panels) as opposed to the multibranch, reactive-like morphology with GFAP overexpression (red) and high proliferation rate (**A** and **C**, bottom left, and **B**, bottom panels) they present after MTLE treatment. All images are maximum projections from approximately 10µm-thick z-stacks. Scale bars are 50µm in the top and 15µm in the bottom panels.

React-NSCs maintain LPA_1-GFP expression as they differentiate into RAs

Given our previous results with inducible Nestin-Cre-ER^{T2}/R26R:YFP transgenic mice indicating that React-NSCs finally differentiate into mature RAs, we wondered whether LPA_1-GFP could be employed as a marker to trace, visualize and, in the future, isolate React-NSCs through their transformation into RAs.

To analyze RA generation from React-NSCs, we used S100β as a marker of mature astrocytes, using its expression as a token for complete differentiation. We quantified

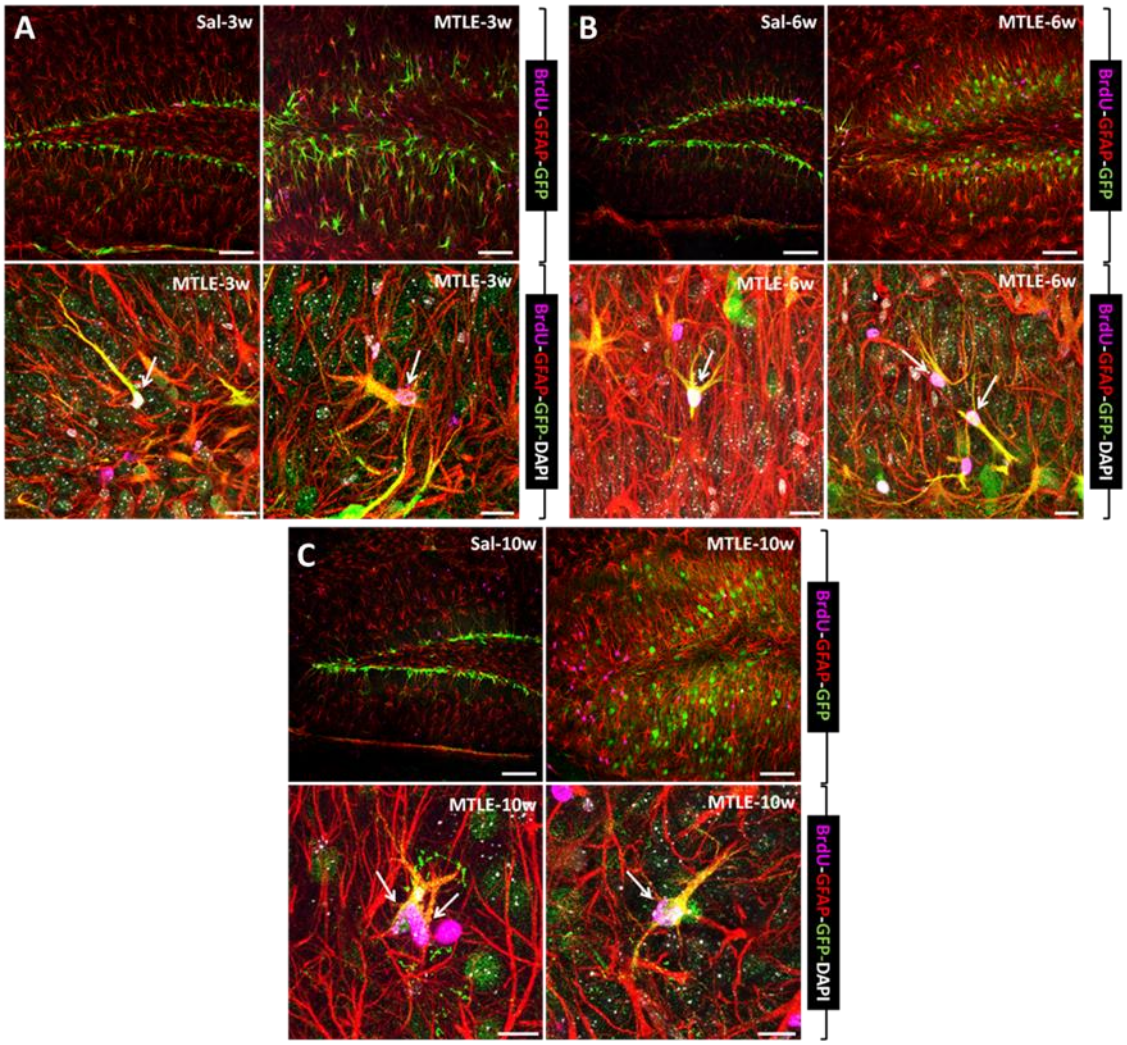

Figure 23. LPA_1-GFP expression is maintained in React-NSCs for several weeks. (**A-C**) Confocal microscopy images showing the appearance of the general DG (top panels) and NSCs (bottom panels) in LPA_1-GFP transgenic mice following Sal or MTLE treatments and analyzed after 3w (**A**), 6w (**B**), or 10w (**C**). In the MTLE group the overall DG and specifically GCL anatomy is altered (**A-C**, top right panels), compared to Sal animals (**A-C**, top left panels), and BrdU-positive React-NSCs (magenta nuclei; arrows in **A-C**, bottom panels) acquire a much more RA-like morphology as revealed by LPA_1-GFP (green) and GFAP (red) immunoreactivity. The contribution of these React-NSC-derived RAs decreases with time suggesting a downregulation of the transgene. Note *de novo* LPA_1-GFP expression in cell bodies in the GCL, presumably corresponding to neurons. All images are maximum projections from approximately 10µm-thick z-stacks. Scale bars are 50µm in the top and 15µm in the bottom panels.

the number of $S100\beta^+LPA_1\text{-}GFP^+GFAP^+$ cells in the DG of Sal and MTLE mice throughout the performed time course and observed an increasing trend over time only in MTLE-treated animals (**Fig. 25A**). This differentiation process was much more evident when S100β expression was represented as a proportion of the total number of NSCs or React-NSCs, defined as $LPA_1\text{-}GFP^+GFAP^+$ cells (**Fig. 25C**). In the short term, up to 2-3w, a low proportion of React-NSC is immunopositive for S100β (**Fig. 25B** and **C**), but especially from 6w after MTLE induction most $LPA_1\text{-}GFP^+$ React-NSCs expressed this mature astrocytic marker (**Fig. 25C** and **D**). As a positive control for

S100β expression, we also quantified the proportion of S100β$^+$ parenchymal astrocytes, *i.e.*, GFAP$^+$ cells devoid of LPA$_1$-GFP expression, and observed no changes between time points or treatments (**Fig. 25E**).

As another proxy of the differentiation process towards RAs, we also quantified the total number of BrdU$^+$ astrocytes and RAs found in the DG. High numbers of division-derived RAs were only observed in MTLE animals (**Fig. 26A**). In addition, instances of BrdU$^+$LPA$_1$-GFP$^+$S100β$^+$ cells were only detected in the MTLE group (**Fig. 26B** and **D**). As occurred in previous quantifications, not achieving normality in our population of BrdU$^+$ astrocytes and RAs prevented us from performing two-way ANOVA. Thus, taking advantage of GFAP expression as a marker of general-astrocytic lineage, we indicated the NSC and React-NSC population as the proportion of LPA$_1$-GFP$^+$ cells devoid of S100β immunolabeling among the GFAP$^+$ population. This helped us isolate the contribution of the undifferentiated React-NSCs to the overall astroglia-like cells and rendered important statistically significant differences. There was a strong reduction in the "pure" React-NSC population over time in MTLE mice, consistent with the differentiation process into RAs (**Fig. 26C**). Moreover, there was a significant decrease in the proportion of the stem cell population in MTLE-treated animals compared to the Sal group.

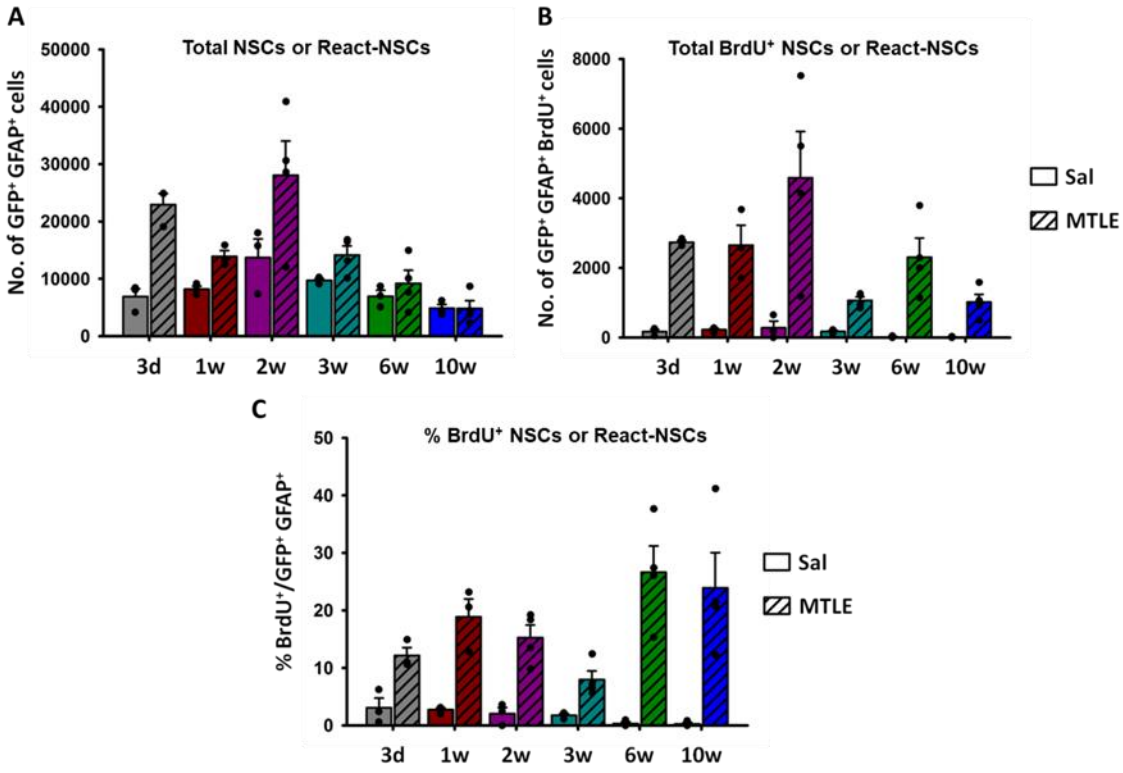

Figure 24. React-NSCs also divide in higher numbers in LPA$_1$-GFP$^+$ mice after MTLE. (**A**) Quantification of the total number of LPA$_1$-GFP$^+$GFAP$^+$ NSCs (Sal) or React-NSCs (MTLE) found in the DG of LPA$_1$-GFP transgenic mice. (**B**) Quantification of the total number of BrdU-labeled NSCs/React-NSCs. (**C**) Quantification of the proportion, expressed in percentage, of BrdU-positive NSCs/React-NSCs for each time point and treatment. Data referring to BrdU$^+$-NSCs/React-NSCs (**B** and **C**) show a clear increasing trend in MTLE-treated animals, but normality was not achieved and thus two-way ANOVA could not be performed. Dots show individual data. Bars show mean ± SEM.

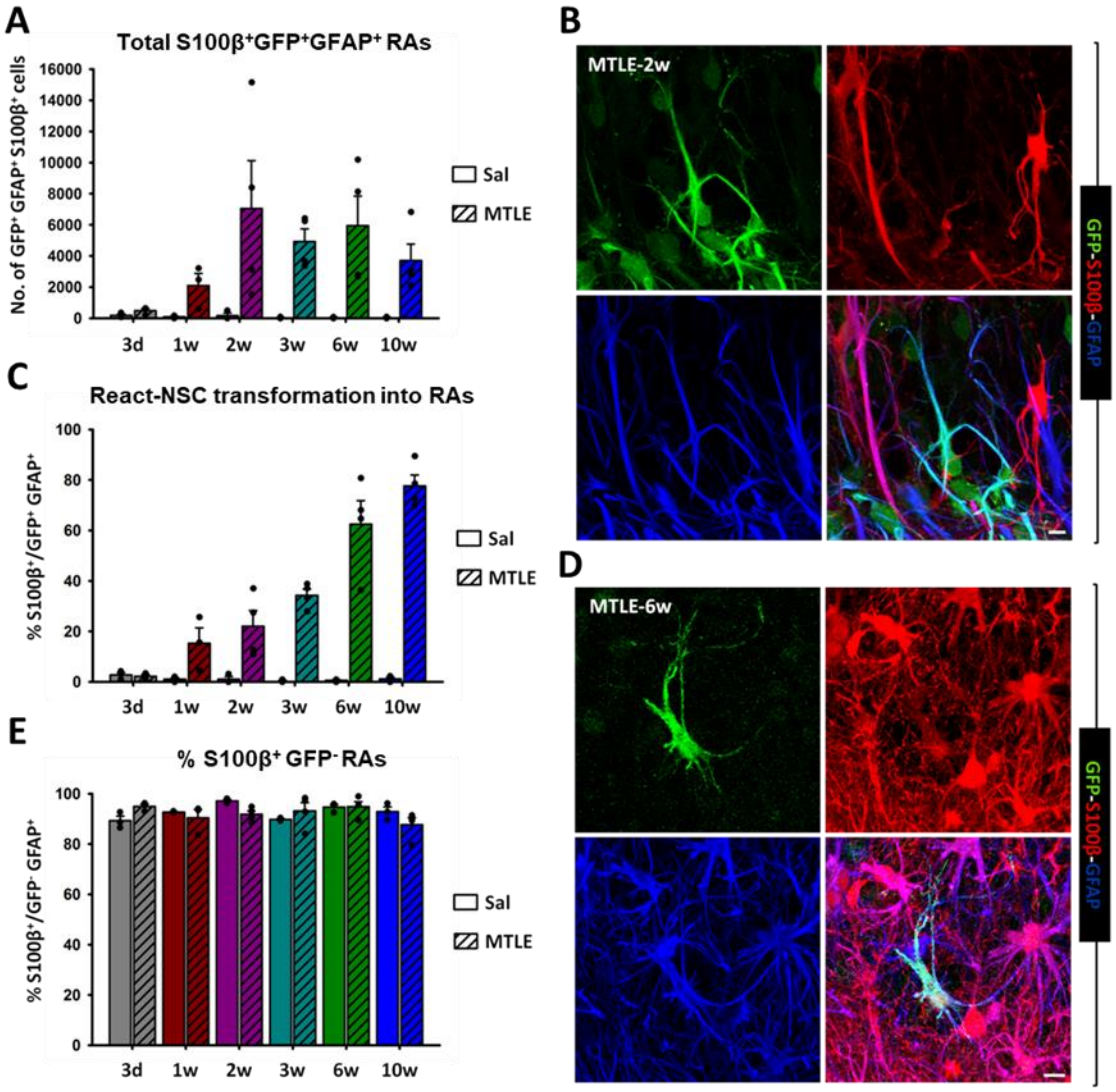

Figure 25. LPA$_1$-GFP$^+$ React-NSCs differentiate into RAs weeks after seizures. (**A**) Quantification of the total number of LPA$_1$-GFP$^+$GFAP$^+$ NSCs (Sal) or React-NSCs (MTLE) that also colocalized with mature astrocytic marker S100β. (**C**) Quantification of the proportion of S100β$^+$ NSCs/React-NSCs. Although not achieving normality necessary for two-way ANOVA performance, remarkable colocalization and increasing trend of this feature showing differentiation into RAs were only observed in MTLE animals. (**B** and **D**) Confocal representative images showing an S100β-negative React-NSC (**B**) 2w after MTLE induction and an S100β-positive (red) React-NSC-derived RA (**D**), as shown by LPA$_1$-GFP persistent expression, at 6w time point. All images are maximum projections from approximately 10µm-thick z-stacks. (**E**) Quantification of the proportion of S100β-expressing GFP-negative astrocytes/RAs to show stable colocalization with general astrocytic marker GFAP. Dots show individual data. Bars show mean ± SEM. Scale bars are 15µm.

These data strongly support the notion that neuronal hyperactivity massively activates NSCs and triggers a change in the fate of their divisions towards the generation of RAs. Furthermore, although the NSC marker LPA$_1$-GFP specifically labels React-NSCs it seems to be downregulated at the later stages of the React-NSC ultimate transformation into RAs. The expression of GFP is however maintained in a small proportion of them even after differentiation is complete.

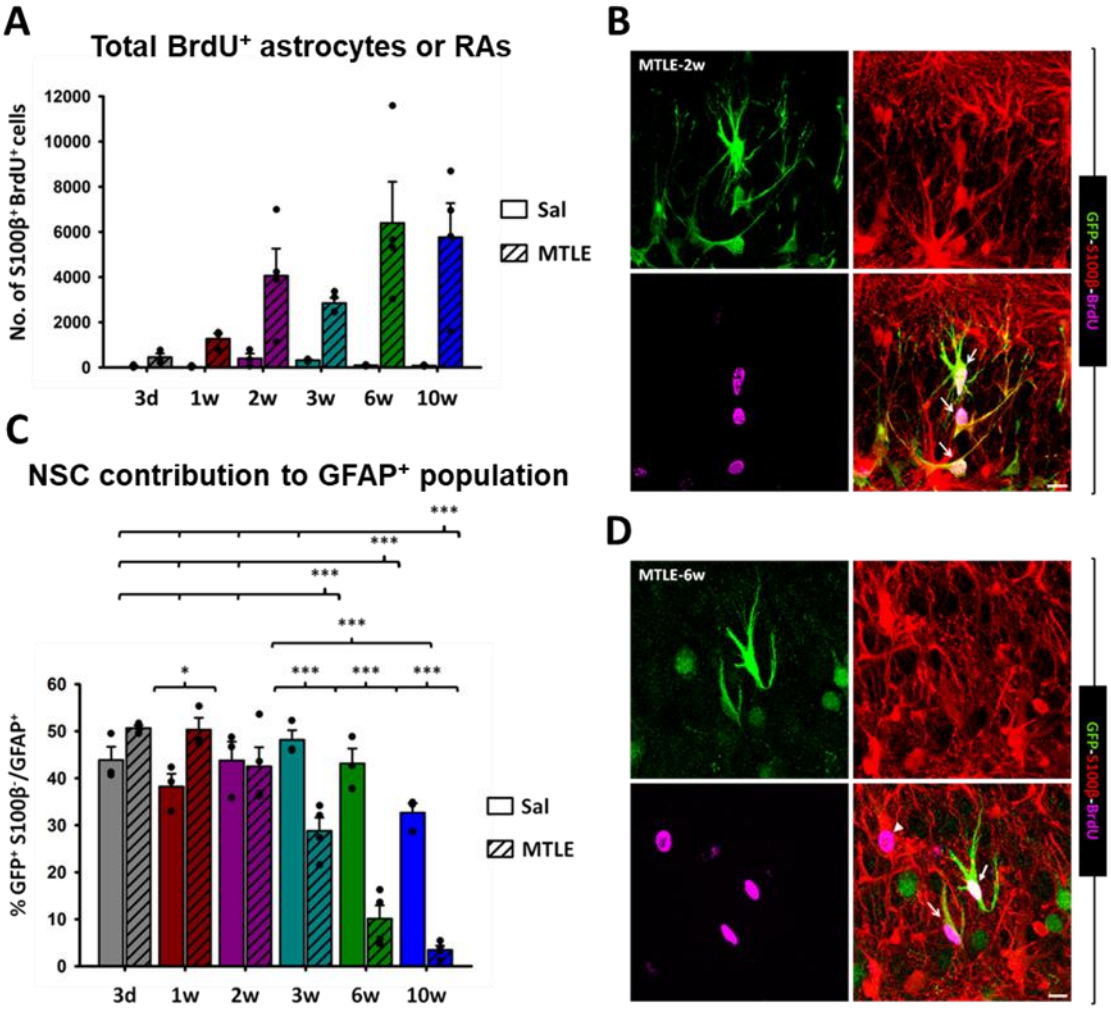

Figure 26. LPA$_1$-GFP$^+$ React-NSC division derives in RAs that exit the stem cell population. (**A**) Quantification of the total number of S100β$^+$ astrocytes (Sal) or RAs (MTLE) with stellate morphology that were also labeled with BrdU. The number of division-derived RAs presented an increasing trend only in MTLE animals. (**C**) Quantification of the proportion of "pure" NSCs/React-NSCs that did not colocalize with astrocytic marker S100β among the GFAP$^+$ glial population in the DG. Note the marked decrease in the contribution of these stem cells weeks after MTLE induction compared to Sal animals. (**B** and **D**) Confocal representative images showing LPA$_1$-GFP$^+$S100β$^+$ with BrdU labeling (open arrows) 2w (**B**) and 6w (**D**) after seizure induction. Note in (**D**) an S100β-negative LPA$_1$-GFP$^+$ React-NSC that had incorporated BrdU (closed arrow) and an LPA$_1$-GFP-negative BrdU$^+$S100β$^+$ RA (arrowhead). All images are maximum projections from approximately 20µm-thick z-stacks. *p < 0.05, ***p < 0.001 by all pairwise multiple comparison by Holm-Sidak post hoc test. Dots show individual data. Bars show mean ± SEM. Scale bars are 15µm.

Neurons start LPA$_1$-GFP expression weeks after seizures

A notable feature we found in the DG of LPA$_1$-GFP after MTLE was *de novo* expression of the transgene in neurons of the GCL. The appearance of GFP staining in this case was more puncta-like and present mostly in only the neuronal nuclei and somata instead of the whole cell body. We quantified the proportion of LPA$_1$-GFP-expressing NeuN$^+$ neurons in Sal and MTLE animals and, remarkably, we did not detect any in Sal mice (**Fig. 27A** and **B**). As we only observed this phenomenon in MTLE

mice, we performed an analysis taking only these data and observed a significant increase in the last two time points (6w and 10w) compared to every previous time point (**Fig. 27B** and **C**). Thus, neurons in the DG start LPA_1-GFP expression following seizures induced in this area.

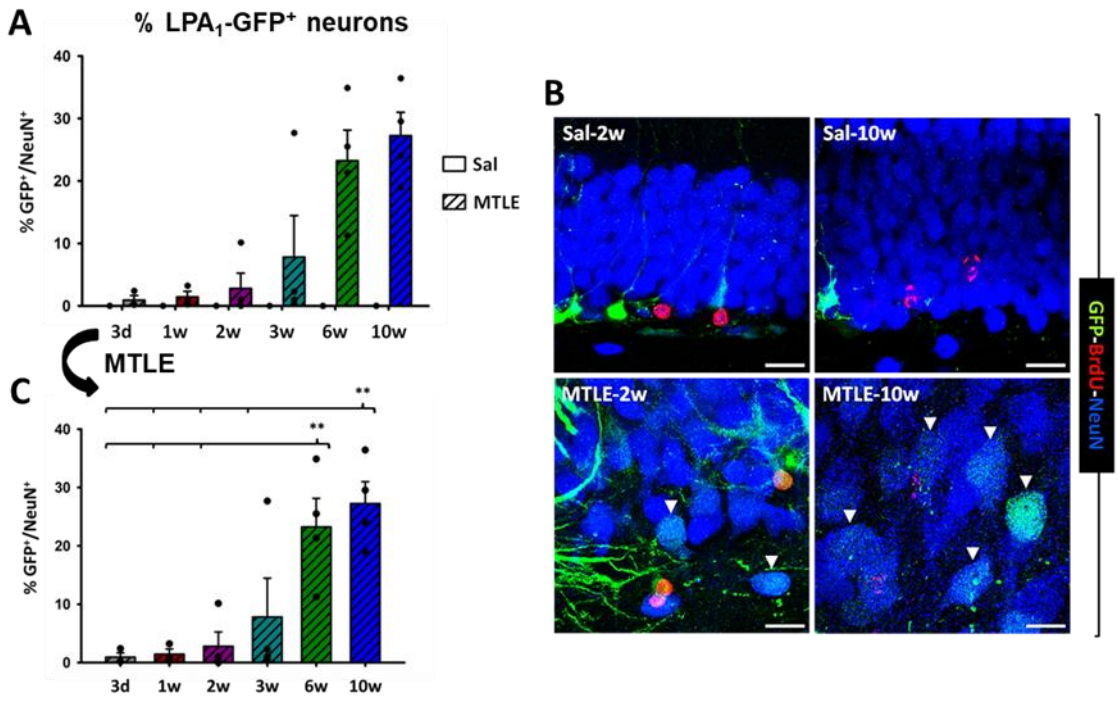

Figure 27. Neurons start LPA_1-GFP expression weeks after MTLE treatment. (**A**) Quantification of the proportion of LPA_1-GFP-expressing neurons ($NeuN^+$ cells located in the GCL) in the DG of Sal and MTLE mice. Normality test failed, but no LPA_1-GFP^+ neurons were detected in Sal animals and thus we performed a one-way ANOVA of data from MTLE animals alone (**C**). In the 6w and 10w time points a significant increase in LPA_1-GFP expression was observed. (**B**) Confocal representative images showing LPA_1-GFP^+NeuN^+ neurons (arrowheads) only in the DG of MTLE-treated mice (bottom panels). All images are maximum projections from approximately 10µm-thick z-stacks. **p < 0.01 by all pairwise multiple comparison by Holm-Sidak post hoc test. Dots show individual data. Bars show mean ± SEM. Scale bars are 15µm.

Ultrastructural analysis confirms specific LPA_1-GFP expression in React-NSCs and reveals novel features

To validate the usefulness of the LPA_1-GFP and further characterize React-NSCs, we resorted to ultrastructural analysis via TEM microscopy. We performed pre-embedding immunohistochemistry for GFP staining in the brains of Sham and MTLE LPA_1-GFP mice 10d after treatment. The reason for Sham treatment instead of Sal in this case was to avoid any type of reactivity induction in NSCs due to the injection in the DG, thus the stereotaxic protocol stopped after drilling the cranium. We focused on React-NSCs in the SGZ of MTLE animals and compared their LPA_1-GFP expression to that of astrocytes in other areas of the DG such as the hilus or the ML (**Fig. 28**). We observed the expected presence of GFP-immunogold particles in the cytoplasm of React-NSCs in MTLE mice (**Fig. 28A**) but did not detect obvious presence of them in astrocytes in the

hilus (**Fig. 28B**) or the ML (**Fig. 28C**). This confirmed that even after seizures LPA_1-GFP expression is restricted to React-NSCs and does not "leak" in parenchymal astrocytes or RAs.

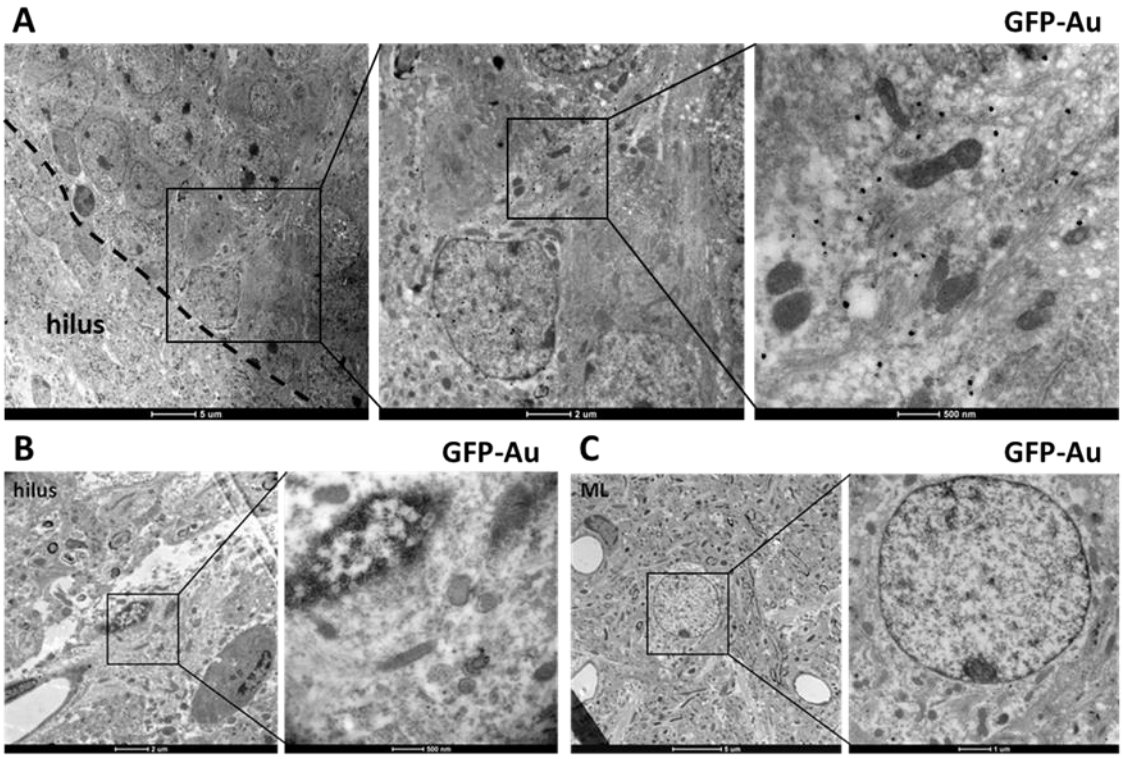

Figure 28. LPA_1-GFP expression is specific for the NSCs in the SGZ and is not observed in astrocytes in adjacent areas. (**A**-**C**) TEM representative images showing ultrathin sections of the DG of an MTLE-10d mouse that were immunogold-treated targeting GFP. (**A**) Detail of a NSC located in the SGZ (dashed line) containing particles of immunogold-labeled GFP (black dots). (**B** and **C**) Astrocytes, recognized by their light cytoplasm, were not positive for LPA_1-GFP neither in the hilus (**B**) nor in the ML (**C**). Scale bars are shown at the bottom of each image.

Remarkably, TEM microscopy imaging revealed high numbers of mitochondria in React-NSCs (**Fig. 29B**). When quantifying these numbers and compared them to those of NSCs in Sham animals, we observed an increasing trend in React-NSCs induced by MTLE treatment. This increase, however, did not show statistical significance (**Fig. 29A**).

The absence of LPA_1 decreases MTLE-induced cell proliferation and React-NSC activation

Continuity of LPA_1-GFP expression during NSC transformation into RAs through React-NSCs (at least for the first weeks after seizure induction and even after differentiation in some of them in the long term) made us ask whether LPA_1 has a function in NSC massive activation and change of fate in MTLE or this behavior is independent on the expression of the receptor. In addition, several reports have attributed to this receptor a function in neurogenesis in the DG (Matas-Rico *et al.*, 2008;

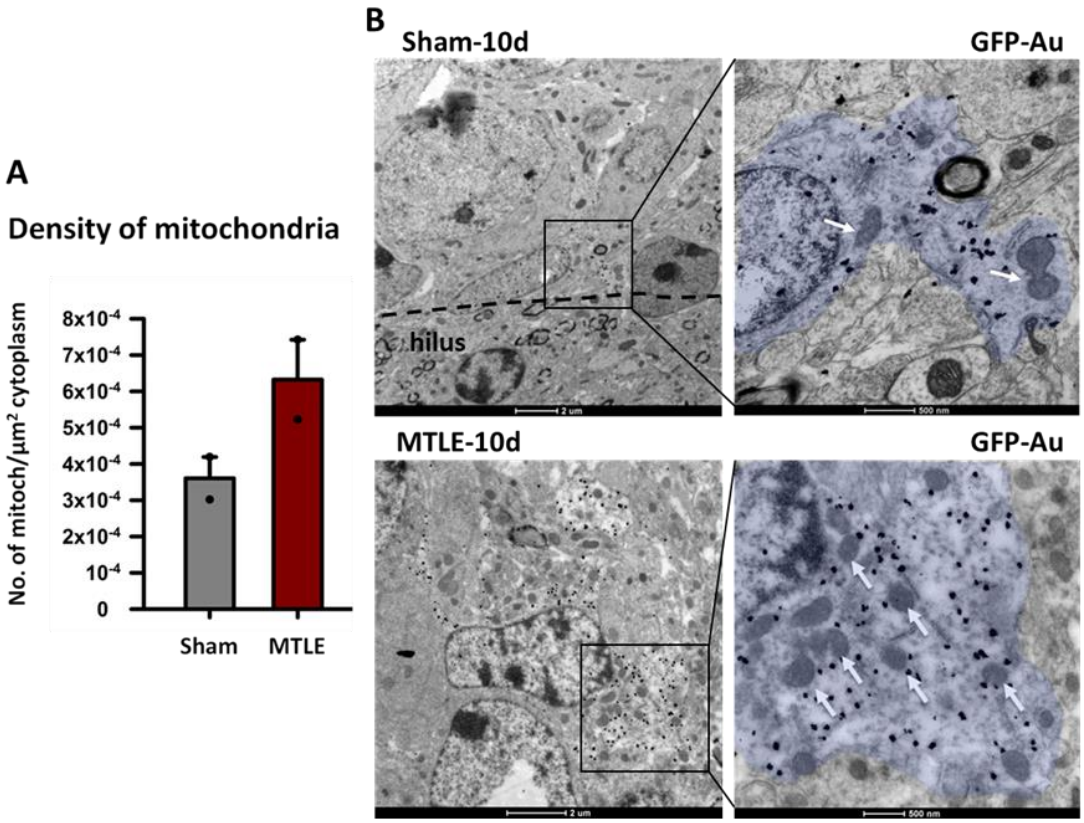

Figure 29. React-NSCs tend to increase their number of mitochondria. (**A**) Quantification of the density of mitochondria, shown as number of mitochondria per unit of cytoplasmic area, in NSCs (Sham) or React-NSCs (MTLE). Density has an increasing trend in MTLE mice, although significant differences were not found yet. (**B**) Representative TEM images showing details of a GFP-positive (black dots) NSC located in the SGZ (dashed line) of the DG of a Sham animal (top panels) and a React-NSC from an MTLE animal (bottom panels). Mitochondria (white arrows) are much more numerous in the cytoplasm of the React-NSC compared to those in the NSC from a Sham mouse. The region corresponding to the cytoplasm of both cells was colored to facilitate the visualization. Scale bars are shown at the bottom of each image.

Walker *et al.*, 2016), a function into which we want to delve. We took advantage of the already generated and described maLPA$_1$ mice, a mouse line devoid of LPA$_1$ expression (Estivill-Torrus *et al.*, 2008), and subjected them and their WT counterparts to MTLE induction. We injected them with BrdU 2d later and analyzed the DG of these animals at 3d and 2w (**Fig. 30A**).

Immunohistochemical staining for nestin, BrdU and GFAP did not reveal any gross anatomical changes between the DG of WT and maLPA$_1$ mice (**Fig. 30D** and **E**). In order to evaluate possible changes in cell proliferation, we quantified the total number of BrdU$^+$ cells in the neurogenic niche of WT and maLPA$_1$ mice. At 3d, a non-significant decrease in the number of overall dividing cells was detected in maLPA$_1$ animals (**Fig. 30B**). By 2w, however, this number was significantly different with almost a 50% reduction in animals devoid of LPA$_1$ (**Fig. 30C**).

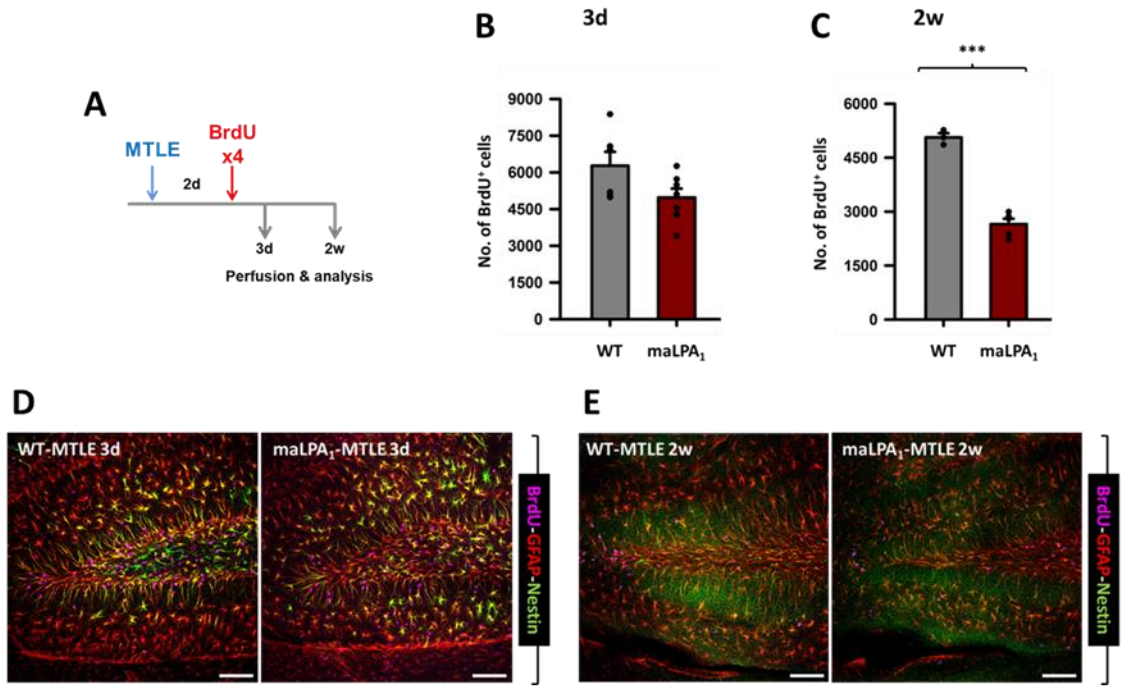

Figure 30. MTLE-induced cell proliferation in the DG decreases in the absence of LPA_1. (**A**) Experimental paradigm applied to $maLPA_1$ mice (a null line for LPA_1) and their WT counterparts. (**B** and **C**) Quantification of the total number of $BrdU^+$ cells found 3d (**B**) and 2w (**C**) after MTLE treatment. A significant decrease in the number of $BrdU^+$ cells was observed in $maLPA_1$ animals at 2w. (**D** and **E**) Confocal representative images showing the general appearance of the DG, stained for nestin, GFAP and BrdU, of WT and $maLPA_1$ mice 3d (**D**) and 2w (**E**) after MTLE induction. No obvious gross anatomy differences could be observed between the two different genotypes. All images are maximum projections from approximately 10µm-thick z-stacks. ***$p < 0.001$ by Student's t test. Dots show individual data. Bars show mean ± SEM. Scale bars are 50µm.

To specifically focus on React-NSCs, we also quantified the percentage of $BrdU^+$ React-NSCs at both time points. Due to the absence of a reporter gene in this mouse line, we followed tight criteria to define this cell type. We employed nestin expression as an indicator to distinguish between React-NSCs and astrocytes or RAs. However, nestin is also expressed in RAs. Therefore, we also took into account the radial morphology of React-NSCs in the short term (3d) to avoid possible contamination of our results by RAs in the GCL (**Fig. 31A** and **C**). We considered the 2w time point to be long enough for React-NSCs to lose their typical radial projection in favor of the more multipolar morphology of RAs, so this feature was not contemplated in the analysis (**Fig. 31B** and **D**). Nevertheless, we expected the contamination by parenchymal astrocyte-division-derived RAs to be improbable due to the scarce proliferative capacity astrocytes usually present, as we have documented in both the Nestin-GFP and the LPA_1-GFP mice even after seizure induction. In both time points, the proportion of $BrdU^+$ React-NSCs was decreased in $maLPA_1$ mice compared to WT animals in a statistically significant manner (**Fig. 31A** and **B**).

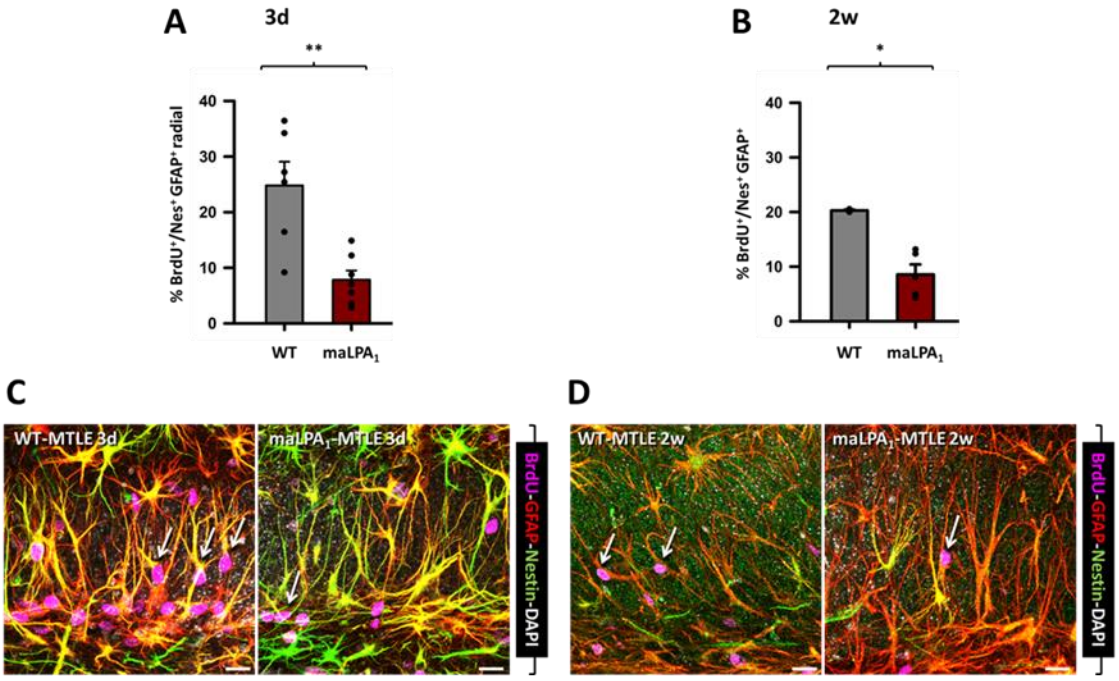

Figure 31. MTLE-induced React-NSC activation decreases in the absence of LPA_1. (**A** and **B**) Quantification of the proportion in percentage of $BrdU^+$ React-NSCs found 3d (**A**) and 2w (**B**) after MTLE treatment. A significant decrease in the percentage of $BrdU^+$ React-NSCs was observed in $maLPA_1$ animals at both 3d and 2w time points. React-NSCs have lost their typically radial morphology by 2w, thus this criterion was not taken into account for the quantifications. (**C** and **D**) Confocal images showing $nestin^+GFAP^+$ NSCs with BrdU incorporated (magenta nuclei, arrows) in the DG of WT and $maLPA_1$ mice 3d (**C**) and 2w (**D**) after MTLE induction. All images are maximum projections from approximately 10µm-thick z-stacks. Titles and arrows were shaded for a better visualization. *$p < 0.05$, **$p < 0.01$ by Student's t test. Dots show individual data. Bars show mean ± SEM. Scale bars are 15µm.

In summary, the constitutive deletion of LPA_1 decreases cell proliferation in the DG and React-NSC activation after MTLE treatment. This effect is much higher than that observed in normal (non-MTLE) mice, suggesting that LPA signaling can be of importance in brain pathophysiology. In contrast, other morphological or anatomical changes in this area due to the absence of this receptor were not obvious suggesting a lack of involvement in the overall reactive gliosis response.

7.4. Seizure induction in the amygdala recapitulates changes observed in the DG

Intraamygdalar KA injection provokes an increase in cell proliferation in the DG

Next, we searched for a manner to isolate the intrinsic effect of neuronal hyperexcitation in the DG avoiding the direct impact of injecting KA into the same area in which we are evaluating the consequences. Both KA and the mechanical damage of the cannula and the injected volume could be argued to contribute to the alterations observed in the MTLE mice. Although the Sal-injected animals show that this is not a real concern we thought that other models of MTLE could give valuable additional information. For instance, we wondered whether seizures generated in another brain area connected with the DG and also frequently involved in the pathophysiology of MTLE, *e.g.*, the amygdala (Fournier *et al.*, 2010), could also affect the stem cell population in the DG. We optimized a model to administer KA in the amygdalar complex with exactitude avoiding contact with the lateral ventricular cavity and CA, so that the injection site was not only restricted to the amygdala but also diffusion of the excitatory substance to the hippocampus was improbable.

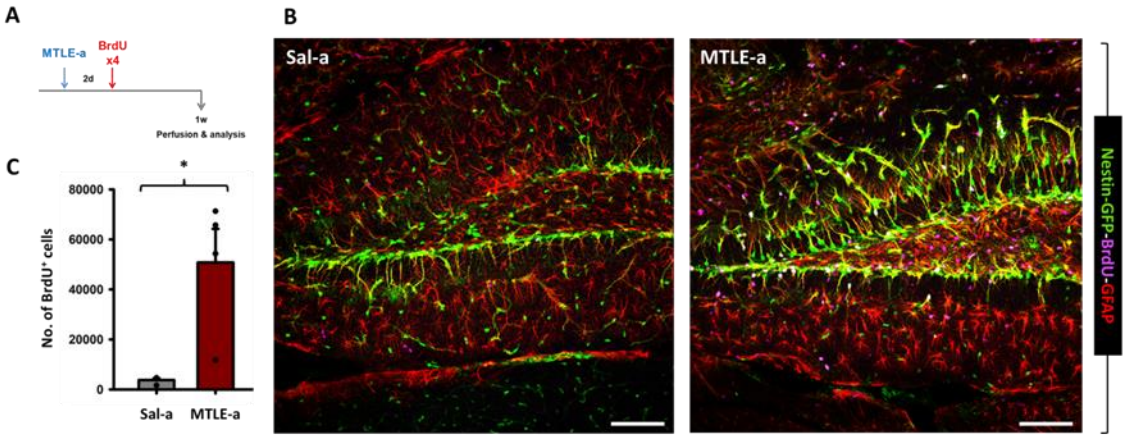

Figure 32. Intraamigdalar induction of MTLE promotes cell proliferation in the DG. (**A**) Experimental paradigm showing the moment of intraamigdalar KA injection and following BrdU administration, performed via 4 injections given 2h apart one from another, and analysis. (**B**) Confocal images showing the general aspect of the DG of a Sal-a and an MTLE-a Nestin-GFP$^+$ animal stained also for GFAP (red) and BrdU (magenta) 1w after the corresponding treatment. Cell division, shown by BrdU$^+$ nuclei, increased in MTLE-a animals even in the hilus, a typical feature of the intrahippocampal MTLE model. All images are maximum projections from approximately 10µm-thick z-stacks. (**C**) Quantification of the total number of BrdU$^+$ nuclei found in the SGZ and GCL of the DG 1w after seizure induction. A significant increase in the number of BrdU$^+$ was observed in MTLE-a-treated animals. *$p < 0.05$ by Student's t test. Dots show individual data. Bars show mean ± SEM. Scale bars are 50µm.

We performed this model of MTLE induction in the amygdala (MTLE-a) in Nestin-GFP transgenic mice and compared their DG to that of saline-injected mice (Sal-a). We also labeled dividing cells and their progeny with BrdU 2d after the procedure and analyzed the tissue 1w after the KA injection (**Fig. 32A**).

We quantified the number of $BrdU^+$ cells and observed a statistically significant increase of more than a 900% in MTLE-a animals compared to those of the Sal-a group (**Fig. 32B** and **C**). Thus, cell proliferation in the DG of animals subjected to MTLE-a induction is strongly promoted, as occurs when MTLE is induced by acting directly in the DG.

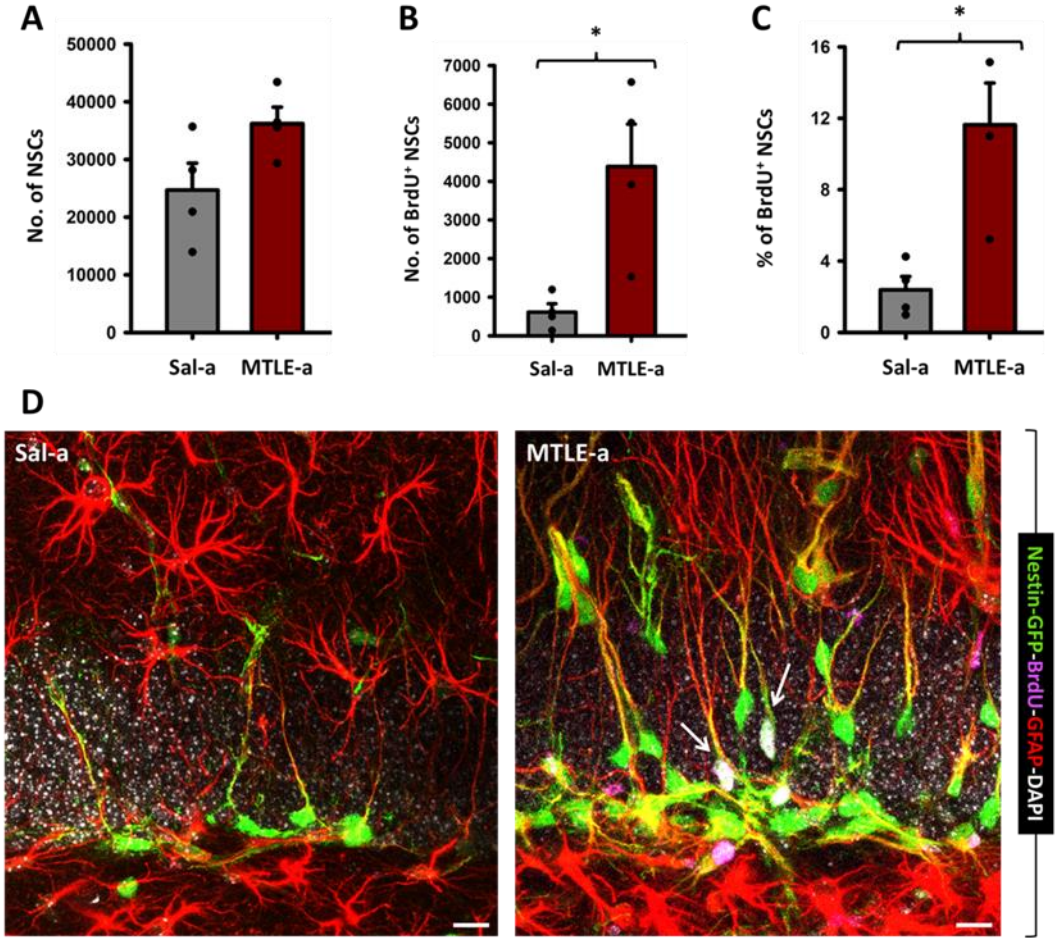

Figure 33. NSCs get recruited with a higher rate and acquire a React-NSC-like morphology in the intraamigdalar MTLE model. (**A**, **B** and **C**) Quantifications of the total number of NSCs (**A**) and $BrdU^+$ NSCs (**B**) and the calculated proportion of the latter among the first (**C**). The total number of $BrdU^+$ NSCs and the proportion of activated NSCs significantly increased after MTLE-a. (**D**) Representative confocal images showing Nestin-GFP^+GFAP^+ NSCs with BrdU immunostaining (magenta nuclei, arrows) in the DG of a Sal-a and an MTLE-a mouse 1w after treatment. Note the change in morphology NSCs suffer also in this epilepsy model. All images are maximum projections from approximately 10µm-thick z-stacks. *$p < 0.05$ by Student's t test. Dots show individual data. Bars show mean ± SEM. Scale bars are 10µm.

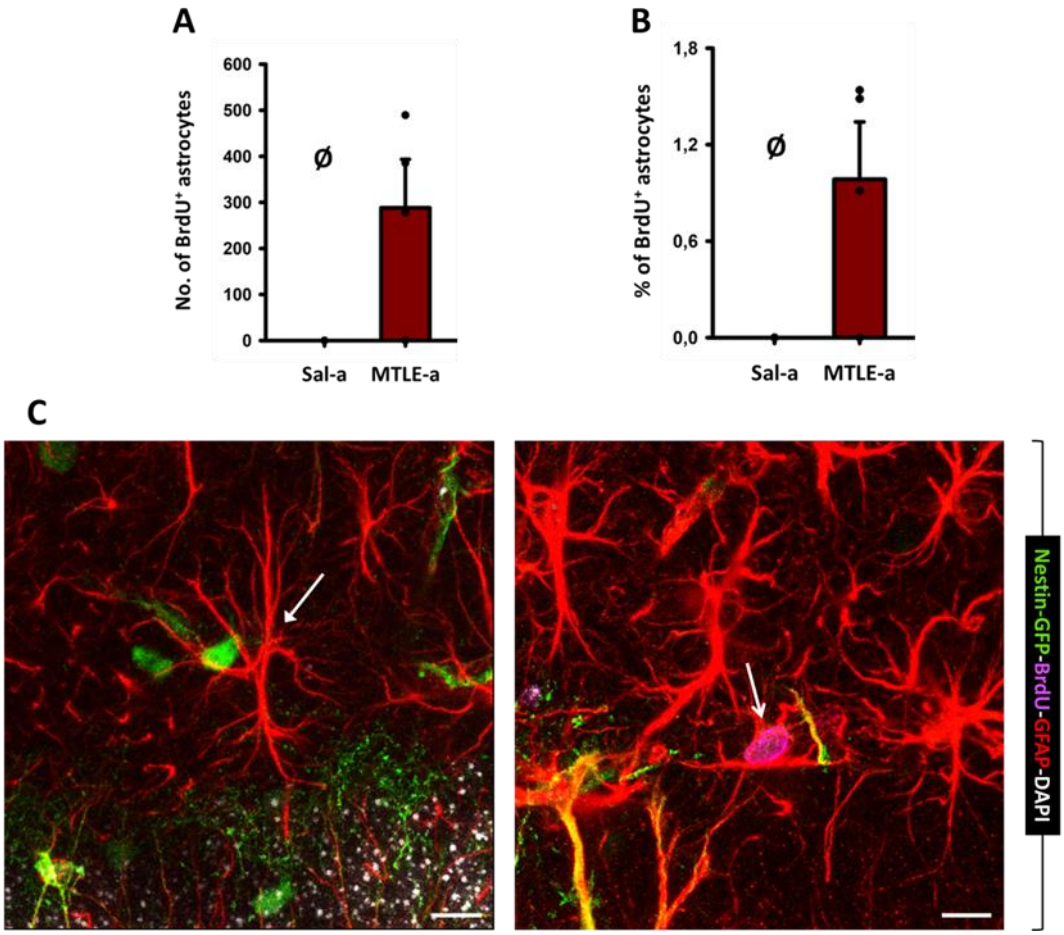

Figure 34. MTLE-a induces division in a small proportion of astrocytes. (**A** and **B**) Quantifications of the total number of BrdU⁺ astrocytes (GFAP⁺ cells with stellate morphology and negative for Nestin-GFP, **A**) and their proportion among the total number of astrocytes (**B**) in Sal-a and MTLE-a mice. No BrdU⁺ astrocytes were found in Sal-a-treated animals. (**C**) Confocal images showing a BrdU-negative astrocyte (closed arrow) in a Sal-a mouse and a BrdU-positive astrocyte (open arrow) in an MTLE-a mouse. All images are maximum projections from 10µm-thick z-stacks. Dots show individual data. Bars show mean ± SEM. Scale bars are 15µm.

MTLE-a increases NSC activation

To further explore the effects of the MTLE-a model in the DG, we focused on NSCs. We quantified the total number of NSCs and the number of those labeled with BrdU and expressed the latter as a proportion, as we have seen that the percentage of activation is a good indicator to describe NSC behavior.

We did not find differences in the total number of NSCs (**Fig. 33A**), but both the number of $BrdU^+$ NSCs and the percentage of $BrdU^+$ NSCs were increased in MTLE-a mice compared to Sal-a mice (**Fig. 33B-D**).

Finally, we also evaluated astrocytic division by quantifying the number of $BrdU^+$ astrocytes and the percentage $BrdU^+$ astrocytes and found instances only in MTLE-a-treated animals (**Fig. 34A-C**). The number of $BrdU^+$ astrocytes found in the DG of some

MTLE-a mice was higher than that in MTLE animals injected directly into the DG, but still was very low and accounted for only a 1% of the total astrocyte number.

These data suggest that neuronal hyperactivity in the amygdala is enough to trigger changes in the DG along the same lines as those produced in the direct model of MTLE induction. MTLE-a increases NSC activation, just like occurs in the intrahippocampal MTLE model, and promotes astrocytic division in the DG. This model of MTLE is useful because it allows us to develop manipulations in the DG to study NSCs and the neurogenic niche, such as retro- or adenoviral vector injections or electrode insertion that would be incompatible with the injection into the DG.

8. Discussion

8. Discussion

8.1. NSCs follow a "disposable" mode of activation

Divisions in the DG render mostly ANP-derived new neurons

BrdU has been largely employed in the study of adult neurogenesis, but normally pulse-and-chase experiments have been performed to label dividing cells in a specific time point. The fact that only a 1-2% of hippocampal NSCs are dividing in a given moment (Encinas *et al.*, 2006; Kronenberg *et al.*, 2003) makes them harder to label and in turn observe their progeny and activation-quiescence behavior. Even though the evidence points at NSCs do not do return to quiescence after activation (Encinas *et al.*, 2011b), a very long cell cycle or too sporadic division makes them easy to miss by the normal division markers and BrdU pulse-and-chase experiments. Resorting to the continuous labeling protocol that we employed in this work we guarantee that every cycling cell was "captured" and therefore they and their progeny could be observable at posterior time points both for proliferation and differentiation analyses.

The results obtained via prolonged exposure to BrdU are in agreement with the well-established notion that NSCs and progenitors in the DG are mostly neurogenic. In the short term, only 1 day after BrdU withdrawal from drinking water, most dividing cells could be readily classified as ANPs by their Nestin-GFP expression, location, morphology and lack of GFAP immunostaining. This result agrees with their high proliferative activity, with 20-25% of them dividing in a given moment (Kronenberg *et al.*, 2003). In addition, the constant exposure to BrdU during their repetitive divisions (2.5 on average) (Encinas *et al.*, 2011b) guarantees that during one of the most vulnerable stages of the neurogenic cascade to the potential dilution of the label keeps there is still access to the nucleotide, so that the dilution below the level of detection turns to be extremely improbable.

The strict criteria employed to categorize BrdU-labeled cells as neurons (NeuN expression, big round or slightly oval nucleus, GCL location and absence of Nestin-GFP labeling) were derived from our aim of clearly separating postmitotic populations from those that putatively can divide at least once more. Nomenclature for stages ranging from differentiating ANPs to mature GCs can vary between authors, due to favoring some factors such as mitotic potential over other such as the expression of certain specific markers. Thus, we avoided differentiating these subdivisions, which rather reflect a continuum, in favor of establishing clear populations in terms of mitotic potential. In the 1w+1d paradigm, the time window existent from the BrdU labeling to the analysis is, presumably, long enough for most of even late ANPs or early NBs to start NeuN expression and enter the neuronal maturation process (Encinas and Enikolopov, 2008). However, although Nestin-GFP coexpression is uncommon sometimes a dim immunolabeling of the transgene can be visualized at the same time

NeuN expression in NBs has started. The expression of GFP can linger longer than the actual expression of nestin, especially in this line that was selected for being the brightest of the initial founder lines (Mignone *et al.*, 2004). Nevertheless, Nestin-GFP-expressing cells were excluded from the neuron category and classified as ANPs. Most often coinciding with this feature, the same exclusion was applied to cells with slightly horizontal oval-like small nucleus characteristic of early-differentiating precursors. All instances of cells belonging to this neuronal lineage but not accomplishing every requirement to be considered already a neuron were therefore classified as ANPs in our quantifications.

The quiescent state in which most NSCs usually remain is complementary to their observed 6% contribution to the overall number of cells that experienced cell division in the DG. Giving a single dose of BrdU, Kronenberg *et al.* defined as NSCs an approximate 4% of $BrdU^+$ cells that did not change much from 2h to 7d (Kronenberg *et al.*, 2003), whereas Encinas *et al.* obtained more than a 10% that was maintained for 10d (Encinas *et al.*, 2011b). Given our continuous model of BrdU administration, it is more probable to label a NSC that is entering the cell cycle as every S phase occurring within the first 7d will have available BrdU to incorporate into the DNA but interestingly the proportions that we quantified with this paradigm are comparable to those from previous studies based on single pulses of BrdU. This result strongly suggests first, that the continuous BrdU administration is not altering the dynamics of proliferation or differentiation; and second, that single or discrete pulses of BrdU are a valid tool as they actually capture most of the information about proliferation and differentiation dynamics. Even though ANP labeling is easier to happen due to their higher mitotic activity, the time lapse before evaluating the tissue is also enough for some of them to start differentiation and, more importantly, die from apoptosis and be phagocytosed. More than two thirds of these neuronal progenitors die in the first 4d (Sierra *et al.*, 2010), reducing their relative contribution to the number of visualized $BrdU^+$ cells. On the contrary, dividing NSCs can remain unchanged for this period. After undergoing three asymmetrical divisions at the population level, NSCs differentiate into astrocytes but fail to express the mature astrocytic marker S100β until 3w later (Encinas *et al.*, 2011b). This period of time mostly coincides with the moment in which other authors had reported to observe $BrdU^+S100\beta^+$ newborn astrocytes in the DG (Steiner *et al.*, 2004; Suh *et al.*, 2007) and also explains the low proportion of them we found in our short-term analysis.

The observed proportion of OPCs among $BrdU^+$ cells also agrees with their known proliferative capacity. However, as noted in Results, most of them were observed in the ML next to the GCL or the hilus next to the SGZ from which they are largely excluded. The 30μm margin we allowed most probably included cells that were excluded in other analyses (Encinas *et al.*, 2011b), thus slightly increasing their contribution to the population of division-derived cells. Still, the deviation that their numbers could induce in the quantification of those of other cell types seems acceptable, as we have

mentioned that the NSC and ANP percentages we obtained are not very different to the ones reported in the bibliography.

When waiting 1m after removing the thymidine analog from drinking water, as expected, the vast majority of $BrdU^+$ cells were neurons, as shown by their NeuN immunolabeling in a big round nucleus located in the GCL. Previous reports employing lineage-tracing techniques or BrdU injections showed similar results, being little differences possibly attributable to variations in the chosen methods (Encinas *et al.*, 2011b; Kronenberg *et al.*, 2003; Suh *et al.*, 2007). This result was consistent between the 1w+1m and 1m+1m paradigms, revealing that the long-term exposure to BrdU does not visibly change the division and maturation dynamics in the DG and again arguing against the toxicity of continuous BrdU administration and validating the use of shorter pulses. A slightly higher percentage of neurons was found in the latter (1m+1m), probably because of the amplification effect ANP divisions are responsible of. Being GCs derived from the most proliferative cells in the neurogenic niche, it seems logical to assume that the more ANPs are labeled (due to prolonged exposure) the higher the contribution of newborn GCs will be in the differentiation analysis. This, in parallel, translates into the reduction of the proportion of the remaining cell types observed in the 1m+1m protocol.

Comparing both differentiation analyses, an interesting shift is also found: whereas in the 1w+1m paradigm the contribution of OPCs was slightly higher than that of astrocytes, it occurs the other way around in the 1m+1m paradigm. Even though OPCs are a highly proliferative cell type, most divisions in the DG take place in the SGZ where NSCs and ANPs are much more frequent (Encinas *et al.*, 2011b). Moreover, OPCs usually locate in areas less densely packed than the GCL and both they and their progeny could "escape" the quantifications after dividing. If so, the 1m+1m-total-long experiment could make this migration more probable to occur and thus reduce their proportion among $BrdU^+$ cells. New astrocytes are most likely derived from NSC divisions, as they were rarely seen in the 1w+1d proliferation analysis and NSCs are known to derive in or give rise to astrocytes (Bonaguidi *et al.*, 2011; Encinas *et al.*, 2011b). When the NSC postmitotic transformation into astrocytes was observed, some of these astrocytes also tended to migrate to the ML or the hilus close to the SGZ (Encinas *et al.*, 2011b). However, although this migration could potentially make them escape too from our quantifications, we believe the upper and lower 30µm margin should be wide enough for us to detect most cells moving from the SGZ. In any case, variations in the percentages of OPCs and astrocytes among $BrdU^+$ cells between both differentiation analyses are not so relevant and could reflect intricate dynamics we cannot evaluate following only *a-posteriori* studies.

BrdU, as can be predicted from its thymidine analog nature, can be toxic and produce morphological and behavioral alterations or trigger cell death (Kolb *et al.*, 1999; Sekerkova *et al.*, 2004; Taupin, 2007). Yet, at the dose we employed we neither observed obvious abnormalities in mice nor cell death in the tissue. We found no reasons to think that our results could have been modified due to the possible influence

of BrdU on cell division of differentiation. The similar proportions we obtained to previous single pulse-and-chase experiments act in support of the validity of our continuous-administration paradigm. Some minor differences with previous results, such as the presence of some BrdU-labeled ANPs 1m after stopping the administration, as commented below, could be due to the prolonged BrdU administration.

ANPs and NSCs do not return to quiescence for a long time after activation

The main goal of these sets of experiments was to address whether NSCs are activated and then enter longer periods of quiescence before entering the cell cycle again, an event that would be easier to miss using single or discrete BrdU experiments. The literature massively argues against this possibility, though, as thousands of papers report only neurons and astrocytes in survival and differentiation studies without mention of BrdU-labeled NSCs. While ANPs and NSCs represented together a high proportion of the cells experiencing division in the proliferation analysis, their contribution was almost abolished when we waited times sufficient for differentiation to occur. 1m after BrdU withdrawal, instead of 1d, ANPs expectedly decreased to less than a 2% as they differentiated into neurons. We may have expected them to drop even more, but the instances found were most probably some of the mentioned rare cases in which an early NB still presents perceptible Nestin-GFP expression. The results at the population level again support the previous idea that ANPs divide consecutively several times, 2.5 on average, and eventually differentiate into GCs (Encinas *et al.*, 2011b; Kempermann *et al.*, 2004; Pilz *et al.*, 2018). Evaluation of the overall reentry into the cell cycle further reinforces the fact that in the short term these cells are continuously proliferating but 1m is enough for the vast majority of them to exit mitosis and start neuronal differentiation and maturation. In fact, as commented before, this period is usually much shorter. The 1m+1m protocol revealed an even more negligible contribution of this cell type to the division-derived population, following these principles.

As for NSCs, their presence among $BrdU^+$ cells was of a scarce 1% in the 1w+1m paradigm. Despite this contribution is very low compared to that of neurons, we could expect $BrdU^+$ NSCs to be less than anecdotal if they also divide consecutively and transform into astrocytes. Even though this might reflect the capacity of some of them to divide symmetrically (Bonaguidi *et al.*, 2012; Bonaguidi *et al.*, 2011), this result can be explained by other causes. Differentiating postmitotic NSCs usually start S100β expression few weeks after the last division, but this process could be a cellular spectrum from short to longer periods in which the multipolar stellate morphology, migration and expression of this marker are progressively acquired. Also, these criteria were all taken into account to define astrocytes but the quantifications for these two cell types (NSCs and astrocytes) were performed in different sets of tissue to get reliable immunohistochemical staining. This is the reason why percentages do not add up to 100% and could reflect that some of the NSCs we found were actually differentiating into astrocytes but did not fulfill all the requirements necessary to be considered mature

astrocytes. To further support this final differentiation, in the 1m+1m paradigm $BrdU^+$ NSCs were abolished in all but one animal in which we observed a single one. The percentage of division-derived cells they represented may have added to that of astrocytes, what would partially explain, in addition to previously mentioned causes, the increase in the latter compared to the proportion of OPCs.

Reentry into the cell cycle, revealed by $Ki67^+BrdU^+$ cells, was high in the proliferation analysis but very low in 1w+1m and 1m+1m differentiation analyses. Given that at the population level both NSCs and ANPs (the most frequent cell types in the SGZ where the majority of divisions take place) divide several consecutive times and exit the cell cycle (Encinas *et al.*, 2011b), these results are consistent with previous observations. Regarding exclusively NSCs, their reentry average is almost twice as high as the level corresponding to the overall $BrdU^+$ population 1d after 1w-long BrdU labeling. This further reinforces their participation in the initial proliferation and their repetitive divisions in the short term. Remarkably, in both experiments in which quantifications were conducted 1m after BrdU removal NSC reentry was not found. $BrdU^+$ NSCs in those evaluations presented very low numbers or were completely absent in some mice, but still not a single one colocalized with Ki67. This means that the few of them that remained as NSCs after division were not dividing again after a 1m period.

NSC quiescence is a majority feature in the DG, but their activation seems a one-way ticket to ride. Once activated, NSCs suffer 3 asymmetric divisions and start differentiating into astrocytes (Encinas *et al.*, 2011b). Even when symmetric division in normal conditions has been reported, a property we have not observed, its probability was very low (Bonaguidi *et al.*, 2011; Pilz *et al.*, 2018) or the criteria utilized to identify NSCs were not unambiguous (Suh *et al.*, 2007). In a clonal analysis based on an inducible Ascl1-tdTomato reporter model, the frequency of NSCs in a clone fell below 0.4 before 20d from labeling had gone by. Moreover, a cycling NSC disappeared less than 10d after activation and, importantly, no repeated shuttling between quiescence and activation was observed. Although in this case no evidence of final astrocytic differentiation was found (instead they reported neuronal differentiation), their results strongly suggested the depletion of activated NSCs (Pilz *et al.*, 2018).

Despite the invaluable information this *in vivo* clonal analysis provided, interpretations extracted from such approach must be taken cautiously. The cortical window the mice had to be implanted with was reported to leave the hippocampus intact, but possible alterations on NSC behavior and the neurogenic niche induced by the invasive surgery remain unknown. In our laboratory we have observed that traumatic brain injury (by controlled cortical impact) increases NSC activation (Durá *et al.*, work in progress) and it is known to alter neurogenesis, therefore it is reasonable to argue that some alterations can be induced by methodology in the *in vivo* two-photon microscopy experiments. In our experiments we have seen the negligible effect the injection of saline, for example, has on NSCs, but this case is an acute treatment performed with the help of a thin cannula instead of the chronic removal of brain tissue. On the other hand, we have also observed that a strong stimulation in the amygdala is able to induce remarkable changes

in the DG; thus, we cannot predict the extent to what this cortical window can cause abnormalities in the circuitry that could lead to a slight disruption of the neurogenic niche and explain some divergences in the results obtained with different methods.

Another approach-derived concern this clonal analysis might present is the choice of Ascl1 to label NSCs and their progeny: Ascl1-expressing cells could represent only a subpopulation of hippocampal stem cells, a possibility the authors even considered (Pilz *et al.*, 2018). Indeed, Ascl1 was reported to be a specific marker of proliferative NSCs and necessary for quiescent ones to get activated (Andersen *et al.*, 2014); so maybe the labeled population is more prone to originate the neurogenic burst than the remaining NSCs. Even though this proactivation protein was reported to be destabilized by Huwe1 to return to quiescence, cell cycle reentry in this study was evaluated only 1d after the thymidine analog ethynyl deoxyuridine (EdU) was administered and still accounted for more than a 75% of NSCs in WT animals (Urban *et al.*, 2016). When the authors also analyzed BrdU-retaining NSCs 3w after labeling both in WT and Huwe1cKO mice, $BrdU^+$ NSCs were significantly reduced in the latter but their numbers were not that high in WT mice. This period of time in which they are not lost could overlap with the astrocytic differentiation process we propose instead of representing a true quiescent state. Nevertheless, Urban and colleagues did not claim a long-term return to quiescence but suggested the existence of a pool of temporarily-resting NSCs that is different from the main quiescent population. To avoid misinterpretations on whether return to quiescence is possible (although not probable) or it just manifests the postmitotic state towards eventual astrocytic differentiation, thorough experiments employing a wider spectrum of time points, especially during the second to third week after labeling, are still needed.

In any scenario, we can claim that at the population level the behavior of most NSCs in the DG matches the "disposable stem cell" model. When a NSC gets activated, its most plausible fate is depletion. Even if some them were able to divide symmetrically, as was reported in Bonaguidi's clonal analysis, the frequency of this event would be very low and not sufficient to counteract the usual depletion (Bonaguidi *et al.*, 2011). The astrogliogenesis we see in parallel to the disappearance of $BrdU^+$ NSCs suggests newborn astrocytes are derived from stem cells after division. If these astrocytes were generated directly from NSC division, however, we would expect a higher representation of them among $BrdU^+$ cells in the initial proliferation analysis than the observed 1 astrocyte per 6 NSCs ratio. NSC ultimate differentiation into astrocytes after activation (Encinas *et al.*, 2011b), on the contrary, meets the requirements needed for the tenfold increase in the proportion of division-derived astrocytes 1m after BrdU withdrawal. Anyway, NSC depletion through division-coupled astrocytic differentiation only explains about half of the stem cell decline and apoptosis has been proposed as a likely contributor (Ziebell *et al.*, 2018). A bump in the road for the whole model to adapt to the real cell behavior is the fact that NSC death or apoptosis is an unobserved process in normal conditions and very infrequent following insult (Sierra *et al.*, 2015). Nevertheless, the non-detectable level of NSC apoptosis could be explained by the rate

at which apoptotic cells are cleared thanks to the prompt microglial phagocytic response (Sierra *et al.*, 2010).

8.2. Seizures in the hippocampus shift NSCs from neurogenesis to reactive astrogliogenesis

Different levels of neuronal hyperactivity affect NSC behavior and can deplete neurogenesis

Given the "disposable" type of activation that NSCs most frequently suffer, a model we supported providing additional proof, we hypothesized that stimuli which induce their entry into the cell cycle would accelerate their division-coupled progressive exhaustion. We have mentioned that NSC activation has been related to neuronal excitability (Pineda and Encinas, 2016) and high levels of hyperexcitation involving seizure generation might even trigger a shift in their properties and disrupt the correct progress of the neurogenic cascade. We were also interested in clarifying whether MTLE increases or impairs neurogenesis and unveiling the mechanisms by which astrogliogenesis is presumably favored in this neurological disorder.

In this study we proved how neuronal hyperexcitation induces NSC activation in the DG. Although this effect was known thanks to previous studies, *e.g.*, utilizing ECS (Segi-Nishida *et al.*, 2008) or intraperitoneal KA models (Huttmann *et al.*, 2003), the studies of the long-term effect were lacking. We characterized the effect of two degrees of neuronal hyperactivation and how, first, NSCs behave in terms of cell division and differentiation, and second, the overall proliferation in the DG and that of other cell types is affected. Neuronal hyperactivity in the form of EA, characterized by abnormal discharges with increased frequency of spikes but that do not induce seizures, was enough to recruit higher numbers of NSCs into the cell cycle in the short term and maintain this enhanced activation state up to 7dpKAi. Meanwhile, ANP proliferation was also increased following EA suggesting that a boost in neurogenesis was triggered. Indeed, the quantifications in inducible Nestin-Cre-ER^{T2}/R26R:YFP transgenic mice, in which we were able to trace NSC-derived progeny, subjected to EA treatment manifested a rise in the number of newborn neurons at 14 and 30dpKAi.

The higher KA concentration employed to trigger convulsive seizures mimicking MTLE provoked a huge increase in NSC activation, but the mode of NSC division the model of MTLE induced was, surprisingly, not the typical ANP-generating asymmetric one. ANP generation was decreased below Sal levels at 7dpKAi, what translated in a persistent decline in neurogenesis as revealed by lineage tracing in Nestin-Cre-ER^{T2}/R26R:YFP mice and the time course we performed on LPA$_1$-GFP mice. As additional evidence to support this change in dynamics, most NSC divisions that were observed belonged to the symmetric category. However, both the mother and daughter NSCs had acquired a hypertrophic multibranched phenotype with enlarged cytoplasm, thus being termed React-NSCs, that seemed incompatible with the generation of

neurogenic progeny. No matter the transgenic line we subjected to MTLE treatment, seizures induced the abolition of neurogenesis in favor of reactive astrogliogenesis.

Provided that NSC activation is mostly coupled with their depletion even in normal conditions, the increased rate of entry into the cell cycle induced by neuronal hyperactivity would expectedly accelerate the loss of the stem cell pool and thus of their neurogenic capabilities. Indeed, following these principles we reported a decrease in both the number of NSCs and that of newborn neurons in the long term after either EA or MTLE treatment (Sierra *et al.*, 2015). This long-lasting impairment of neurogenesis would lead to the loss of the cognitive functions related to this process and the restorative potential to replace the neurons lost due to excitotoxicity.

The level of AHN correlates with acquisition of spatial memories (Kempermann and Gage, 2002) and it has also been reported to have a role in hippocampal-dependent associative learning (Saxe *et al.*, 2006) as well as in responses to stress and depression (Snyder *et al.*, 2011). Interestingly, epileptic patients have a high incidence of memory impairment (Gargaro *et al.*, 2013) and anxiety and depression (Heuser *et al.*, 2009). Intuitively, it has been speculated that increasing neurogenesis could benefit these patients. However, given our data enhancing neurogenesis in MTLE does not seem a good strategy as NSCs, the origin of the cascade itself, present an affected division behavior. Instead, therapeutic strategies should try to prevent the NSC massive activation that leads to reactive astrogliogenesis.

8.3. LPA_1-GFP mice, a new tool to study NSCs and React-NSCs

React-NSCs derive in RAs maintaining LPA_1 expression during most of their differentiation process

React-NSCs not only lose their neurogenic capabilities, as their divisions render mainly more React-NSCs and neurogenesis was observed to be depleted, but progressively differentiate into RAs. Whereas in EA animals the change in NSC and ANP divisions was merely quantitative, MTLE completely changed the fate of NSC-derived cells. React-NSCs in Nestin-Cre-ER^{T2}/R26R:YFP mice unambiguously gave rise to RAs, which ended up being the most represented cell type among YFP^+ cells. In support of these data, LPA_1-GFP^+ React-NSCs also differentiated into RAs in a process that often involved a progressive loss of the transgene expression.

Reactive astrogliosis is a common hallmark of MTLE (O'Dell *et al.*, 2012), but usually RAs are derived from parenchymal astrocytes in this and other neuropathological conditions (Norton *et al.*, 1992; Sofroniew, 2009; Zamanian *et al.*, 2012). RAs have impaired glutamate buffering due to altered expression of glutamate transporters such as GLAST and release cytokines with proepileptogenic potential such as IL-1β (Devinsky *et al.*, 2013). Furthermore, different models employed to induce reactive astrogliogenesis in the hippocampus led to increased neuronal hyperexcitability

(Ortinski *et al.*, 2010) and the development of spontaneous seizures (Robel *et al.*, 2015). These data strongly suggest that impaired astrocytic function favors the development of secondary recurrent seizures. According to our results, React-NSCs can also originate RAs and thus partially contribute to the gliosis that is part of hippocampal sclerosis. This addition to stem cell multipotency was also proved for the subventricular NSCs, which under stroke conditions leave their niche to become RAs that indeed contribute to the glial scar formation in the site of injury (Faiz *et al.*, 2015).

The React-NSC phenotype constitutes a new property of NSCs with critical functional implications: neurogenesis becomes chronically impaired due to the disruption of the neurogenic cascade, that no longer produces neuronal progenitors, and the steady decay of the stem cell pool coupled to their conversion into RAs. These RAs, as we have just mentioned, in turn could exacerbate MTLE. Therefore, characterizing this transformation should open a window of opportunity in which React-NSCs or React-NSC-derived RAs are functionally different from parenchymal astrocyte-derived RAs and the transition step can be redirected. Here, we provide insight into the expression of a specific NSC marker, revealed by LPA_1-GFP transgenic mouse, that labels this transition into RAs and further up to the apparent complete differentiation in a subpopulation of them.

The molecular mechanisms leading to this transformation must be further studied, and in particular we can emphasize the importance of LPA_1. Even though nestin-based mouse lines have been extremely useful tools in the study of NSCs, they lose potential in the research on their acquisition of a reactive phenotype that leads to the generation of RAs. Nestin is also expressed by RAs (Clarke *et al.*, 1994), what makes us impossible to distinguish between React-NSC-derived RAs and those derived from parenchymal astrocytes on the basis of its expression. However, in this work we did not find evidence of LPA_1-GFP expression in astrocytes other than RAs differentiated from React-NSCs. This makes LPA_1-GFP transgenic strain a very valuable tool for the specific purpose of studying the transition from React-NSC to RAs, as it allows us to define a conspicuous difference to tell them from other RAs. As a proof of principle, we are in the laboratory isolating NSCs and React-NSCs from LPA_1-GFP mice and we have found, for instance, a huge increase in the expression of IL-1β in React-NSCs when compared to control NSCs (Martín-Suárez *et al.*, work in progress). A schematic representation of the conclusions we reached regarding LPA_1 were summarized in **Fig. 35**.

We have reported the observation of React-NSCs and their massive activation after seizures, but they do not manifest this response following other pathophysiological alterations. Specifically, neuronal hyperexcitation in the form of EA activated NSCs in higher numbers but only seizures caused by the MTLE model qualitatively changed their division type and fate. Moreover, inflammation alone provoked by LPS injection did not exert even similar effects on NSC morphology and activation. Thus, in spite of NSC similarities with astrocytes (Seri *et al.*, 2001), molecular pathways leading to NSC transformation into React-NSCs and eventually into RAs could be not the same as in the

reactive gliosis derived from parenchymal astrocytes. There are, however, common features between astroglial and NSC reactivity. In addition to their hypertrophic phenotype, interestingly, we have reported an increasing trend in the number of mitochondria in React-NSCs following MTLE treatment. A rise in this number is also a characteristic of RAs (Maxwell and Kruger, 1965), which strengthen the biogenesis of mitochondria to cope with the increased demand for energy, *e.g.*, under sepsis conditions (Wang *et al.*, 2014; Zhao *et al.*, 2017). Nevertheless, in our TEM analysis no obvious changes in the number of mitochondria in astrocytes or RAs 10d after seizure induction were observed compared to Sham animals.

The increase in the number of mitochondria during NSC acquisition of their reactive phenotype could also be interpreted as an effort to fulfill the energetic requirements necessary to maintain the high rate of division they present. Furthermore, mitochondria usually suffer fission events during the G2 and M phases of the cell cycle to facilitate the equal distribution to each of the daughter cells after mitosis (Mishra and Chan, 2014). This reason, yet, is not probably applicable to the previously reported increase in the number of mitochondria in RAs, since we have shown in several experiments that astrocytic division is very infrequent even following damage. Thus, this peculiarity could represent another difference between astrocytic and NSC reactivity acquisition in MTLE. Increasing numbers of mitochondria in parenchymal RAs might not be common to reactive astrogliosis as an overall mechanism but exclusive to specific responses, for example, to stimuli that induce injury of the ultrastructure of the mitochondria (Zhao *et al.*, 2017). This argument, still, is weakened by the fact that oxidative stress has been indeed reported in the hippocampi of epileptic patients, mainly in neurons but also in astrocytes (Ristic *et al.*, 2015). In any scenario, in the future we will perform further analyses to elucidate whether the increase in the number of mitochondria is a real difference between cell types and/or between treatments.

More important than the presumable ultrastructural differences between NSCs and React-NSCs we could find, we would like to emphasize the suitability of the LPA_1-GFP transgenic mouse for TEM studies, especially for those focused on React-NSCs. The specificity of the transgene expression in this lineage was validated by the fact that an almost complete absence of immunogold labeling was found in astrocytes located in adjacent areas to the SGZ or GCL even after a reactive response could have been provoked by the MTLE model. This reactivity, for instance, would have contaminated some sets of results if we had employed nestin-based transgenic strains due to *de novo* nestin expression in RAs, unless performing approaches to avoid the interference of this *a posteriori* expression like the one we applied on inducible Nestin-Cre-ER^{T2}/R26R:YFP mice.

LPA_1 contributes to React-NSC activation

We have reported the persisting LPA_1-GFP expression in React-NSCs and even in a subpopulation of React-NSC-derived RAs after differentiation, but the specific function of the receptor in this transformation remains elusive. In normal conditions, its absence

has been related to decreased neurogenesis (Matas-Rico *et al.*, 2008) and increased neuronal survival *in vivo* without a rise in cell proliferation was promoted by the agonist LPA (Walker *et al.*, 2016), but React-NSCs are a novel property of NSC multipotency and remain to be specifically characterized. MTLE induction in maLPA$_1$ mice, devoid of LPA$_1$ expression, did not lead to conspicuous morphological differences in React-NSCs compared to their WT counterparts. No obvious anatomical or tissue changes in the DG between these two mouse genotypes were observed, either. Nevertheless, a strong effect on overall cell division and React-NSC activation was shown.

Even though under normal conditions maLPA$_1$ mice had been reported to have reduced cell proliferation compared to WT mice (Matas-Rico *et al.*, 2008), we did not observe such decrease to be significantly different 3d after MTLE treatment. It seems probable that the stimulation of cell division after seizures is so high that the baseline levels are covered up by this increase. By 2w, however, BrdU$^+$ cells were decreased almost a 50% in maLPA$_1$ compared to WT animals, suggesting an accumulative effect on proliferation of the absence of the receptor.

Regarding NSCs exclusively, React-NSC activation rate in the MTLE model was much higher in WT animals than in maLPA$_1$ animals both at 3d and 2w time points, although it remained higher than NSC activation in normal conditions. Despite we did not include control (Sal-injected) mice in this experiment as we wanted information about React-NSCs and not normal NSCs, we can consider some speculations comparing MTLE data with those of MTLE mice of our reporter transgenic strains. For example, the approximate 8% of dividing React-NSCs in maLPA$_1$ mice at both time points that we found was lower than any proportion of dividing React-NSCs in our LPA$_1$-GFP animals up to 2w after MTLE treatment. On the contrary, the percentages we obtained in WT animals were slightly higher than any of LPA$_1$-GFP mice in those first three time points. Thus, the different genetic background between mouse lines that for sure can give rise to divergences in results in this case do nothing but emphasize the relevance of LPA$_1$ expression. This is so because the large differences observed between WT and maLPA$_1$ animals must be only due to the presence or absence, respectively, of this receptor.

Whether the absence of LPA$_1$ expression leads to differences in basal NSC activation or not, a possibility we will study in the near future, our results strongly suggest that it has an important role in the massive activation React-NSCs suffer following MTLE treatment. However, the fast React-NSC-phenotype acquisition was found no matter the genotype the animals presented. Therefore, it seems that the action of this receptor in NSCs is restricted to their entry into the cell cycle, at least after seizures. React-NSC conversion into RAs and their contribution to the reactive gliosis, a characteristic of hippocampal sclerosis in MTLE patients, would then be an independent mechanism on React-NSC high rates of division in pathways in which LPA$_1$ is involved. This might be interpreted as a fateful discovery, since possible therapeutic targets would only act in one of the features appearing in MTLE. Yet, the fact that in this pathological condition both the mother and daughter cells of a React-NSC division differentiate into RAs

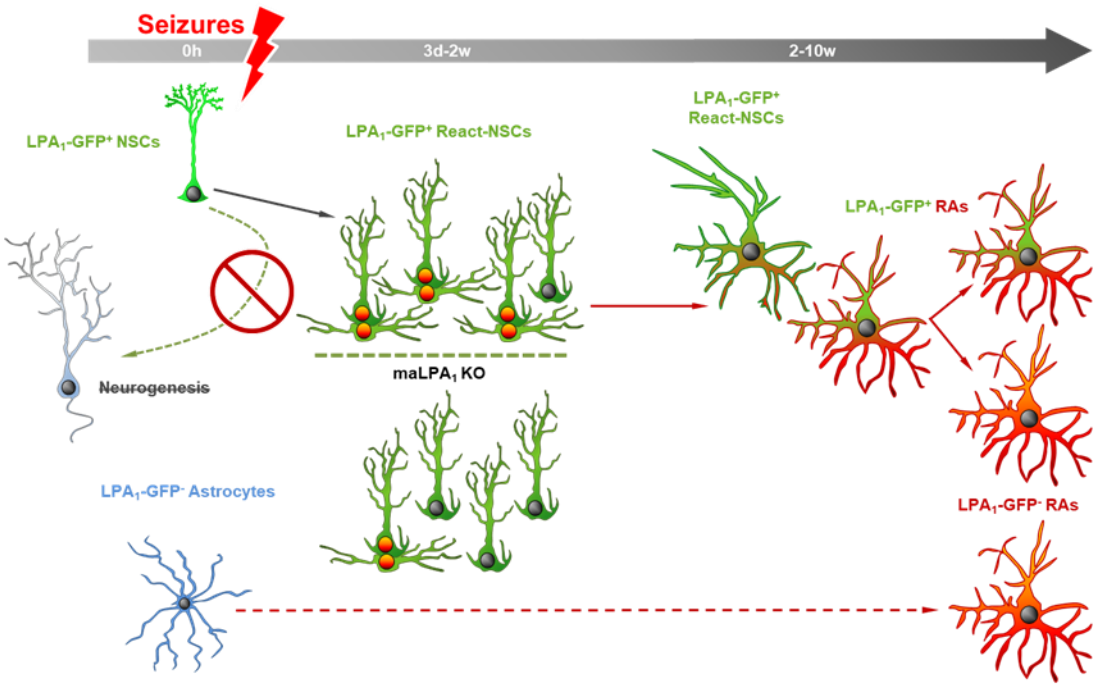

Figure 35. LPA_1 labels seizure-induced hippocampal React-NSCs and controls their activation. When neuronal hyperactivity is high enough to trigger seizures in the hippocampus, NSCs get massively activated but the neurogenic cascade is abolished. Instead, both they and their progeny transform into React-NSCs that progressively differentiate into RAs. Evaluating this transition with LPA_1-GFP labeling, the resulting populations consist of RAs negative for the transgene expression, RAs with persisting LPA_1-GFP expression and a subpopulation of putative LPA_1-GFP$^+$ React-NSCs that do not colocalize the mature astrocytic marker S100β. LPA_1-GFP-negative RAs can also derive from parenchymal astrocytes. In the absence of LPA_1, like in maLPA_1 KO mice, however, the massive activation that NSCs suffer following seizures is significantly reduced.

suggests the more React-NSCs get activated, the higher their contribution to reactive astrogliosis must be. In this scenario, LPA_1 antagonists would partly prevent the fraction of the glial scar of which React-NSC massive activation is presumably responsible.

LPA_1 starts to be expressed by GCs weeks after the onset of seizures in MTLE

Another noteworthy discovery we reported is the surprising *de novo* LPA_1-GFP expression in neurons only in MTLE-treated mice. LPA_1 expression analysis has been problematic since its regulatory functions in AHN was first proposed (Hecht *et al.*, 1996) due to the difficulty in getting a good specific antibody against the receptor and the contradictory effects that its ligand LPA has been reported to have. For example, we have documented specific LPA_1 expression in NSCs via immunohistochemistry and LPA_1-GFP reporter supporting recently published data (Hochgerner *et al.*, 2018; Walker *et al.*, 2016). However, it has been claimed to have functions preventing neuronal differentiation and inhibiting neurosphere formation from human embryonic stem cells (Dottori *et al.*, 2008). On the other hand, other authors have described that neurosphere formation from primary cultured hippocampal precursor cells and net neurogenesis *in*

vivo were increased by the agonist LPA (Walker *et al.*, 2016). Results of both studies suggest that LPA_1 signaling pathways have functions in the neurogenic cascade beyond the NSC stage, even though LPA_1 expression is fast downregulated in ANPs.

Moreover, LPA receptor activation induced by gintonin has been reported to enhance both excitatory and inhibitory synaptic transmission in the adult rat hippocampus (Park *et al.*, 2015). Even more specifically, LPA signaling has been proposed to play a role in the regulation of KA-induced cell death, but this was especially observed in CA3 and the receptor whose expression was affected in the DG, decreasing its immunoreactivity, was LPA_3 and not LPA_1 (Lee *et al.*, 2014). If this last result has something to do with the start of the transgene expression that we observed in GCs we cannot know for sure, as we found this result weeks after KA injection and the authors of this paper only evaluated the acute effect on the expression of these receptors up to 24h later. As other pathological conditions such as GCL dispersion can be observed in MTLE, the start of LPA_1 expression could be part of the group of mechanisms that the neuronal population manifests to try to adapt to the new recurrent circuitry or even prevent excitotoxicity-induced cell death.

Interestingly, brain sections of mice devoid of LPA_1 expression of the same strain we employed ($maLPA_1$) showed no gross anatomical abnormalities in the hippocampal formation but indeed presented a reduced volume in this region (Castilla-Ortega *et al.*, 2011; Matas-Rico *et al.*, 2008). However, this volume reduction was not observed in the DG suggesting a normal embryonic development in this specific area. More intriguingly, adult neurogenesis in terms of cell proliferation was decreased in $maLPA_1$ mice in such a way that environmental enrichment was not able to rescue the normal phenotype (Matas-Rico *et al.*, 2008) and chronic stress-induced impairment was more aggravated than in WT animals (Castilla-Ortega *et al.*, 2011). These results support the hypothesis that LPA has a positive effect on AHN, although it remains to elucidate the manner by which it could affect only newborn-neuron survival *in vivo* without expression of the receptor LPA_1 in late progenitors (Walker *et al.*, 2016). Whether this action is exerted via the activation of other receptors or other intricate mechanisms are involved deserves further research. An interesting interpretation of these results, however, is that embryonic and adult neurogeneses are not regulated by the same pathways suggesting that AHN would not be a remnant of the developmental process.

8.4. Intraamygdalar injection of KA is an alternative valid model of MTLE

Lastly, we have implemented an MTLE model originating seizures in the amygdalar complex that triggers changes in the neurogenic niche of the DG. Optimizing the KA injection site for our purposes of avoiding contact with the hippocampus or the lateral ventricle (that could lead to a more widespread distribution of the drug) we now have an alternative method to induce seizures that does not exert its action directly into the DG. We have reported that inflammation alone, which could have been facilitated by injury, is not enough to activate NSCs in higher numbers or induce the phenotypical React-

NSC change that we observed in the intrahippocampal MTLE model. However, KA *per se* could provoke widespread effects in the DG that would exacerbate those attributable specifically to neuronal hyperexcitation. In addition, this model will help us technically since it allows us to perform manipulations in the DG such as the insertion of permanent electrodes to carry out electrophysiological and electroencephalographic recordings or the injection of viral vectors.

Previous works have reported the epileptic behavior that is observed in animals treated with this model (Berger *et al.*, 1989; Mouri *et al.*, 2008), whereas we focused on describing the neurogenic niche. We have observed in MTLE-a animals an increase in cell proliferation in a similar fashion as in the intrahippocampal MTLE model. More importantly, NSC activation was induced by MTLE-a up to levels comparable to those in the short term after direct injection into the. Although not quantified, we found indicators of NSC reactivity similar to the ones in the React-NSC phenotype (Sierra *et al.*, 2015) such as GFAP overexpression and apical process thickening but in a milder manner. We also observed $BrdU^+$ astrocytes in MTLE-a mice, whereas in Sal-a mice none was found. The number of these division-derived astrocytes, although low, was even higher than in MTLE mice, but administration paradigms were slightly different and could be a reason for this divergence.

These results reveal that more important than the epileptogenic site, provided that it is connected to the hippocampus, is the level of neuronal hyperactivity that is ultimately triggered in the DG. It seems that once a threshold in neuronal excitation is exceeded NSCs stop their normal neurogenic program, acquire a reactive phenotype and both they and their progeny differentiate into RAs. Even though long-term evaluations must be performed to validate this hypothesis in MTLE-a mice, the appearance of NSCs, their daughter cells and the overall neurogenic niche suggest they will follow a similar evolution as that discussed for React-NSCs and their progeny in MTLE but probably in a slower manner.

We have seen that, avoiding the damage produced by the physical injection and the local action of KA in the DG, neuronal hyperactivity alone is capable of altering cell proliferation and NSC activation and reactivity. Nevertheless, it would be necessary to analyze reactivity and inflammation parameters and compare them between models to validate that the neurogenic alterations are a consequence of the sole hyperexcitation and are not exacerbated by the local injection of the glutamate agonist.

Other areas such as the rhinal and piriform cortices are highly epileptogenic regions that are broadly interconnected with other limbic areas (Vismer *et al.*, 2015). Induction of SE has even been performed in the piriform cortex (Milhaud *et al.*, 2003), but approaches to limbic seizures with KA, out of the direct injection, have more often employed the intraamygdalar injection to visualize influences to the hippocampus (Alves *et al.*, 2017; Kobayashi *et al.*, 2002). An additional reason to choose this model is the fact that aberrant AHN due to amygdaloid seizure induction has been reported (Fournier *et al.*, 2010; Fournier *et al.*, 2013). Even though the authors utilized kindling

instead of KA administration in these works, the relevant effect the stimulation of this circuitry showed in the DG made the amygdala an adequate target for our research purposes. Moreover, the epileptogenic cortices are generally associative region-related areas in which neuronal hyperactivity could lead to widespread effects in the brain; whereas the amygdalar complex is a more specific location from where we find more difficult the diffusion of KA to other hippocampus-related circuits.

In any case, the alterations in the neurogenic niche we described following MTLE-a are preliminary proof that must be further explored, especially in terms of final differentiation of the React-NSC-like cells and the possible contribution of the reported seizure-induced changes to hippocampal sclerosis.

9. Conclusions

9. Conclusions

1. **NSCs follow a "disposable/one-time only" model of activation and do not cycle between periods of cell division and quiescence.**

2. **NSCs, when activated, reenter the cell cycle with a very high probability in the short term but they neither remain as NSCs nor reenter the cell cycle in the long term.**

3. **Reentry into the cell cycle is probable in the neurogenic niche in the short term but negligible after cell differentiation.**

4. **Long-term BrdU labeling does not alter cell division or differentiation dynamics in the DG neurogenic niche and is therefore a valid tool to study AHN.**

5. **Neuronal hyperexcitation in the form of EA increases cell proliferation and NSC activation in the DG but does not change differentiation or the neurogenic capability of NSCs.**

6. **A higher level of neuronal hyperexcitation, in the form of MTLE, massively activates NSCs, induces React-NSCs and switches them to symmetric cell division that abolishes neurogenesis.**

7. **Seizure induced-React-NSCs and their progeny differentiate into RAs in the DG thus contributing to hippocampal sclerosis.**

8. **Inflammation (LPS-induced) alone does not trigger an increase in cell proliferation or NSC activation, as they are observed after neuronal hyperexcitation.**

9. **NSCs in the DG specifically express LPA_1 and LPA_1-GFP.**

10. **MTLE-induced React-NSCs maintain LPA_1-GFP expression until their final transformation into RAs, remaining in some of these React-NSC-derived RAs as a characteristic that distinguishes them from other RAs.**

11. **The proportion of undifferentiated React-NSCs, based on LPA_1-GFP expression, decreases over time in MTLE.**

12. **Neurons in the GCL start LPA_1-GFP expression weeks after induction of MTLE.**

13. **Ultrastructural analysis by TEM confirms the utility of LPA_1-GFP transgenic mice to study NSCs and React-NSCs and revealing an increasing trend in the number of mitochondria in the latter.**

14. **In the absence of LPA_1 MTLE-induced cell proliferation and NSC activation in the DG are decreased.**

15. **An alternative model of MTLE based on the intraamigdalar injection of KA also increases cell proliferation, NSC activation and induction of React-NSCs in the DG.**

10. Bibliography

10. Bibliography

Ables, J.L., Decarolis, N.A., Johnson, M.A., Rivera, P.D., Gao, Z., Cooper, D.C., Radtke, F., Hsieh, J., and Eisch, A.J. (2010). Notch1 is required for maintenance of the reservoir of adult hippocampal stem cells. J Neurosci *30*, 10484-10492.

Adlaf, E.W., Vaden, R.J., Niver, A.J., Manuel, A.F., Onyilo, V.C., Araujo, M.T., Dieni, C.V., Vo, H.T., King, G.D., Wadiche, J.I., *et al.* (2017). Adult-born neurons modify excitatory synaptic transmission to existing neurons. Elife *6*.

Aimone, J.B. (2016). Computational Modeling of Adult Neurogenesis. Cold Spring Harb Perspect Biol *8*, a018960.

Aimone, J.B., Li, Y., Lee, S.W., Clemenson, G.D., Deng, W., and Gage, F.H. (2014). Regulation and function of adult neurogenesis: from genes to cognition. Physiol Rev *94*, 991-1026.

Akers, K.G., Martinez-Canabal, A., Restivo, L., Yiu, A.P., De Cristofaro, A., Hsiang, H.L., Wheeler, A.L., Guskjolen, A., Niibori, Y., Shoji, H., *et al.* (2014). Hippocampal neurogenesis regulates forgetting during adulthood and infancy. Science *344*, 598-602.

Altman, J. (1969). Autoradiographic and histological studies of postnatal neurogenesis. IV. Cell proliferation and migration in the anterior forebrain, with special reference to persisting neurogenesis in the olfactory bulb. J Comp Neurol *137*, 433-457.

Altman, J. (2011). The Discovery of Adult Mammalian Neurogenesis. In Neurogenesis in the Adult Brain I: Neurobiology, T. Seki, K. Sawamoto, J.M. Parent, and A. Alvarez-Buylla, eds. (Tokyo: Springer Japan), pp. 3-46.

Altman, J., and Das, G.D. (1965). Autoradiographic and histological evidence of postnatal hippocampal neurogenesis in rats. J Comp Neurol *124*, 319-335.

Altman, J., and Das, G.D. (1967). Postnatal neurogenesis in the guinea-pig. Nature *214*, 1098-1101.

Alunni, A., Krecsmarik, M., Bosco, A., Galant, S., Pan, L., Moens, C.B., and Bally-Cuif, L. (2013). Notch3 signaling gates cell cycle entry and limits neural stem cell amplification in the adult pallium. Development *140*, 3335-3347.

Alves, M., Gomez-Villafuertes, R., Delanty, N., Farrell, M.A., O'Brien, D.F., Miras-Portugal, M.T., Hernandez, M.D., Henshall, D.C., and Engel, T. (2017). Expression and function of the metabotropic purinergic P2Y receptor family in experimental seizure models and patients with drug-refractory epilepsy. Epilepsia *58*, 1603-1614.

Amaral, D.G., and Witter, M.P. (1989). The three-dimensional organization of the hippocampal formation: A review of anatomical data. Neuroscience *31*, 571-591.

Andersen, J., Urban, N., Achimastou, A., Ito, A., Simic, M., Ullom, K., Martynoga, B., Lebel, M., Goritz, C., Frisen, J., *et al.* (2014). A transcriptional mechanism integrating inputs from extracellular signals to activate hippocampal stem cells. Neuron *83*, 1085-1097.

Angevine, J.B., Jr. (1965). Time of neuron origin in the hippocampal region. An autoradiographic study in the mouse. Exp Neurol Suppl, Suppl 2:1-70.

Ashton, R.S., Conway, A., Pangarkar, C., Bergen, J., Lim, K.I., Shah, P., Bissell, M., and Schaffer, D.V. (2012). Astrocytes regulate adult hippocampal neurogenesis through ephrin-B signaling. Nat Neurosci *15*, 1399-1406.

Babb, T.L., Pereira-Leite, J., Mathern, G.W., and Pretorius, J.K. (1995). Kainic acid induced hippocampal seizures in rats: comparisons of acute and chronic seizures using intrahippocampal versus systemic injections. Ital J Neurol Sci *16*, 39-44.

Bachstetter, A.D., Morganti, J.M., Jernberg, J., Schlunk, A., Mitchell, S.H., Brewster, K.W., Hudson, C.E., Cole, M.J., Harrison, J.K., Bickford, P.C., *et al.* (2011). Fractalkine and CX 3 CR1 regulate hippocampal neurogenesis in adult and aged rats. Neurobiol Aging *32*, 2030-2044.

Bae, E.K., Jung, K.H., Chu, K., Lee, S.T., Kim, J.H., Park, K.I., Kim, M., Chung, C.K., Lee, S.K., and Roh, J.K. (2010). Neuropathologic and clinical features of human medial temporal lobe epilepsy. J Clin Neurol *6*, 73-80.

Banerjee, S.B., Rajendran, R., Dias, B.G., Ladiwala, U., Tole, S., and Vaidya, V.A. (2005). Recruitment of the Sonic hedgehog signalling cascade in electroconvulsive seizure-mediated regulation of adult rat hippocampal neurogenesis. Eur J Neurosci *22*, 1570-1580.

Bao, H., Asrican, B., Li, W., Gu, B., Wen, Z., Lim, S.A., Haniff, I., Ramakrishnan, C., Deisseroth, K., Philpot, B., *et al.* (2017). Long-Range GABAergic Inputs Regulate Neural Stem Cell Quiescence and Control Adult Hippocampal Neurogenesis. Cell Stem Cell *21*, 604-617 e605.

Barkho, B.Z., Song, H., Aimone, J.B., Smrt, R.D., Kuwabara, T., Nakashima, K., Gage, F.H., and Zhao, X. (2006). Identification of astrocyte-expressed factors that modulate neural stem/progenitor cell differentiation. Stem Cells Dev *15*, 407-421.

Basak, O., Giachino, C., Fiorini, E., Macdonald, H.R., and Taylor, V. (2012). Neurogenic subventricular zone stem/progenitor cells are Notch1-dependent in their active but not quiescent state. J Neurosci *32*, 5654-5666.

Basu, J., and Siegelbaum, S.A. (2015). The Corticohippocampal Circuit, Synaptic Plasticity, and Memory. Cold Spring Harb Perspect Biol *7*.

Bayer, S.A. (1985). Neuron production in the hippocampus and olfactory bulb of the adult rat brain: addition or replacement? Ann N Y Acad Sci *457*, 163-172.

Bedard, A., and Parent, A. (2004). Evidence of newly generated neurons in the human olfactory bulb. Brain Res Dev Brain Res *151*, 159-168.

Bergami, M., Rimondini, R., Santi, S., Blum, R., Gotz, M., and Canossa, M. (2008). Deletion of TrkB in adult progenitors alters newborn neuron integration into hippocampal circuits and increases anxiety-like behavior. Proc Natl Acad Sci U S A *105*, 15570-15575.

Berger, M.L., Lassmann, H., and Hornykiewicz, O. (1989). Limbic seizures without brain damage after injection of low doses of kainic acid into the amygdala of freely moving rats. Brain Res *489*, 261-272.

Bielefeld, P., Mooney, C., Henshall, D.C., and Fitzsimons, C.P. (2017). miRNA-Mediated Regulation of Adult Hippocampal Neurogenesis; Implications for Epilepsy. Brain Plast *3*, 43-59.

Blumcke, I., Schewe, J.C., Normann, S., Brustle, O., Schramm, J., Elger, C.E., and Wiestler, O.D. (2001). Increase of nestin-immunoreactive neural precursor cells in the dentate gyrus of pediatric patients with early-onset temporal lobe epilepsy. Hippocampus *11*, 311-321.

Boldrini, M., Fulmore, C.A., Tartt, A.N., Simeon, L.R., Pavlova, I., Poposka, V., Rosoklija, G.B., Stankov, A., Arango, V., Dwork, A.J., *et al.* (2018). Human Hippocampal Neurogenesis Persists throughout Aging. Cell Stem Cell *22*, 589-599 e585.

Bonaguidi, M.A., Peng, C.Y., McGuire, T., Falciglia, G., Gobeske, K.T., Czeisler, C., and Kessler, J.A. (2008). Noggin expands neural stem cells in the adult hippocampus. J Neurosci *28*, 9194-9204.

Bonaguidi, M.A., Song, J., Ming, G.L., and Song, H. (2012). A unifying hypothesis on mammalian neural stem cell properties in the adult hippocampus. Curr Opin Neurobiol *22*, 754-761.

Bonaguidi, M.A., Wheeler, M.A., Shapiro, J.S., Stadel, R.P., Sun, G.J., Ming, G.L., and Song, H. (2011). In vivo clonal analysis reveals self-renewing and multipotent adult neural stem cell characteristics. Cell *145*, 1142-1155.

Bouilleret, V., Ridoux, V., Depaulis, A., Marescaux, C., Nehlig, A., and Le Gal La Salle, G. (1999). Recurrent seizures and hippocampal sclerosis following intrahippocampal kainate injection in adult mice: electroencephalography, histopathology and synaptic reorganization similar to mesial temporal lobe epilepsy. Neuroscience *89*, 717-729.

Brandt, M.D., Jessberger, S., Steiner, B., Kronenberg, G., Reuter, K., Bick-Sander, A., von der Behrens, W., and Kempermann, G. (2003). Transient calretinin expression

defines early postmitotic step of neuronal differentiation in adult hippocampal neurogenesis of mice. Mol Cell Neurosci *24*, 603-613.

Braun, S.M., Pilz, G.A., Machado, R.A., Moss, J., Becher, B., Toni, N., and Jessberger, S. (2015). Programming Hippocampal Neural Stem/Progenitor Cells into Oligodendrocytes Enhances Remyelination in the Adult Brain after Injury. Cell Rep *11*, 1679-1685.

Buckmaster, P.S., Zhang, G.F., and Yamawaki, R. (2002). Axon sprouting in a model of temporal lobe epilepsy creates a predominantly excitatory feedback circuit. J Neurosci *22*, 6650-6658.

Cameron, H.A., and McKay, R.D. (1999). Restoring production of hippocampal neurons in old age. Nat Neurosci *2*, 894-897.

Castilla-Ortega, E., Hoyo-Becerra, C., Pedraza, C., Chun, J., Rodriguez De Fonseca, F., Estivill-Torrus, G., and Santin, L.J. (2011). Aggravation of chronic stress effects on hippocampal neurogenesis and spatial memory in LPA(1) receptor knockout mice. PLoS One *6*, e25522.

Cha, B.H., Akman, C., Silveira, D.C., Liu, X., and Holmes, G.L. (2004). Spontaneous recurrent seizure following status epilepticus enhances dentate gyrus neurogenesis. Brain Dev *26*, 394-397.

Cho, K.O., Lybrand, Z.R., Ito, N., Brulet, R., Tafacory, F., Zhang, L., Good, L., Ure, K., Kernie, S.G., Birnbaum, S.G., *et al.* (2015). Aberrant hippocampal neurogenesis contributes to epilepsy and associated cognitive decline. Nat Commun *6*, 6606.

Cipriani, S., Ferrer, I., Aronica, E., Kovacs, G.G., Verney, C., Nardelli, J., Khung, S., Delezoide, A.L., Milenkovic, I., Rasika, S., *et al.* (2018). Hippocampal Radial Glial Subtypes and Their Neurogenic Potential in Human Fetuses and Healthy and Alzheimer's Disease Adults. Cereb Cortex *28*, 2458-2478.

Clarke, S.R., Shetty, A.K., Bradley, J.L., and Turner, D.A. (1994). Reactive astrocytes express the embryonic intermediate neurofilament nestin. Neuroreport *5*, 1885-1888.

Codega, P., Silva-Vargas, V., Paul, A., Maldonado-Soto, A.R., Deleo, A.M., Pastrana, E., and Doetsch, F. (2014). Prospective identification and purification of quiescent adult neural stem cells from their in vivo niche. Neuron *82*, 545-559.

Contos, J.J., Fukushima, N., Weiner, J.A., Kaushal, D., and Chun, J. (2000). Requirement for the lpA1 lysophosphatidic acid receptor gene in normal suckling behavior. Proc Natl Acad Sci U S A *97*, 13384-13389.

Curtis, M.A., Kam, M., Nannmark, U., Anderson, M.F., Axell, M.Z., Wikkelso, C., Holtas, S., van Roon-Mom, W.M., Bjork-Eriksson, T., Nordborg, C., *et al.* (2007). Human neuroblasts migrate to the olfactory bulb via a lateral ventricular extension. Science *315*, 1243-1249.

de Lanerolle, N.C., Kim, J.H., Williamson, A., Spencer, S.S., Zaveri, H.P., Eid, T., and Spencer, D.D. (2003). A retrospective analysis of hippocampal pathology in human temporal lobe epilepsy: evidence for distinctive patient subcategories. Epilepsia *44*, 677-687.

Deng, W., Zhao, C., and Gage, F.H. (2011). Integration of New Neurons into the Adult Hippocampus. In Neurogenesis in the Adult Brain I: Neurobiology, T. Seki, K. Sawamoto, J.M. Parent, and A. Alvarez-Buylla, eds. (Tokyo: Springer Japan), pp. 237-255.

Devinsky, O., Vezzani, A., Najjar, S., De Lanerolle, N.C., and Rogawski, M.A. (2013). Glia and epilepsy: excitability and inflammation. Trends Neurosci *36*, 174-184.

Doetsch, F., and Alvarez-Buylla, A. (1996). Network of tangential pathways for neuronal migration in adult mammalian brain. Proc Natl Acad Sci U S A *93*, 14895-14900.

Doetsch, F., Garcia-Verdugo, J.M., and Alvarez-Buylla, A. (1997). Cellular composition and three-dimensional organization of the subventricular germinal zone in the adult mammalian brain. J Neurosci *17*, 5046-5061.

Dottori, M., Leung, J., Turnley, A.M., and Pebay, A. (2008). Lysophosphatidic acid inhibits neuronal differentiation of neural stem/progenitor cells derived from human embryonic stem cells. Stem Cells *26*, 1146-1154.

Eckenhoff, M.F., and Rakic, P. (1984). Radial organization of the hippocampal dentate gyrus: a Golgi, ultrastructural, and immunocytochemical analysis in the developing rhesus monkey. J Comp Neurol *223*, 1-21.

Ehm, O., Goritz, C., Covic, M., Schaffner, I., Schwarz, T.J., Karaca, E., Kempkes, B., Kremmer, E., Pfrieger, F.W., Espinosa, L., *et al.* (2010). RBPJkappa-dependent signaling is essential for long-term maintenance of neural stem cells in the adult hippocampus. J Neurosci *30*, 13794-13807.

Encinas, J.M., and Enikolopov, G. (2008). Identifying and quantitating neural stem and progenitor cells in the adult brain. Methods Cell Biol *85*, 243-272.

Encinas, J.M., Hamani, C., Lozano, A.M., and Enikolopov, G. (2011a). Neurogenic hippocampal targets of deep brain stimulation. J Comp Neurol *519*, 6-20.

Encinas, J.M., Michurina, T.V., Peunova, N., Park, J.H., Tordo, J., Peterson, D.A., Fishell, G., Koulakov, A., and Enikolopov, G. (2011b). Division-coupled astrocytic differentiation and age-related depletion of neural stem cells in the adult hippocampus. Cell Stem Cell *8*, 566-579.

Encinas, J.M., and Sierra, A. (2012). Neural stem cell deforestation as the main force driving the age-related decline in adult hippocampal neurogenesis. Behav Brain Res *227*, 433-439.

Encinas, J.M., Vaahtokari, A., and Enikolopov, G. (2006). Fluoxetine targets early progenitor cells in the adult brain. Proc Natl Acad Sci U S A *103*, 8233-8238.

Engel, J., Jr. (1993). Update on surgical treatment of the epilepsies. Summary of the Second International Palm Desert Conference on the Surgical Treatment of the Epilepsies (1992). Neurology *43*, 1612-1617.

Engel, T., Martinez-Villarreal, J., Henke, C., Jimenez-Mateos, E.M., Sanz-Rodriguez, A., Alves, M., Hernandez-Santana, Y., Brennan, G.P., Kenny, A., Campbell, A., *et al.* (2017). Spatiotemporal progression of ubiquitin-proteasome system inhibition after status epilepticus suggests protective adaptation against hippocampal injury. Mol Neurodegener *12*, 21.

Eriksson, P.S., Perfilieva, E., Bjork-Eriksson, T., Alborn, A.M., Nordborg, C., Peterson, D.A., and Gage, F.H. (1998). Neurogenesis in the adult human hippocampus. Nat Med *4*, 1313-1317.

Erkanli, G., Ercan, F., Sirvanci, S., Yananli, H.R., Onat, F., and San, T. (2007). Time-dependent changes in distribution of basic fibroblast growth factor immunoreactive cells in rat hippocampus after status epilepticus. Neurol Res *29*, 816-823.

Esposito, M.S., Piatti, V.C., Laplagne, D.A., Morgenstern, N.A., Ferrari, C.C., Pitossi, F.J., and Schinder, A.F. (2005). Neuronal differentiation in the adult hippocampus recapitulates embryonic development. J Neurosci *25*, 10074-10086.

Estivill-Torrus, G., Llebrez-Zayas, P., Matas-Rico, E., Santin, L., Pedraza, C., De Diego, I., Del Arco, I., Fernandez-Llebrez, P., Chun, J., and De Fonseca, F.R. (2008). Absence of LPA1 signaling results in defective cortical development. Cereb Cortex *18*, 938-950.

Faigle, R., and Song, H. (2013). Signaling mechanisms regulating adult neural stem cells and neurogenesis. Biochim Biophys Acta *1830*, 2435-2448.

Faiz, M., Sachewsky, N., Gascon, S., Bang, K.W., Morshead, C.M., and Nagy, A. (2015). Adult Neural Stem Cells from the Subventricular Zone Give Rise to Reactive Astrocytes in the Cortex after Stroke. Cell Stem Cell *17*, 624-634.

Filippov, V., Kronenberg, G., Pivneva, T., Reuter, K., Steiner, B., Wang, L.P., Yamaguchi, M., Kettenmann, H., and Kempermann, G. (2003). Subpopulation of nestin-expressing progenitor cells in the adult murine hippocampus shows electrophysiological and morphological characteristics of astrocytes. Mol Cell Neurosci *23*, 373-382.

Finch, D.M., Wong, E.E., Derian, E.L., Chen, X.H., Nowlin-Finch, N.L., and Brothers, L.A. (1986). Neurophysiology of limbic system pathways in the rat: projections from the amygdala to the entorhinal cortex. Brain Res *370*, 273-284.

Fournier, N.M., Andersen, D.R., Botterill, J.J., Sterner, E.Y., Lussier, A.L., Caruncho, H.J., and Kalynchuk, L.E. (2010). The effect of amygdala kindling on hippocampal neurogenesis coincides with decreased reelin and DISC1 expression in the adult dentate gyrus. Hippocampus *20*, 659-671.

Fournier, N.M., Botterill, J.J., Marks, W.N., Guskjolen, A.J., and Kalynchuk, L.E. (2013). Impaired recruitment of seizure-generated neurons into functional memory networks of the adult dentate gyrus following long-term amygdala kindling. Exp Neurol *244*, 96-104.

Franklin, K.B.J., and Paxinos, G. (1997). The Mouse Brain in Stereotaxic Coordinates (San Diego: Academic Press).

Gao, X., Enikolopov, G., and Chen, J. (2009). Moderate traumatic brain injury promotes proliferation of quiescent neural progenitors in the adult hippocampus. Exp Neurol *219*, 516-523.

Garcia, A.D., Doan, N.B., Imura, T., Bush, T.G., and Sofroniew, M.V. (2004). GFAP-expressing progenitors are the principal source of constitutive neurogenesis in adult mouse forebrain. Nat Neurosci *7*, 1233-1241.

Gargaro, A.C., Sakamoto, A.C., Bianchin, M.M., Geraldi Cde, V., Scorsi-Rosset, S., Coimbra, E.R., Carlotti, C.G., Jr., Assirati, J.A., and Velasco, T.R. (2013). Atypical neuropsychological profiles and cognitive outcome in mesial temporal lobe epilepsy. Epilepsy Behav *27*, 461-469.

Ge, S., Goh, E.L., Sailor, K.A., Kitabatake, Y., Ming, G.L., and Song, H. (2006). GABA regulates synaptic integration of newly generated neurons in the adult brain. Nature *439*, 589-593.

Ge, S., Yang, C.H., Hsu, K.S., Ming, G.L., and Song, H. (2007). A critical period for enhanced synaptic plasticity in newly generated neurons of the adult brain. Neuron *54*, 559-566.

Giachino, C., Barz, M., Tchorz, J.S., Tome, M., Gassmann, M., Bischofberger, J., Bettler, B., and Taylor, V. (2014). GABA suppresses neurogenesis in the adult hippocampus through GABAB receptors. Development *141*, 83-90.

Giachino, C., and Taylor, V. (2014). Notching up neural stem cell homogeneity in homeostasis and disease. Front Neurosci *8*, 32.

Goldman, S.A., and Nottebohm, F. (1983). Neuronal production, migration, and differentiation in a vocal control nucleus of the adult female canary brain. Proc Natl Acad Sci U S A *80*, 2390-2394.

Gong, S., Zheng, C., Doughty, M.L., Losos, K., Didkovsky, N., Schambra, U.B., Nowak, N.J., Joyner, A., Leblanc, G., Hatten, M.E., *et al.* (2003). A gene expression

atlas of the central nervous system based on bacterial artificial chromosomes. Nature *425*, 917-925.

Gould, E. (2007). How widespread is adult neurogenesis in mammals? Nat Rev Neurosci *8*, 481-488.

Gould, E., Cameron, H.A., Daniels, D.C., Woolley, C.S., and McEwen, B.S. (1992). Adrenal hormones suppress cell division in the adult rat dentate gyrus. J Neurosci *12*, 3642-3650.

Gould, E., McEwen, B.S., Tanapat, P., Galea, L.A., and Fuchs, E. (1997). Neurogenesis in the dentate gyrus of the adult tree shrew is regulated by psychosocial stress and NMDA receptor activation. J Neurosci *17*, 2492-2498.

Gould, E., Reeves, A.J., Fallah, M., Tanapat, P., Gross, C.G., and Fuchs, E. (1999). Hippocampal neurogenesis in adult Old World primates. Proc Natl Acad Sci U S A *96*, 5263-5267.

Gould, E., Tanapat, P., McEwen, B.S., Flugge, G., and Fuchs, E. (1998). Proliferation of granule cell precursors in the dentate gyrus of adult monkeys is diminished by stress. Proc Natl Acad Sci U S A *95*, 3168-3171.

Gratzner, H.G. (1982). Monoclonal antibody to 5-bromo- and 5-iododeoxyuridine: A new reagent for detection of DNA replication. Science *218*, 474-475.

Harrison, S.M., Reavill, C., Brown, G., Brown, J.T., Cluderay, J.E., Crook, B., Davies, C.H., Dawson, L.A., Grau, E., Heidbreder, C., *et al.* (2003). LPA1 receptor-deficient mice have phenotypic changes observed in psychiatric disease. Mol Cell Neurosci *24*, 1170-1179.

Hattiangady, B., Rao, M.S., and Shetty, A.K. (2004). Chronic temporal lobe epilepsy is associated with severely declined dentate neurogenesis in the adult hippocampus. Neurobiol Dis *17*, 473-490.

Hattiangady, B., and Shetty, A.K. (2010). Decreased neuronal differentiation of newly generated cells underlies reduced hippocampal neurogenesis in chronic temporal lobe epilepsy. Hippocampus *20*, 97-112.

Hecht, J.H., Weiner, J.A., Post, S.R., and Chun, J. (1996). Ventricular zone gene-1 (vzg-1) encodes a lysophosphatidic acid receptor expressed in neurogenic regions of the developing cerebral cortex. The Journal of Cell Biology *135*, 1071-1083.

Hester, M.S., and Danzer, S.C. (2013). Accumulation of abnormal adult-generated hippocampal granule cells predicts seizure frequency and severity. J Neurosci *33*, 8926-8936.

Heuser, K., Tauboll, E., Nagelhus, E.A., Cvancarova, M., Petter Ottersen, O., and Gjerstad, L. (2009). Phenotypic characteristics of temporal lobe epilepsy: the impact of hippocampal sclerosis. Acta Neurol Scand Suppl, 8-13.

Hochgerner, H., Zeisel, A., Lonnerberg, P., and Linnarsson, S. (2018). Conserved properties of dentate gyrus neurogenesis across postnatal development revealed by single-cell RNA sequencing. Nat Neurosci *21*, 290-299.

Hodge, R.D., Kowalczyk, T.D., Wolf, S.A., Encinas, J.M., Rippey, C., Enikolopov, G., Kempermann, G., and Hevner, R.F. (2008). Intermediate progenitors in adult hippocampal neurogenesis: Tbr2 expression and coordinate regulation of neuronal output. J Neurosci *28*, 3707-3717.

Huttmann, K., Sadgrove, M., Wallraff, A., Hinterkeuser, S., Kirchhoff, F., Steinhauser, C., and Gray, W.P. (2003). Seizures preferentially stimulate proliferation of radial glia-like astrocytes in the adult dentate gyrus: functional and immunocytochemical analysis. Eur J Neurosci *18*, 2769-2778.

Imayoshi, I., and Kageyama, R. (2014). bHLH factors in self-renewal, multipotency, and fate choice of neural progenitor cells. Neuron *82*, 9-23.

Imayoshi, I., Ohtsuka, T., Metzger, D., Chambon, P., and Kageyama, R. (2006). Temporal regulation of Cre recombinase activity in neural stem cells. Genesis *44*, 233-238.

Imayoshi, I., Sakamoto, M., Ohtsuka, T., Takao, K., Miyakawa, T., Yamaguchi, M., Mori, K., Ikeda, T., Itohara, S., and Kageyama, R. (2008). Roles of continuous neurogenesis in the structural and functional integrity of the adult forebrain. Nat Neurosci *11*, 1153-1161.

Imayoshi, I., Sakamoto, M., Yamaguchi, M., Mori, K., and Kageyama, R. (2010). Essential roles of Notch signaling in maintenance of neural stem cells in developing and adult brains. J Neurosci *30*, 3489-3498.

Indulekha, C.L., Sanalkumar, R., Thekkuveettil, A., and James, J. (2010). Seizure induces activation of multiple subtypes of neural progenitors and growth factors in hippocampus with neuronal maturation confined to dentate gyrus. Biochem Biophys Res Commun *393*, 864-871.

Jang, M.H., Bonaguidi, M.A., Kitabatake, Y., Sun, J., Song, J., Kang, E., Jun, H., Zhong, C., Su, Y., Guo, J.U., *et al.* (2013). Secreted frizzled-related protein 3 regulates activity-dependent adult hippocampal neurogenesis. Cell Stem Cell *12*, 215-223.

Jessberger, S., and Kempermann, G. (2003). Adult-born hippocampal neurons mature into activity-dependent responsiveness. Eur J Neurosci *18*, 2707-2712.

Jun, H., Mohammed Qasim Hussaini, S., Cho, C.H., Welby, J., and Jang, M.H. (2015). Gadd45b Mediates Electroconvulsive Shock Induced Proliferation of Hippocampal Neural Stem Cells. Brain Stimul *8*, 1021-1024.

Jung, K.H., Chu, K., Kim, M., Jeong, S.W., Song, Y.M., Lee, S.T., Kim, J.Y., Lee, S.K., and Roh, J.K. (2004). Continuous cytosine-b-D-arabinofuranoside infusion reduces ectopic granule cells in adult rat hippocampus with attenuation of spontaneous recurrent seizures following pilocarpine-induced status epilepticus. Eur J Neurosci *19*, 3219-3226.

Kang, K., Lee, S.W., Han, J.E., Choi, J.W., and Song, M.R. (2014). The complex morphology of reactive astrocytes controlled by fibroblast growth factor signaling. Glia *62*, 1328-1344.

Kaplan, M.S., and Bell, D.H. (1984). Mitotic neuroblasts in the 9-day-old and 11-month-old rodent hippocampus. J Neurosci *4*, 1429-1441.

Kaplan, M.S., and Hinds, J.W. (1977). Neurogenesis in the adult rat: electron microscopic analysis of light radioautographs. Science *197*, 1092-1094.

Kawaguchi, A., Miyata, T., Sawamoto, K., Takashita, N., Murayama, A., Akamatsu, W., Ogawa, M., Okabe, M., Tano, Y., Goldman, S.A., *et al.* (2001). Nestin-EGFP transgenic mice: visualization of the self-renewal and multipotency of CNS stem cells. Mol Cell Neurosci *17*, 259-273.

Kempermann, G. (2011a). The pessimist's and optimist's views of adult neurogenesis. Cell *145*, 1009-1011.

Kempermann, G. (2011b). Regulation of Adult Neurogenesis by Environment and Learning. In Neurogenesis in the Adult Brain I: Neurobiology, T. Seki, K. Sawamoto, J.M. Parent, and A. Alvarez-Buylla, eds. (Tokyo: Springer Japan), pp. 271-284.

Kempermann, G., and Gage, F.H. (2002). Genetic determinants of adult hippocampal neurogenesis correlate with acquisition, but not probe trial performance, in the water maze task. Eur J Neurosci *16*, 129-136.

Kempermann, G., Jessberger, S., Steiner, B., and Kronenberg, G. (2004). Milestones of neuronal development in the adult hippocampus. Trends Neurosci *27*, 447-452.

Kobayashi, S., Ohno, K., Iwakuma, M., Kaneda, Y., and Saji, M. (2002). Synaptotagmin I hypothalamic knockdown prevents amygdaloid seizure-induced damage of hippocampal neurons but not of entorhinal neurons. Neurosci Res *44*, 455-465.

Kolb, B., Pedersen, B., Ballermann, M., Gibb, R., and Whishaw, I.Q. (1999). Embryonic and postnatal injections of bromodeoxyuridine produce age-dependent morphological and behavioral abnormalities. J Neurosci *19*, 2337-2346.

Kornack, D.R., and Rakic, P. (1999). Continuation of neurogenesis in the hippocampus of the adult macaque monkey. Proc Natl Acad Sci U S A *96*, 5768-5773.

Kosaka, T., and Hama, K. (1986). Three-dimensional structure of astrocytes in the rat dentate gyrus. J Comp Neurol *249*, 242-260.

Kralic, J.E., Ledergerber, D.A., and Fritschy, J.M. (2005). Disruption of the neurogenic potential of the dentate gyrus in a mouse model of temporal lobe epilepsy with focal seizures. Eur J Neurosci *22*, 1916-1927.

Kronenberg, G., Reuter, K., Steiner, B., Brandt, M.D., Jessberger, S., Yamaguchi, M., and Kempermann, G. (2003). Subpopulations of proliferating cells of the adult hippocampus respond differently to physiologic neurogenic stimuli. J Comp Neurol *467*, 455-463.

Kuhn, H.G., Dickinson-Anson, H., and Gage, F.H. (1996). Neurogenesis in the dentate gyrus of the adult rat: age-related decrease of neuronal progenitor proliferation. J Neurosci *16*, 2027-2033.

Lagace, D.C., Whitman, M.C., Noonan, M.A., Ables, J.L., DeCarolis, N.A., Arguello, A.A., Donovan, M.H., Fischer, S.J., Farnbauch, L.A., Beech, R.D., *et al.* (2007). Dynamic contribution of nestin-expressing stem cells to adult neurogenesis. J Neurosci *27*, 12623-12629.

Lazarini, F., and Lledo, P.M. (2011). Is adult neurogenesis essential for olfaction? Trends Neurosci *34*, 20-30.

Lee, J.-K., Kwon, M.-S., Kim, H.R., Kim, H.-G., Sim, Y.-B., Park, S.-H., and Suh, H.-W. (2014). Temporal expression of hippocampal lysophosphatidic acid receptors and their roles in kainic acid-induced neurotoxicity. Genes & Genomics *36*, 239-246.

Lehtinen, M.K., Zappaterra, M.W., Chen, X., Yang, Y.J., Hill, A.D., Lun, M., Maynard, T., Gonzalez, D., Kim, S., Ye, P., *et al.* (2011). The cerebrospinal fluid provides a proliferative niche for neural progenitor cells. Neuron *69*, 893-905.

Lendahl, U., Zimmerman, L.B., and McKay, R.D. (1990). CNS stem cells express a new class of intermediate filament protein. Cell *60*, 585-595.

Lepousez, G., Valley, M.T., and Lledo, P.M. (2013). The impact of adult neurogenesis on olfactory bulb circuits and computations. Annu Rev Physiol *75*, 339-363.

Leuner, B., Kozorovitskiy, Y., Gross, C.G., and Gould, E. (2007). Diminished adult neurogenesis in the marmoset brain precedes old age. Proc Natl Acad Sci U S A *104*, 17169-17173.

Lie, D.C., Colamarino, S.A., Song, H.J., Desire, L., Mira, H., Consiglio, A., Lein, E.S., Jessberger, S., Lansford, H., Dearie, A.R., *et al.* (2005). Wnt signalling regulates adult hippocampal neurogenesis. Nature *437*, 1370-1375.

Lim, D.A., and Alvarez-Buylla, A. (2014). Adult neural stem cells stake their ground. Trends Neurosci *37*, 563-571.

Liu, S., Wang, J., Zhu, D., Fu, Y., Lukowiak, K., and Lu, Y.M. (2003). Generation of functional inhibitory neurons in the adult rat hippocampus. J Neurosci *23*, 732-736.

Lois, C., and Alvarez-Buylla, A. (1993). Proliferating subventricular zone cells in the adult mammalian forebrain can differentiate into neurons and glia. Proc Natl Acad Sci U S A *90*, 2074-2077.

Lois, C., and Alvarez-Buylla, A. (1994). Long-distance neuronal migration in the adult mammalian brain. Science *264*, 1145-1148.

Lorente de Nó, R. (1934). Studies on the structure of the cerebral cortex. II. Continuation of the study of the ammonic system. Journal für Psychologie und Neurologie *46*, 113-177.

Lugert, S., Basak, O., Knuckles, P., Haussler, U., Fabel, K., Gotz, M., Haas, C.A., Kempermann, G., Taylor, V., and Giachino, C. (2010). Quiescent and active hippocampal neural stem cells with distinct morphologies respond selectively to physiological and pathological stimuli and aging. Cell Stem Cell *6*, 445-456.

Lugert, S., and Taylor, V. (2011). Neural stem cells: disposable, end-state glia? Cell Stem Cell *8*, 464-465.

Matas-Rico, E., Garcia-Diaz, B., Llebrez-Zayas, P., Lopez-Barroso, D., Santin, L., Pedraza, C., Smith-Fernandez, A., Fernandez-Llebrez, P., Tellez, T., Redondo, M., *et al.* (2008). Deletion of lysophosphatidic acid receptor LPA1 reduces neurogenesis in the mouse dentate gyrus. Mol Cell Neurosci *39*, 342-355.

Maxwell, D.S., and Kruger, L. (1965). The Fine Structure of Astrocytes in the Cerebral Cortex and Their Response to Focal Injury Produced by Heavy Ionizing Particles. J Cell Biol *25*, 141-157.

McCabe, B.K., Silveira, D.C., Cilio, M.R., Cha, B.H., Liu, X., Sogawa, Y., and Holmes, G.L. (2001). Reduced neurogenesis after neonatal seizures. J Neurosci *21*, 2094-2103.

McLean, I.W., and Nakane, P.K. (1974). Periodate-lysine-paraformaldehyde fixative. A new fixation for immunoelectron microscopy. J Histochem Cytochem *22*, 1077-1083.

Merkle, F.T., Mirzadeh, Z., and Alvarez-Buylla, A. (2007). Mosaic organization of neural stem cells in the adult brain. Science *317*, 381-384.

Merkle, F.T., Tramontin, A.D., Garcia-Verdugo, J.M., and Alvarez-Buylla, A. (2004). Radial glia give rise to adult neural stem cells in the subventricular zone. Proc Natl Acad Sci U S A *101*, 17528-17532.

Mich, J.K., Signer, R.A., Nakada, D., Pineda, A., Burgess, R.J., Vue, T.Y., Johnson, J.E., and Morrison, S.J. (2014). Prospective identification of functionally distinct stem cells and neurosphere-initiating cells in adult mouse forebrain. Elife *3*, e02669.

Mignone, J.L., Kukekov, V., Chiang, A.S., Steindler, D., and Enikolopov, G. (2004). Neural stem and progenitor cells in nestin-GFP transgenic mice. J Comp Neurol *469*, 311-324.

Milhaud, D., Rondouin, G., Lerner-Natoli, M., Bockaert, J., and Lafon-Cazal, M. (2003). Neuroprotective activity of antazoline against neuronal damage induced by limbic status epilepticus. Neuroscience *120*, 475-484.

Mineyeva, O.A., Enikolopov, G., and Koulakov, A.A. (2018). Spatial geometry of stem cell proliferation in the adult hippocampus. Sci Rep *8*, 3444.

Ming, G.L., and Song, H. (2011). Adult neurogenesis in the mammalian brain: significant answers and significant questions. Neuron *70*, 687-702.

Mira, H., Andreu, Z., Suh, H., Lie, D.C., Jessberger, S., Consiglio, A., San Emeterio, J., Hortiguela, R., Marques-Torrejon, M.A., Nakashima, K., *et al.* (2010). Signaling through BMPR-IA regulates quiescence and long-term activity of neural stem cells in the adult hippocampus. Cell Stem Cell *7*, 78-89.

Mirzadeh, Z., Merkle, F.T., Soriano-Navarro, M., Garcia-Verdugo, J.M., and Alvarez-Buylla, A. (2008). Neural stem cells confer unique pinwheel architecture to the ventricular surface in neurogenic regions of the adult brain. Cell Stem Cell *3*, 265-278.

Mishra, P., and Chan, D.C. (2014). Mitochondrial dynamics and inheritance during cell division, development and disease. Nat Rev Mol Cell Biol *15*, 634-646.

Mouri, G., Jimenez-Mateos, E., Engel, T., Dunleavy, M., Hatazaki, S., Paucard, A., Matsushima, S., Taki, W., and Henshall, D.C. (2008). Unilateral hippocampal CA3-predominant damage and short latency epileptogenesis after intra-amygdala microinjection of kainic acid in mice. Brain Res *1213*, 140-151.

Nadler, J.V., Perry, B.W., and Cotman, C.W. (1980). Selective reinnervation of hippocampal area CA1 and the fascia dentata after destruction of CA3-CA4 afferents with kainic acid. Brain Res *182*, 1-9.

Nakao, K., Matsuyama, K., Matsuki, N., and Ikegaya, Y. (2004). Amygdala stimulation modulates hippocampal synaptic plasticity. Proc Natl Acad Sci U S A *101*, 14270-14275.

Nitta, N., Heinrich, C., Hirai, H., and Suzuki, F. (2008). Granule cell dispersion develops without neurogenesis and does not fully depend on astroglial cell generation in a mouse model of temporal lobe epilepsy. Epilepsia *49*, 1711-1722.

Norton, W.T., Aquino, D.A., Hozumi, I., Chiu, F.C., and Brosnan, C.F. (1992). Quantitative aspects of reactive gliosis: a review. Neurochem Res *17*, 877-885.

Nottebohm, F. (2011). Song Learning in Birds Offers a Model for Neuronal Replacement in Adult Brain. In Neurogenesis in the Adult Brain I: Neurobiology, T. Seki, K. Sawamoto, J.M. Parent, and A. Alvarez-Buylla, eds. (Tokyo: Springer Japan), pp. 47-84.

O'Dell, C.M., Das, A., Wallace, G.t., Ray, S.K., and Banik, N.L. (2012). Understanding the basic mechanisms underlying seizures in mesial temporal lobe epilepsy and possible therapeutic targets: a review. J Neurosci Res *90*, 913-924.

Okamoto, M., Inoue, K., Iwamura, H., Terashima, K., Soya, H., Asashima, M., and Kuwabara, T. (2011). Reduction in paracrine Wnt3 factors during aging causes impaired adult neurogenesis. FASEB J *25*, 3570-3582.

Okazaki, M.M., Molnar, P., and Nadler, J.V. (1999). Recurrent mossy fiber pathway in rat dentate gyrus: synaptic currents evoked in presence and absence of seizure-induced growth. J Neurophysiol *81*, 1645-1660.

Ortinski, P.I., Dong, J., Mungenast, A., Yue, C., Takano, H., Watson, D.J., Haydon, P.G., and Coulter, D.A. (2010). Selective induction of astrocytic gliosis generates deficits in neuronal inhibition. Nat Neurosci *13*, 584-591.

Overstreet Wadiche, L., Bromberg, D.A., Bensen, A.L., and Westbrook, G.L. (2005). GABAergic signaling to newborn neurons in dentate gyrus. J Neurophysiol *94*, 4528-4532.

Packard, M.G., Cahill, L., and McGaugh, J.L. (1994). Amygdala modulation of hippocampal-dependent and caudate nucleus-dependent memory processes. Proc Natl Acad Sci U S A *91*, 8477-8481.

Paradisi, M., Fernandez, M., Del Vecchio, G., Lizzo, G., Marucci, G., Giulioni, M., Pozzati, E., Antonelli, T., Lanzoni, G., Bagnara, G.P., *et al.* (2010). Ex vivo study of dentate gyrus neurogenesis in human pharmacoresistant temporal lobe epilepsy. Neuropathol Appl Neurobiol *36*, 535-550.

Parent, J.M., Tada, E., Fike, J.R., and Lowenstein, D.H. (1999). Inhibition of dentate granule cell neurogenesis with brain irradiation does not prevent seizure-induced mossy fiber synaptic reorganization in the rat. J Neurosci *19*, 4508-4519.

Parent, J.M., Yu, T.W., Leibowitz, R.T., Geschwind, D.H., Sloviter, R.S., and Lowenstein, D.H. (1997). Dentate granule cell neurogenesis is increased by seizures and contributes to aberrant network reorganization in the adult rat hippocampus. J Neurosci *17*, 3727-3738.

Park, H., Kim, S., Rhee, J., Kim, H.J., Han, J.S., Nah, S.Y., and Chung, C. (2015). Synaptic enhancement induced by gintonin via lysophosphatidic acid receptor activation in central synapses. J Neurophysiol *113*, 1493-1500.

Pascual-Brazo, J., Baekelandt, V., and Encinas, J.M. (2014). Neurogenesis as a new target for the development of antidepressant drugs. Curr Pharm Des *20*, 3763-3775.

Pastrana, E., Cheng, L.C., and Doetsch, F. (2009). Simultaneous prospective purification of adult subventricular zone neural stem cells and their progeny. Proc Natl Acad Sci U S A *106*, 6387-6392.

Paton, J.A., and Nottebohm, F.N. (1984). Neurons generated in the adult brain are recruited into functional circuits. Science *225*, 1046-1048.

Petreanu, L., and Alvarez-Buylla, A. (2002). Maturation and death of adult-born olfactory bulb granule neurons: role of olfaction. J Neurosci *22*, 6106-6113.

Petrik, D., Myoga, M.H., Grade, S., Gerkau, N.J., Pusch, M., Rose, C.R., Grothe, B., and Gotz, M. (2018). Epithelial Sodium Channel Regulates Adult Neural Stem Cell Proliferation in a Flow-Dependent Manner. Cell Stem Cell *22*, 865-878 e868.

Pilz, G.A., Bottes, S., Betizeau, M., Jorg, D.J., Carta, S., Simons, B.D., Helmchen, F., and Jessberger, S. (2018). Live imaging of neurogenesis in the adult mouse hippocampus. Science *359*, 658-662.

Pineda, J.R., and Encinas, J.M. (2016). The Contradictory Effects of Neuronal Hyperexcitation on Adult Hippocampal Neurogenesis. Front Neurosci *10*, 74.

Ponti, G., Obernier, K., Guinto, C., Jose, L., Bonfanti, L., and Alvarez-Buylla, A. (2013). Cell cycle and lineage progression of neural progenitors in the ventricular-subventricular zones of adult mice. Proc Natl Acad Sci U S A *110*, E1045-1054.

Qu, Q., Sun, G., Li, W., Yang, S., Ye, P., Zhao, C., Yu, R.T., Gage, F.H., Evans, R.M., and Shi, Y. (2010). Orphan nuclear receptor TLX activates Wnt/beta-catenin signalling to stimulate neural stem cell proliferation and self-renewal. Nat Cell Biol *12*, 31-40; sup pp 31-39.

Rakic, P. (1985). Limits of neurogenesis in primates. Science *227*, 1054-1056.

Rakic, P., and Nowakowski, R.S. (1981). The time of origin of neurons in the hippocampal region of the rhesus monkey. J Comp Neurol *196*, 99-128.

Ramirez-Amaya, V., Marrone, D.F., Gage, F.H., Worley, P.F., and Barnes, C.A. (2006). Integration of new neurons into functional neural networks. J Neurosci *26*, 12237-12241.

Ramón y Cajal, S. (1928). Degeneration and regeneration of the nervous system (London: Oxford University Press).

Ramón y Cajal, S. (1995). Histology of the nervous system of man and vertebrates (New York: Oxford University Press).

Reynolds, B.A., and Weiss, S. (1992). Generation of neurons and astrocytes from isolated cells of the adult mammalian central nervous system. Science *255*, 1707-1710.

Ristic, A.J., Savic, D., Sokic, D., Bogdanovic Pristov, J., Nestorov, J., Bascarevic, V., Raicevic, S., Savic, S., and Spasojevic, I. (2015). Hippocampal antioxidative system in mesial temporal lobe epilepsy. Epilepsia *56*, 789-799.

Riva, M.A., Gale, K., and Mocchetti, I. (1992). Basic fibroblast growth factor mRNA increases in specific brain regions following convulsive seizures. Brain Res Mol Brain Res *15*, 311-318.

Robel, S., Buckingham, S.C., Boni, J.L., Campbell, S.L., Danbolt, N.C., Riedemann, T., Sutor, B., and Sontheimer, H. (2015). Reactive astrogliosis causes the development of spontaneous seizures. J Neurosci *35*, 3330-3345.

Sakamoto, M., Ieki, N., Miyoshi, G., Mochimaru, D., Miyachi, H., Imura, T., Yamaguchi, M., Fishell, G., Mori, K., Kageyama, R., *et al.* (2014). Continuous postnatal neurogenesis contributes to formation of the olfactory bulb neural circuits and flexible olfactory associative learning. J Neurosci *34*, 5788-5799.

Sanai, N., Berger, M.S., Garcia-Verdugo, J.M., and Alvarez-Buylla, A. (2007). Comment on "Human neuroblasts migrate to the olfactory bulb via a lateral ventricular extension". Science *318*, 393; author reply 393.

Sanai, N., Nguyen, T., Ihrie, R.A., Mirzadeh, Z., Tsai, H.H., Wong, M., Gupta, N., Berger, M.S., Huang, E., Garcia-Verdugo, J.M., *et al.* (2011). Corridors of migrating neurons in the human brain and their decline during infancy. Nature *478*, 382-386.

Sanai, N., Tramontin, A.D., Quinones-Hinojosa, A., Barbaro, N.M., Gupta, N., Kunwar, S., Lawton, M.T., McDermott, M.W., Parsa, A.T., Manuel-Garcia Verdugo, J., *et al.* (2004). Unique astrocyte ribbon in adult human brain contains neural stem cells but lacks chain migration. Nature *427*, 740-744.

Saxe, M.D., Battaglia, F., Wang, J.W., Malleret, G., David, D.J., Monckton, J.E., Garcia, A.D., Sofroniew, M.V., Kandel, E.R., Santarelli, L., *et al.* (2006). Ablation of hippocampal neurogenesis impairs contextual fear conditioning and synaptic plasticity in the dentate gyrus. Proc Natl Acad Sci U S A *103*, 17501-17506.

Scharfman, H.E. (2000). Epileptogenesis in the parahippocampal region. Parallels with the dentate gyrus. Ann N Y Acad Sci *911*, 305-327.

Scharfman, H.E., Sollas, A.L., Berger, R.E., and Goodman, J.H. (2003). Electrophysiological evidence of monosynaptic excitatory transmission between granule cells after seizure-induced mossy fiber sprouting. J Neurophysiol *90*, 2536-2547.

Schmidt-Hieber, C., Jonas, P., and Bischofberger, J. (2004). Enhanced synaptic plasticity in newly generated granule cells of the adult hippocampus. Nature *429*, 184-187.

Scholzen, T., and Gerdes, J. (2000). The Ki-67 protein: from the known and the unknown. J Cell Physiol *182*, 311-322.

Segi-Nishida, E., Warner-Schmidt, J.L., and Duman, R.S. (2008). Electroconvulsive seizure and VEGF increase the proliferation of neural stem-like cells in rat hippocampus. Proc Natl Acad Sci U S A *105*, 11352-11357.

Seib, D.R., Corsini, N.S., Ellwanger, K., Plaas, C., Mateos, A., Pitzer, C., Niehrs, C., Celikel, T., and Martin-Villalba, A. (2013). Loss of Dickkopf-1 restores neurogenesis in old age and counteracts cognitive decline. Cell Stem Cell *12*, 204-214.

Sejersen, T., and Lendahl, U. (1993). Transient expression of the intermediate filament nestin during skeletal muscle development. J Cell Sci *106 (Pt 4)*, 1291-1300.

Sekerkova, G., Ilijic, E., and Mugnaini, E. (2004). Bromodeoxyuridine administered during neurogenesis of the projection neurons causes cerebellar defects in rat. J Comp Neurol *470*, 221-239.

Seri, B., Garcia-Verdugo, J.M., Collado-Morente, L., McEwen, B.S., and Alvarez-Buylla, A. (2004). Cell types, lineage, and architecture of the germinal zone in the adult dentate gyrus. J Comp Neurol *478*, 359-378.

Seri, B., Garcia-Verdugo, J.M., McEwen, B.S., and Alvarez-Buylla, A. (2001). Astrocytes give rise to new neurons in the adult mammalian hippocampus. J Neurosci *21*, 7153-7160.

Sharma, A.K., Reams, R.Y., Jordan, W.H., Miller, M.A., Thacker, H.L., and Snyder, P.W. (2007). Mesial temporal lobe epilepsy: pathogenesis, induced rodent models and lesions. Toxicol Pathol *35*, 984-999.

Shetty, A.K., Zaman, V., and Shetty, G.A. (2003). Hippocampal neurotrophin levels in a kainate model of temporal lobe epilepsy: a lack of correlation between brain-derived neurotrophic factor content and progression of aberrant dentate mossy fiber sprouting. J Neurochem *87*, 147-159.

Shimojo, H., Ohtsuka, T., and Kageyama, R. (2008). Oscillations in notch signaling regulate maintenance of neural progenitors. Neuron *58*, 52-64.

Shors, T.J., Miesegaes, G., Beylin, A., Zhao, M., Rydel, T., and Gould, E. (2001). Neurogenesis in the adult is involved in the formation of trace memories. Nature *410*, 372-376.

Sierra, A., Encinas, J.M., Deudero, J.J., Chancey, J.H., Enikolopov, G., Overstreet-Wadiche, L.S., Tsirka, S.E., and Maletic-Savatic, M. (2010). Microglia shape adult

hippocampal neurogenesis through apoptosis-coupled phagocytosis. Cell Stem Cell *7*, 483-495.

Sierra, A., Martin-Suarez, S., Valcarcel-Martin, R., Pascual-Brazo, J., Aelvoet, S.A., Abiega, O., Deudero, J.J., Brewster, A.L., Bernales, I., Anderson, A.E., *et al.* (2015). Neuronal hyperactivity accelerates depletion of neural stem cells and impairs hippocampal neurogenesis. Cell Stem Cell *16*, 488-503.

Sirerol-Piquer, M.S., Cebrian-Silla, A., Alfaro-Cervello, C., Gomez-Pinedo, U., Soriano-Navarro, M., and Verdugo, J.M. (2012). GFP immunogold staining, from light to electron microscopy, in mammalian cells. Micron *43*, 589-599.

Sirko, S., Behrendt, G., Johansson, P.A., Tripathi, P., Costa, M., Bek, S., Heinrich, C., Tiedt, S., Colak, D., Dichgans, M., *et al.* (2013). Reactive glia in the injured brain acquire stem cell properties in response to sonic hedgehog. [corrected]. Cell Stem Cell *12*, 426-439.

Snyder, J.S., Soumier, A., Brewer, M., Pickel, J., and Cameron, H.A. (2011). Adult hippocampal neurogenesis buffers stress responses and depressive behaviour. Nature *476*, 458-461.

Sofroniew, M.V. (2009). Molecular dissection of reactive astrogliosis and glial scar formation. Trends Neurosci *32*, 638-647.

Song, J., Zhong, C., Bonaguidi, M.A., Sun, G.J., Hsu, D., Gu, Y., Meletis, K., Huang, Z.J., Ge, S., Enikolopov, G., *et al.* (2012). Neuronal circuitry mechanism regulating adult quiescent neural stem-cell fate decision. Nature *489*, 150-154.

Sorrells, S.F., Paredes, M.F., Cebrian-Silla, A., Sandoval, K., Qi, D., Kelley, K.W., James, D., Mayer, S., Chang, J., Auguste, K.I., *et al.* (2018). Human hippocampal neurogenesis drops sharply in children to undetectable levels in adults. Nature *555*, 377-381.

Spalding, K.L., Bergmann, O., Alkass, K., Bernard, S., Salehpour, M., Huttner, H.B., Bostrom, E., Westerlund, I., Vial, C., Buchholz, B.A., *et al.* (2013). Dynamics of hippocampal neurogenesis in adult humans. Cell *153*, 1219-1227.

Spassky, N., Merkle, F.T., Flames, N., Tramontin, A.D., Garcia-Verdugo, J.M., and Alvarez-Buylla, A. (2005). Adult ependymal cells are postmitotic and are derived from radial glial cells during embryogenesis. J Neurosci *25*, 10-18.

Stanfield, B.B., and Trice, J.E. (1988). Evidence that granule cells generated in the dentate gyrus of adult rats extend axonal projections. Exp Brain Res *72*, 399-406.

Steiner, B., Kronenberg, G., Jessberger, S., Brandt, M.D., Reuter, K., and Kempermann, G. (2004). Differential regulation of gliogenesis in the context of adult hippocampal neurogenesis in mice. Glia *46*, 41-52.

Stepan, J., Dine, J., and Eder, M. (2015). Functional optical probing of the hippocampal trisynaptic circuit in vitro: network dynamics, filter properties, and polysynaptic induction of CA1 LTP. Front Neurosci *9*, 160.

Suh, H., Consiglio, A., Ray, J., Sawai, T., D'Amour, K.A., and Gage, F.H. (2007). In vivo fate analysis reveals the multipotent and self-renewal capacities of Sox2+ neural stem cells in the adult hippocampus. Cell Stem Cell *1*, 515-528.

Tashiro, A., Sandler, V.M., Toni, N., Zhao, C., and Gage, F.H. (2006). NMDA-receptor-mediated, cell-specific integration of new neurons in adult dentate gyrus. Nature *442*, 929-933.

Tauck, D.L., and Nadler, J.V. (1985). Evidence of functional mossy fiber sprouting in hippocampal formation of kainic acid-treated rats. J Neurosci *5*, 1016-1022.

Taupin, P. (2007). BrdU immunohistochemistry for studying adult neurogenesis: paradigms, pitfalls, limitations, and validation. Brain Res Rev *53*, 198-214.

Taylor, V. (2011). Hippocampal stem cells: so they are multipotent! J Mol Cell Biol *3*, 270-272.

Terling, C., Rass, A., Mitsiadis, T.A., Fried, K., Lendahl, U., and Wroblewski, J. (1995). Expression of the intermediate filament nestin during rodent tooth development. Int J Dev Biol *39*, 947-956.

Toni, N., Laplagne, D.A., Zhao, C., Lombardi, G., Ribak, C.E., Gage, F.H., and Schinder, A.F. (2008). Neurons born in the adult dentate gyrus form functional synapses with target cells. Nat Neurosci *11*, 901-907.

Toni, N., Teng, E.M., Bushong, E.A., Aimone, J.B., Zhao, C., Consiglio, A., van Praag, H., Martone, M.E., Ellisman, M.H., and Gage, F.H. (2007). Synapse formation on neurons born in the adult hippocampus. Nat Neurosci *10*, 727-734.

Tronche, F., Kellendonk, C., Kretz, O., Gass, P., Anlag, K., Orban, P.C., Bock, R., Klein, R., and Schutz, G. (1999). Disruption of the glucocorticoid receptor gene in the nervous system results in reduced anxiety. Nat Genet *23*, 99-103.

Urban, N., and Guillemot, F. (2014). Neurogenesis in the embryonic and adult brain: same regulators, different roles. Front Cell Neurosci *8*, 396.

Urban, N., van den Berg, D.L., Forget, A., Andersen, J., Demmers, J.A., Hunt, C., Ayrault, O., and Guillemot, F. (2016). Return to quiescence of mouse neural stem cells by degradation of a proactivation protein. Science *353*, 292-295.

van Praag, H., Christie, B.R., Sejnowski, T.J., and Gage, F.H. (1999). Running enhances neurogenesis, learning, and long-term potentiation in mice. Proc Natl Acad Sci U S A *96*, 13427-13431.

van Praag, H., Schinder, A.F., Christie, B.R., Toni, N., Palmer, T.D., and Gage, F.H. (2002). Functional neurogenesis in the adult hippocampus. Nature *415*, 1030-1034.

van Strien, N.M., Cappaert, N.L., and Witter, M.P. (2009). The anatomy of memory: an interactive overview of the parahippocampal-hippocampal network. Nat Rev Neurosci *10*, 272-282.

Vismer, M.S., Forcelli, P.A., Skopin, M.D., Gale, K., and Koubeissi, M.Z. (2015). The piriform, perirhinal, and entorhinal cortex in seizure generation. Front Neural Circuits *9*, 27.

Walker, T.L., Overall, R.W., Vogler, S., Sykes, A.M., Ruhwald, S., Lasse, D., Ichwan, M., Fabel, K., and Kempermann, G. (2016). Lysophosphatidic Acid Receptor Is a Functional Marker of Adult Hippocampal Precursor Cells. Stem Cell Reports *6*, 552-565.

Walter, J., Keiner, S., Witte, O.W., and Redecker, C. (2011). Age-related effects on hippocampal precursor cell subpopulations and neurogenesis. Neurobiol Aging *32*, 1906-1914.

Wang, C., Liu, F., Liu, Y.Y., Zhao, C.H., You, Y., Wang, L., Zhang, J., Wei, B., Ma, T., Zhang, Q., *et al.* (2011). Identification and characterization of neuroblasts in the subventricular zone and rostral migratory stream of the adult human brain. Cell Res *21*, 1534-1550.

Wang, Y., Chen, Z., Zhang, Y., Fang, S., and Zeng, Q. (2014). Mitochondrial biogenesis of astrocytes is increased under experimental septic conditions. Chin Med J (Engl) *127*, 1837-1842.

Waterhouse, E.G., An, J.J., Orefice, L.L., Baydyuk, M., Liao, G.Y., Zheng, K., Lu, B., and Xu, B. (2012). BDNF promotes differentiation and maturation of adult-born neurons through GABAergic transmission. J Neurosci *32*, 14318-14330.

Weiner, J.A., Hecht, J.H., and Chun, J. (1998). Lysophosphatidic acid receptor gene vzg-1/lpA1/edg-2 is expressed by mature oligodendrocytes during myelination in the postnatal murine brain. J Comp Neurol *398*, 587-598.

Whitlock, J.R., Heynen, A.J., Shuler, M.G., and Bear, M.F. (2006). Learning induces long-term potentiation in the hippocampus. Science *313*, 1093-1097.

Wieser, H.G. (2004). ILAE Commission Report. Mesial temporal lobe epilepsy with hippocampal sclerosis. Epilepsia *45*, 695-714.

Witter, M.P., Wouterlood, F.G., Naber, P.A., and Van Haeften, T. (2000). Anatomical organization of the parahippocampal-hippocampal network. Ann N Y Acad Sci *911*, 1-24.

Wu, M.V., and Hen, R. (2013). The young and the restless: regulation of adult neurogenesis by Wnt signaling. Cell Stem Cell *12*, 139-140.

Yamaguchi, M., Saito, H., Suzuki, M., and Mori, K. (2000). Visualization of neurogenesis in the central nervous system using nestin promoter-GFP transgenic mice. Neuroreport *11*, 1991-1996.

Yoshimura, S., Takagi, Y., Harada, J., Teramoto, T., Thomas, S.S., Waeber, C., Bakowska, J.C., Breakefield, X.O., and Moskowitz, M.A. (2001). FGF-2 regulation of neurogenesis in adult hippocampus after brain injury. Proc Natl Acad Sci U S A *98*, 5874-5879.

Zamanian, J.L., Xu, L., Foo, L.C., Nouri, N., Zhou, L., Giffard, R.G., and Barres, B.A. (2012). Genomic analysis of reactive astrogliosis. J Neurosci *32*, 6391-6410.

Zhao, C., Deng, W., and Gage, F.H. (2008). Mechanisms and functional implications of adult neurogenesis. Cell *132*, 645-660.

Zhao, C., Teng, E.M., Summers, R.G., Jr., Ming, G.L., and Gage, F.H. (2006). Distinct morphological stages of dentate granule neuron maturation in the adult mouse hippocampus. J Neurosci *26*, 3-11.

Zhao, Y.Z., Gao, Z.Y., Ma, L.Q., Zhuang, Y.Y., and Guan, F.L. (2017). Research on biogenesis of mitochondria in astrocytes in sepsis-associated encephalopathy models. Eur Rev Med Pharmacol Sci *21*, 3924-3934.

Ziebell, F., Dehler, S., Martin-Villalba, A., and Marciniak-Czochra, A. (2018). Revealing age-related changes of adult hippocampal neurogenesis using mathematical models. Development *145*.

Zimmerman, L., Parr, B., Lendahl, U., Cunningham, M., McKay, R., Gavin, B., Mann, J., Vassileva, G., and McMahon, A. (1994). Independent regulatory elements in the nestin gene direct transgene expression to neural stem cells or muscle precursors. Neuron *12*, 11-24.

Zulewski, H., Abraham, E.J., Gerlach, M.J., Daniel, P.B., Moritz, W., Muller, B., Vallejo, M., Thomas, M.K., and Habener, J.F. (2001). Multipotential nestin-positive stem cells isolated from adult pancreatic islets differentiate ex vivo into pancreatic endocrine, exocrine, and hepatic phenotypes. Diabetes *50*, 521-533.